

THE DESIGN OF STEEL FIBRE REINFORCED CONCRETE STRUCTURES



WORKSHOP PROCEEDING

FROM A

NORDIC MINISEMINAR

STOCKHOLM - SWEDEN

12. JUNE 2001

PREFACE

In several Nordic universities, research institutes, and companies, research and development are devoted to steel fibre reinforced concrete structures. The Swedish Concrete Association published a report on steel fibre reinforced concrete in 1995. At that time, it was considered to be one of the world's most modern and straightforward handbooks on the design of steel fibre reinforced concrete structures. Since then, six years have passed. Several doctoral and licentiate dissertations have been devoted completely or partly to steel fibre reinforced concrete. The material technology has developed further and some new and more advanced computation models have been suggested. Furthermore, new test methods have been developed; especially those dealing with pure tension are interesting since such methods are necessary to improve the understanding of the structural behaviour of steel fibre reinforced concrete.

In order to exchange information and new research results, the Royal Institute of Technology (KTH) invited to a Nordic workshop on the design of steel fibre reinforced concrete structures in June 2001 in Stockholm. The aim was to provide the attendees with the state of the art on design of steel fibre reinforced concrete structures and to give impact and ideas to the continuing research and development in this area. Since 1975, more than 60 Nordic workshops have been organised by the research committee of the Nordic Concrete Federation. This workshop assembled 27 participants from Denmark, Norway and Sweden. A total number of 14 oral presentations were given. They are all summarised in these proceedings.

In the final discussion it was concluded that the views of the various speakers are somewhat contradictory. Some speakers stated that the current design rules are too complicated. Others said that they are too simple since they do not treat the structural behaviour sufficiently adequately. Some researchers claimed that current design praxis is too conservative whereas others argued that all aspects that may have a negative impact on the design are not included. Restrain stresses are too often neglected. On the other hand, the material development continues. This means that steel fibre reinforced concrete might be more competitive in the future. A unanimous meeting concluded, however, that we have to continue our work with both improvements of the design methods and modelling of the material behaviour.

Stockholm, November 2001

Johan Silfwerbrand

Organiser of the workshop and member of the Research Committee of the Nordic Concrete Federation

CONTENTS:

List of Participants	vii
Peter Mjörnell Experiences with Betongrapport Nr. 4 and the Need for Recognised Guidelines	1
Bo Westerberg Some Quistions Concerning the design of Steel Fibre Concrete Slabs on Ground	11
Johan Silfwerbrand Improvements of the Swedish Concrete Association's Method for Design of SFRC Slabs on Grade.	23
Tor K. Sandaker, Arne Vatnar & Øyvind Bjøntegaard Competitive Concrete Solutions for Industrial and Residential Buildings	33
Bo Malmberg Design of Fibre Reinforced Floors - Practical Experiences.	45
Lutfi Ay Yield and Failure Criteria of Fibrous Cement Based Composites	55
Henrik Stang Determination of Fracture Mechanical Properties for FRC	61
Jonas Carlswärd A Test Method for Studying Crack Development in Steel Fibre Reinforced Concrete Overlays Due to Restrained Deformation	71
Jonas Holmgren & Bert Norlin Properties and Use of the Round, Determinately Supported Concrete Panel for Testing of Fibre reinforced Concrete	81
Ulf Nilsson Load Bearing Capacity of Steel Fibre Reinforced Shotcrete Linings	93
Erik Nordström Steel Fibre Corrosion in Cracks - A design Problem for Shotcrete Applications?	103
Manouchehr Hassanzadeh Flexural Behaviour of Steel-Fibre-Reinforced High-Performance Concrete	113
Ghassam Hassanzadeh & Håkon Sundquist Influence of Steel Fibre Reinforcement on Punching Shear Capacity of Column Supported Flat Slabs.	123
Keivan Noghabai Behaviour of Fibre Reinforced Concrete for Different Strictures.	137

LIST OF PARTICIPANTS:

Pär Andreasson	NCC, Solna	Sweden
Lutfi Ay	KTH, Stockholm	Sweden
Geir Bjørnbakk.....	Veidekke, Oslo	Norway
Jan Erik carlsen	Selmer Skanska, Oslo	Norway
Jonas Carlswärd	Betongindustri, Stockholm	Sweden
Ali Farhang	ELU Konsult, Stockholm.....	Sweden
Patrik Groth	NCC, Solna	Sweden
Magnus Hansson	Bekaert, Göteborg.....	Sweden
Peter Harryson	Chalmers, Göteborg.....	Sweden
Ghassem Hassanzadeh	KTH, Stockholm	Sweden
Manouchehr Hassanzadeh	LTH, Lund	Sweden
Jerry Hedebratt.....	KTH, Stockholm	Sweden
Jonas Holmgren.....	KTH, Stockholm	Sweden
Ingemar Löfgren	Chalmers, Göteborg.....	Sweden
Bo Malmberg	J&W, Karlstad.....	Sweden
Alf Egil Mathisen.....	Veidekke, Oslo	Norway
Peter Mjörnell	Bekaert, Göteborg.....	Sweden
Ulf Nilsson.....	KTH, Stockholm	Sweden
Keivan Noghabai.....	LTU, Luleå.....	Sweden
Erik Nordström	Vattenfall Utvikling, Älvkarleby.....	Sweden
Samir Redha.....	Vägverket, Borlänge.....	Sweden
Tor K. Sandaker	Norconsult, Sandvika.....	Norway
Johan Silfwerbrand.....	KTH, Stockholm	Sweden

Henrik Stang	DTU, Lyngby	Denmark
Åke Thorsén.....	Cementa, Danderyd	Sweden
Stefan Tyrbo	J&W, Stockholm	Sweden
Bo Westerberg	Týrens, Stockholm.....	Sweden

Experiences with Betongrapport Nr 4 and the Need for Recognised Guidelines



Peter Mjörnell
M.Sc. Sales Manager Northern Europe
Bekaert Svenska AB
Första Långgatan 28 B, 413 27 Göteborg, Sweden
E-mail: peter.mjoernell@bekaert.com

ABSTRACT

The Betongrapport nr 4 of the Swedish Concrete Society has brought design of steel fibre reinforced design forward since 1995. It has proved to be complex to apply and interpret for many engineers not working with steel fibre reinforced concrete regularly, however. Especially the presentation of performance of steel fibre reinforcement still tends to cause confusion.

Key words: flooring design, performance classes, steel fibre reinforced concrete.

1. INTRODUCTION

While the Betongrapport nr 4 [1] can be used for general design problems, flooring design is the most common for steel fibre reinforced concrete today. Focus will be on flooring in this paper.

1.1 Early Flooring Design

Before Betongrapport nr 4 was introduced Bekaert based its flooring design on older Dutch recommendations. The models were somewhat crude with only elastic analysis and the load redistribution of a plate on ground was taken into account by using an enhanced design stress. Basically the Dutch CUR [2] recommendation specify that there is a link between the flexural toughness and the increased load bearing capacity of a plate on ground. The following stress enhancement formula was used:

$$f_{flresk} = (1,6 - h) \left(1 + \frac{R_{10,30} - 30}{70} \right) f_{tk} \quad (1)$$

f_{flresk} is flexural residual strength for a plate on ground

This model was derived by studying the behaviour of point loaded plates on ground. Bekaert do not use this model anymore but is still being used by many designers, especially in the Benelux countries. Today, Bekaert normally design floors based on the British recommendation TR 34 [3], apart from the Nordic countries.

Another approach still being widely practised is design based on the assumption that steel fibre reinforcement increases the first crack strength. The assumption is normally supported by carefully selected test results. Most research institutes do not support this hypothesis today, for moderate dosages of steel fibres, but the model is still in practice. Many designers still possess limited knowledge of steel fibre reinforced concrete and may accept a design based on an increased first crack strength.

Others still do not design floors at all. Some contractors have one solution for all floors regardless of loading. E.g. 150 mm and 40 kg/m³ of a specific fibre. This solution is then expected to work on all grounds and loading conditions.

2. DESIGN BASED ON BETONGRAPPORT NR 4

2.1 Flooring design

Quite early Bekaert attempted to adopt our design methods to the Betongrapport nr 4 in the Nordic countries. The first hand calculations were done by Carl Lindquist already in 1995. In the summer of 1995 the first big floor, calculated according to Betongrapport nr 4, was casted in Gothenburg. It was a floor of 10 000 m², 130 mm thick and reinforced with 35 kg/m³ Dramix ZC 80/0.60.

A design program was developed, together with a design manual [4]. This program is still in use after several updates and is still one of our most important design tools in the Nordic countries. The shortcoming of Betongrapport nr 4 is mostly in dealing with structures only subjected to shrinkage stresses.

The design model has been recognised in Denmark, Finland and Norway as being an acceptable way to design steel fibre reinforced concrete for the time being.

In the rest of the world Bekaert normally design floors according to TR 34 of the British Concrete Society. There is also a manual and a design program to support this. The basic philosophy is the same and also this model rest partly on Betongrapport nr 4 and “Handledning för dimensionering av fiberbetonggolv”[5].

Bekaert is now in the introduction phase of a new generation on design programs for steel fire reinforced floors. Apart from a more modern program layout and printing facilities it is also very flexible to enable easy adjustments to national requirements. The basic ultimate stresses are calculated using the original formulas of Losberg [6].

The new program will be able to handle different sets of material characteristics and other input that may vary in national recommendations. It will also be accessible over Internet from this autumn on, for selected individuals and companies.

2.2 Other design

When designing structural applications such as segmental lining and other precast structures Bekaert basically apply the same approach. For important structures and/or repetitive solutions there is often the possibility to test the specific material or even to do full scale testing. Steel fibre reinforced segmental lining for TBM's are often tested full scale, as an example.

2.3 Experiences in flooring

Since 1995 some 5 million m² floors have been reinforced with Dramix® in the Nordic area and most of these floors have been designed according to Betongrapport nr 4.

Most of these floors have worked very well and there are no indications that the models are off from a structural point of view. During this period we have no record of any floor, that has not worked as expected in terms of load capacity.

An interesting conclusion was that the older CUR models gave very similar results as the calculations according to Betongrapport nr 4. There was often good correlation between thickness and reinforcement for most loading conditions even if the calculated stresses were different naturally.

Occasional problems occurring have been more related to practical issues not covered by the design model. Common problems are, as with all floors, shrinkage cracks, curling problems, joint problems and finishing issues. These difficulties are not specific for steel fibre reinforced floors and can only be addressed through a good co-operation between the designer, contractor and the material supplier. In fact, many contractors experience less such difficulties with steel fibre reinforced concrete compared to traditionally reinforced floors.

The concrete composition is crucial for several reasons. The shrinkage should be moderate while still maintaining a relative high slump. A suitable superplasticizer is recommended in most cases. The sieve curves are especially important when mixing high dosages of high performance steel fibres. The concrete should have an increased amount of material 0-2 mm to reduce problems with fibres at the surface. The amount of large aggregates should be limited.

2.4 Successful floor types

Two types of floors, which are described as type A and C in Betongrapport nr 4, generally give the best results. Saw cut floors with joint distances between 10-20 m have proved difficult in our experience. Even if it is possible to avoid shrinkage cracks with a good reinforcement, you often face serious problems at the joints. It is then better to increase the joint distances to a maximum and make an extra effort to protect the large joint openings.

Type A. Small plates with saw-cut joints

These floors are often casted with a Laserscreed in bays of about 1500 m² and cut the day after. Joint distances are often limited to 6-8 m and should be at maximum 10 m. The thickness and reinforcement depend on loading and ground conditions but a thinner floor give more curling.

Minimum thickness is about 120 mm but a thicker floor is preferred. (Incidentally, it can be mentioned that 150 mm is a required minimum thickness in many countries for concrete floors.) Traditionally “type A” floors were casted on low a friction sub-base but this is more and more in question. Cracks are very rare and instead there are often problems with series of plates moving to create dominant joints. The friction should certainly be high enough to open most joints on these floors. This means that the foil may be skipped in some cases.

Type B. Floors without contraction joints.

These floors have proved to work very well throughout Europe, including the Nordic area, and now make up a serious share of the larger heavy industrial floors. The floors are cast with a Laserscreed in bays of about 2000 m² and there are no joints or visible cracks in these bays. The joint openings are large however, often 1 cm or more, and need to be protected with a steel edge. A very low friction to the sub-base is then needed, along with excellent execution and a low shrinkage concrete. The jointless floors should be minimum 140 mm thick and reinforced to a toughness of more than 60 %. Minimum reinforcement is then 35 kg/m³ Dramix RC-65/60-BN. Ω-joints are often selected as day joints to combine mould, steel protection and free horizontal movements.

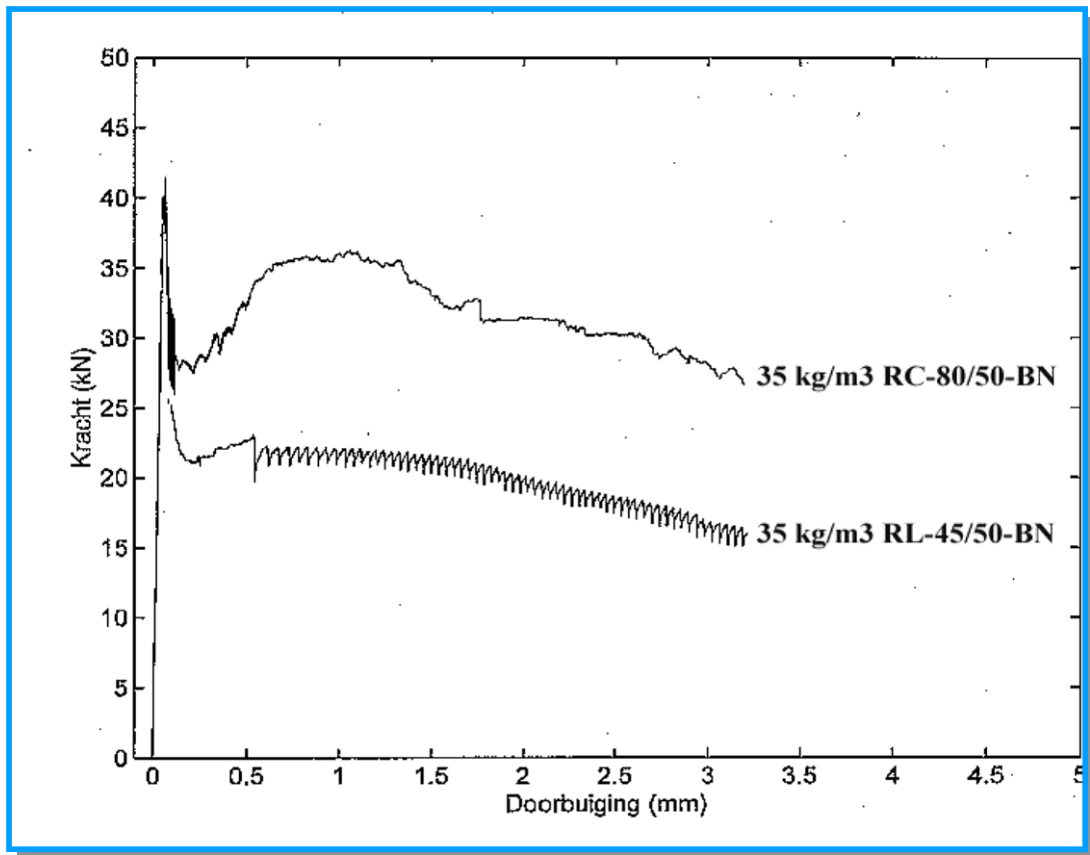
3. PRESENTATION OF RESULTS

3.1 Testing of steel fibre reinforced concrete

There are several good ways to test the flexural properties of steel fibre concrete and still better methods to determine both the flexural and tensile properties will probably come into practice in the next few years. E.g. the RILEM suggestions. The most important thing is that there are generally accepted methods per market and that most parties recognise them. In most of Europe the JSCE-SF4 is still predominant, while in the Nordic it is more common to use the ASTM C 1018. Unless there is a rather strict way to compare the performance of different alternatives the market very rapidly deteriorates into a dosage based market and become the dumping ground of low-end steel fibres. The tunnel market in Norway is a good example where low-end steel fibres are used in many tunnels today.

The performance of steel fibre concrete depends as much on the choice of steel fibre as the dosage. The following two load-deflection curves show the performance of two fibres of the same length, dosage and geometry, tested according to JSCE-SF4. It is however very difficult for most engineers to tell the difference by just looking at the products.

It is clear that the same dosage (35 kg/m³) of Dramix® fibres can give residual strengths varying between 50 and 80 %. Both fibres are 50 mm long and the RC-80/50-BN fibre is 0,62 mm thick while the RL-45/50-BN is 1,05 mm thick.



Source: K.U. Leuven (P.V.:R/28527-B/96)
(P.V.:R/28642/96)

Figure 1 – Load-deflection curves

3.2 Today's presentation of performance and function

Steel fibre structures are presented to designers and end clients in different ways today. “Don't worry – We take care of everything” is mingled with more or less correct presentations of performance, properties and functional capacities. We see that the Betongrapport nr 4 was a big step forward, even if we still see designs based on tests proving an increased first crack strength of the concrete.

The Betongrapport nr 4 is perceived a bit complicated in terms of performance and it may be difficult to see what to really ask for as a designer (or from whom for that matter).

In cases where a post crack performance is specified, normally the steel fibre producer or distributor make a design and take responsibility for the relative flexural toughness (R-values). The attractive parts of this approach is that it is easy to understand, it has been in practice for long, and it is low cost in testing. The disadvantage is that you have no absolute assurance that the selected concrete will give exactly the same flexural strength as when testing. Bekaert do

normally accept this uncertainty for floors but not for more advanced structures. Apart from input and modelling information, our design program for Betongrapport nr 4 give the following final output today.

⑥ DRAMIX® FÖRSLAG

Baserat på givna förutsättningar föreslås följande lösning:

Plattans tjocklek	:	140	mm
Dosering	:	35	kg/m³
Fibertyp	:	RC-65/60-BN	
Betong	:	K 30	
Fogavstånd	:	9000 x 8000	mm

Ovanstående förslag motsvarar följande hållfastheter vid provning enligt ASTM C 1018:92.

Residualhållfasthet (%) Motsvarande spänning (MPa)

$$R_{10,20} = 64 \qquad f_{fresk} = R_{10,20} \times 1,2 \times f_{fcr} = 2,36$$

$$R_{10,39} = 61 \qquad f_{fresk} = R_{10,39} \times 1,2 \times f_{fcr} = 2,25$$

⑦ KOMMENTARER

Figure 2 – Program printout

The relative flexural toughnesses and the equivalent flexural strengths are presented at needed deflections, to compare to eventual material tests performed on the project. However, it is today rather unusual that such tests really take place. It may happen infrequently on large important projects but not on smaller projects.

The new design program will contain more detailed information and will also more clearly distinguish between ultimate and serviceability state.

4. DISCUSSION AND FUTURE TRENDS

4.1 Requirements and alternatives

It is easy to criticise the relative approach and just state that each and every concrete mix has to be individually tested. The cost of testing would be prohibitive on all but very large flooring projects however. It is a sure route towards a market situation where individual companies provide company based assurances. Flooring design will become less transparent and it will not enhance the quality of flooring.

We also see a rapid development in some countries towards steel fibre reinforced alternatives for smaller repetitive applications, often marketed by the ready mix industry. Here we find small house foundations, compression layers, cellar walls and similar applications. Also in this fast growing segment there is a need for guidelines.

Regardless what test models are selected per country, it is important to have simple and clear presentation of performance. If we select $R_{10,30}$, $R_{e1,5}$, I_x , $f_{1,5\text{mm}}$ or the RILEM recommendation, is perhaps of less importance. Our solutions today, based on Betongrapport nr 4, present performance at deflections corresponding to $R_{10,20}$ and $R_{10,x}$. "X" depends on the expected maximum crack width of the construction in mind. This further complicates an already difficult message for many engineers.

Another requirement is for the test itself to be relatively simple to perform and not too costly. The amount of testing that can be prescribed will depend largely on the cost per test.

4.2 When to test and by whom?

Testing can either be prescribed at especially important projects or that each supplier get some sort of approved performance per product. This has been suggested in Finland with the BY 8 B certification. It indicates what sort of toughness a specific product will give at different dosages. In principle you test at an approved test institute and get an official fibre identification chart.

The other question is who should be responsible for what? Is it the steel fibre supplier that should be responsible for the performance and function? Should responsibility lie with the contractor casting the floor, or perhaps with the ready mix producer, marketing steel fibre reinforced concrete? The fibre supplier normally takes most of the responsibility now, as the fibre supplier often sets the design rules for its products. There is a trend in some European countries towards a larger involvement of the ready mix producers. This development points in the direction of more or less official performance classes for steel fibre reinforced concrete.

4.3 Performance classes

In Germany there are plans to establish a DBV-Merkblatt that regulate different levels of performance for steel fibre concrete. Beam tests will be used to establish equivalent flexural strengths for different fibres and dosages. Performance will be studied at two pre-defined deflections. The smaller deflection ($\rho_{cr} + 0,65$ mm) will be for serviceability studies and the larger deflection ($\rho_{cr} + 3,15$ mm) will be for the ultimate limit state. The following classes are being considered:

Table 1 – Performance classes according to DBV-Merkblatt – **DRAFT**

Class	Min-value for equivalent flexural strength (MPa)
0	< 1,0
0,4	> 1,0
0,6	> 1,5
0,8	> 2,0
1,0	> 2,5
1,2	≥ 3,0

The classes obviously refer to the calculated pure tensile strength when using the common conversion factor of 0,37.

Theoretically performance should be tested at each concrete plant but in practice each producer will probably test at representative plants and use the data at other plants. The minimum number of beams will be six per dosage. It is easy to understand the vast number of tests required to test at all plants.

In Benelux similar ideas will be introduced but there the steel fibre producers will probably establish performance classes for selected types of concrete. It will probably be based on relative performance measures.

Performance classes have been discussed in the Nordic before and now could be the time to attempt to classify performance for steel fibre reinforced concrete. This would counter some of the confusion and make steel fibre reinforced concrete even more acceptable in the future.

Perhaps there may be possibilities to combine the practical approach applied in Betongrapport nr 4, with the more recent work in the Danish Materials Technology Development Program, MUP2 [7]. Also this work point in the direction of performance classification, although from a different angle.

Another source of inspiration could be the new updated Norwegian rock support guide [8]. It suggests performance classes based on both beam tests and plate tests and it also indicates what

tests to be done. For the highest class (2) it is prescribed to test with the right mix on the project, while else it is enough to declare the performance based on general official testing.

REFERENCES

1. Svenska Betongföreningen, “Betongrapport nr 4. Stålfiberbetong – rekommendationer för konstruktion, utförande och provning.”, Utgåva 2, November 1997, 135 pp.
2. Dutch Concrete Society, “Ontwerpen van elastisch ondersteunde betonvloeren”, CUR-Aanbeveling 36, Second edition 2000, first published in 1994
3. The British Concrete Society, “Concrete Industrial Ground Floors; A Guide to their design and Construction – TR 34”, Second edition, February 1995
4. Thoof, H “Stålfiberarmerade betonggolv på mark beräknade enligt svenska betongföreningens betongrapport nr 4-1995”, NV Bekaert SA, Zwevegem, Belgium, 1997
5. Skarendahl, Å, & Westerberg, B., “Handledning för dimensionering av fiberbetonggolv”, CBI rapport 1:89, Stockholm, 1989
6. Losberg, A., “Design methods for structurally reinforced concrete pavements”, CTH Handlingar 250, 1961
7. Stang, H., & Forbes Olesen, J., “Design Basis For FRC Structures” MUP2, DTU, Copenhagen 1999.
8. Norsk Betongförening, “Sprayed Concrete for Rock Support – Technical Specification, Guidelines and Test Methods”, Publication no 7, 1999.

Some Questions Concerning the Design of Steel Fibre Concrete Slabs on Ground



Bo Westerberg
Adj Professor

Tyréns Byggkonsult
SE-11886 Stockholm
E-mail: bo.westerberg@tyrens.se

Royal Institute of Technology
Department of Structural Engineering
SE 10044 Stockholm
E-mail: bo.westerberg@struct.kth.se

ABSTRACT

Current Swedish practise in the design of steel fibre concrete slabs on ground is reviewed and discussed.

Key words: steel fibre concrete, slabs on ground, plastic analysis, punching

1. INTRODUCTION

A concentrated load on a slab on ground is carried more or less directly by the subgrade. However, due to the stiffness of the slab, the subgrade reaction (ground pressure) is spread over an area outside the load, which creates bending moments and shear in the slab, see figure 1.

The design with regard to these effects is the subject of this paper, and the title suggests that there may be uncertainties and questions concerning this. In general, the author does not have the answers to the questions, but maybe some of the answers can be found in other contributions to this seminar.

In the following, “fibre concrete” means steel fibre reinforced concrete, “reinforced concrete” means concrete with ordinary reinforcement whereas “plain concrete” means no reinforcement at all.

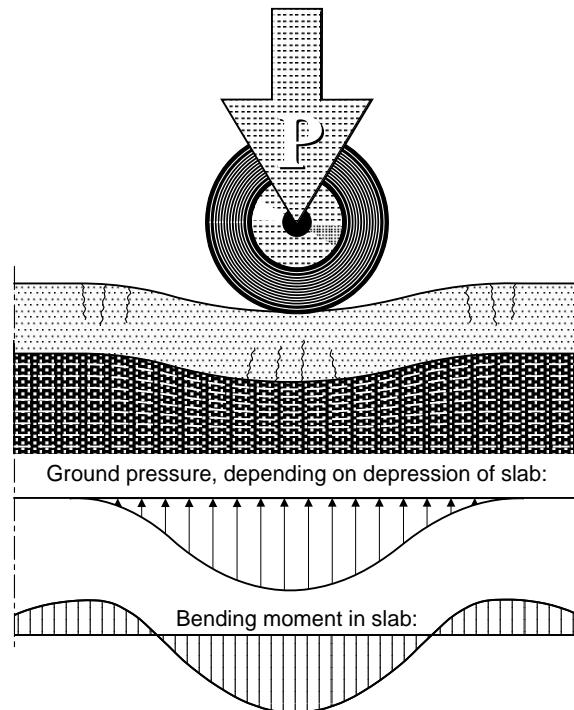


Figure 1. Illustration of a slab on ground subjected to a concentrated load.

In the traditional design of floors and pavements of plain concrete, the maximum bending moment from an elastic analysis is compared to the maximum flexural capacity of the slab, i.e. the cracking moment. When the maximum capacity is reached for positive moment, the negative moment is far below maximum, see curve 1 in figure 2 (the other curves will be discussed later).

Figure 2. Examples of moment distributions for an interior concentrated load (far from edges and corners).

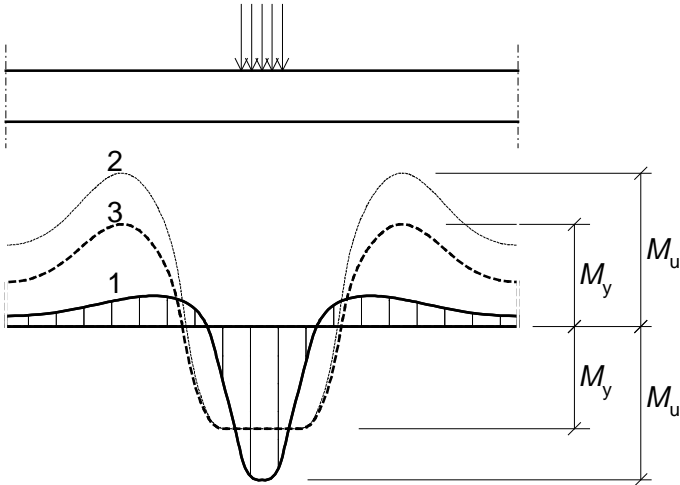
M_u = ultimate moment

M_y = yield moment

Curve 1: elastic analysis

Curve 2: plastic analysis with yield capacity for positive and maximum capacity for negative moment

Curve 3: plastic analysis with yield moment for positive and negative moments



Fibre concrete slabs are sometimes (still) designed in the same way. This gives little or no benefit from the fibres, since the maximum moment capacity does not increase much with the addition of fibres, see figure 3. The effect of fibres is not significant until *after cracking*.¹

¹ The conventional representation of the mechanical properties of fibre concrete is the *flexural stress*, see figure 3, which is a way to express the *moment independently of the cross section depth*. Thus, in describing the behaviour one may use either *moment* or *stress*. This should be remembered if the text may seem inconsistent in this respect.

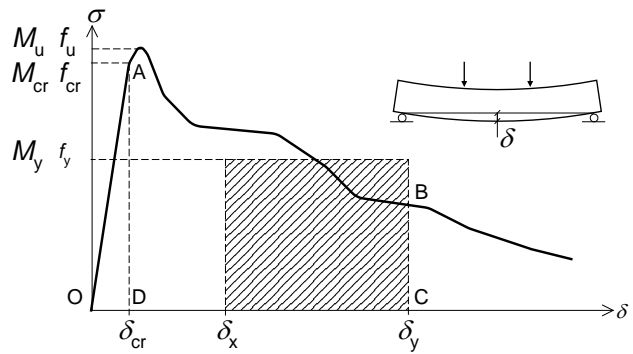
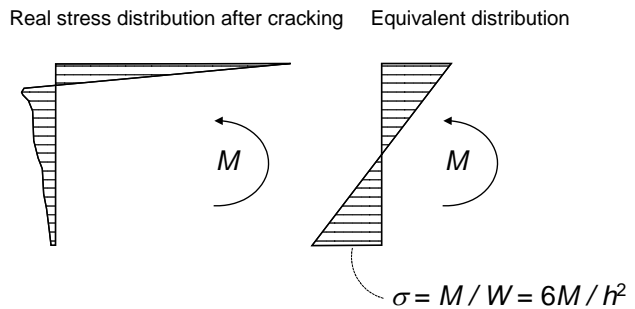


Figure 3.
Typical relationship between load (moment or stress) and deformation (deflection) for a fibre concrete, resulting from a standard flexural test.

After cracking the flexural stress is expressed as an equivalent stress, based on linear distribution.

M_{cr} = cracking moment
 M_u = maximum moment
 M_y = “yield” moment



2. PLASTIC ANALYSIS FOR FIBRE REINFORCED CONCRETE

2.1 General

With fibres a bending moment can be taken even after cracking. The load can be increased beyond “positive” cracking, if there is room for a sufficient increase of the negative moment to compensate for the decrease of positive moment. The load can then be increased until the negative moment reaches the maximum capacity, while the positive moment stays at some “yield” level. See curve 2 in figure 3. In a genuinely plastic approach, a “yield moment” would be assumed in both directions, curve 3, but this would normally give a lower load capacity.

Yield line analysis of the slab together with an elastic model for the subgrade was treated by Losberg [1], and the failure criterion (curve 2 or 3) was also addressed. Reinforced concrete, which is dealt with in [1], has a behaviour suitable for plastic analysis. This is not true for fibre concrete, as can be seen in figure 3. Here, the definition of a “yield moment” and the choice of failure criterion are both more or less open questions.

2.2 Definition of yield moment

For fibre concrete, a fictitious “yield moment” must be defined. It should represent the average moment in yield lines (cracks). One way is to use yield strength = residual strength, by definition the average stress within a certain deformation interval $\delta_x - \delta_y$; see figure 3.

Let A_y be the area OABCD up to deflection δ_y , and A_x corresponding to δ_x . Then
 $f_{res,x,y} = (A_y - A_x) / (\delta_y - \delta_x)$

The areas can be expressed in terms of the toughness index:

$A_x = A_{cr} \cdot I_x$ and $A_y = A_{cr} \cdot I_y$ where A_{cr} is the triangular area OAD up to cracking, $A_{cr} = f_{cr} \cdot \delta_{cr} / 2$

From the definition of toughness index also follows: $\delta_x = \delta_{cr} \cdot (x + 1)/2$, $\delta_y = \delta_{cr} \cdot (y + 1)/2$

Using these expressions, the residual strength can be written, after simplification:

$$f_{res,x,y} = f_{cr} \cdot (I_y - I_x) / (y - x) = f_{cr} \cdot R_{x,y}, \text{ where } R_{x,y} \text{ is the residual strength factor}$$

The deformation interval varies. In Sweden $R_{10,30}$ is often used, corresponding to $5,5 - 15,5 \times \delta_{cr}$. Some countries go from δ_{cr} to a fixed value in mm, e.g. 1,5 or 3 mm. Thus, the residual strength for a given fibre concrete may differ, see figure 4. Comparisons must also consider the size of test beams, which influences the value of δ_{cr} .

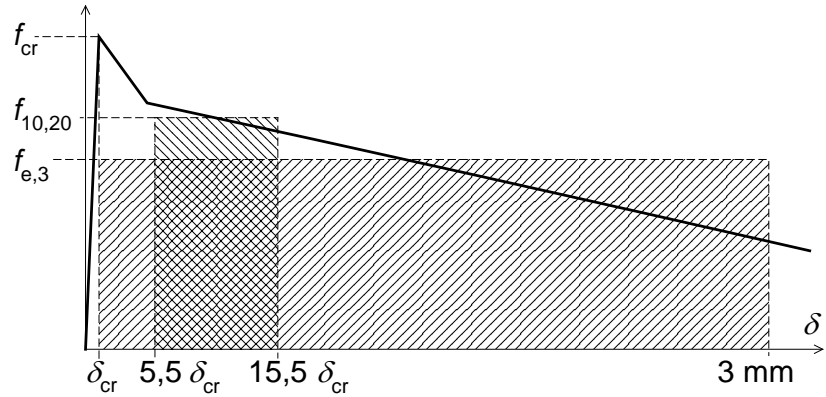


Figure 4. Example of different definitions of residual strength, based on $\delta_{cr} = 0,05 \text{ mm}$.

2.3 Failure criterion

For reinforced concrete slabs on ground, the following failure criteria are proposed in [1]:

1. Reinforcement in one layer: after yielding for positive moment, the slab cracks for negative moments around the load, i.e. cracking moment is used in negative yield lines.
2. Reinforcement in two layers: yield moment in both positive and negative yield lines.

The first case seems to support a failure criterion according to curve 2 in figure 3. However, there are fundamental differences. For reinforced concrete the yield moment is normally *higher* than the cracking moment, but for fibre concrete it is *lower*. Reinforced concrete can have large deformations in the ultimate limit state, whereas the deformation capacity of fibre concrete is limited. Therefore, models developed for reinforced concrete should be applied to fibre concrete with caution. This leads to a recommendation to use the genuinely plastic approach, i.e. curve 3 in figure 3, *yield capacity for both positive and negative moments*.

3. STIFFNESS PARAMETERS

3.1 General

The subgrade is assumed to behave elastically in [1]. Then there are two models, illustrated in figure 5. The choice of model will not be further discussed here; it is usually governed by what type of information is available for the subgrade.

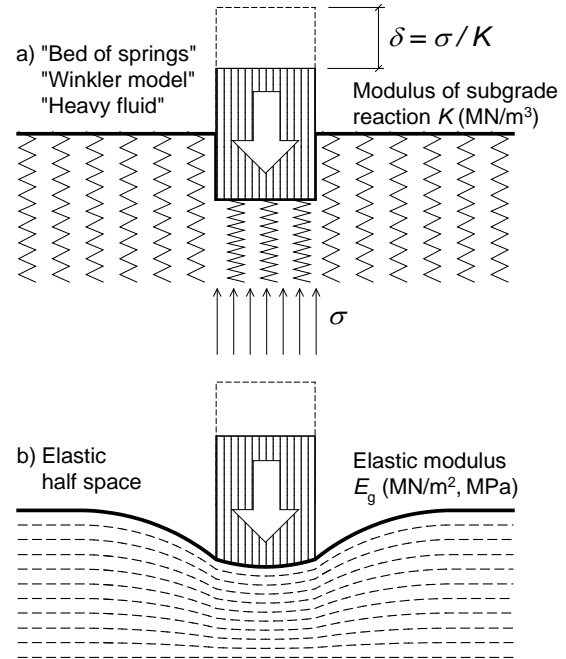


Figure 5.
Alternative models for the subgrade.

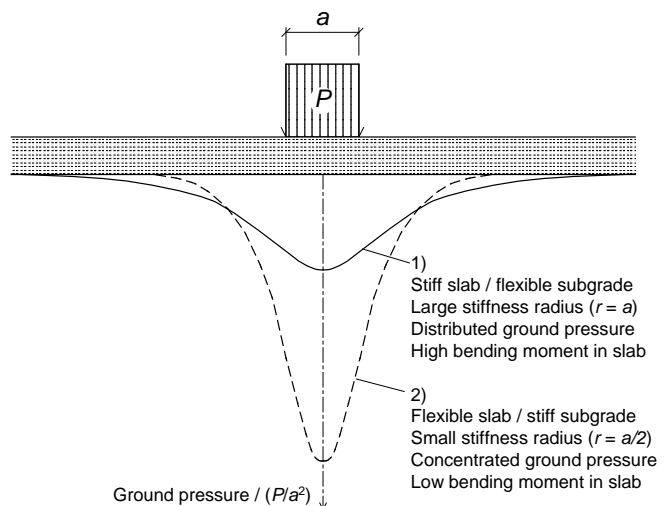
A governing parameter for the bending moment in the slab is the ratio between the stiffness of the slab and that of the subgrade. This ratio is usually expressed in terms of a so-called *stiffness radius*, r ; this is a fictitious length parameter without a direct physical meaning, but with an effect on the bending moment similar to that of a span length. The stiffness radius is

$$r = \sqrt[4]{EI/K} \text{ or } r = \sqrt[3]{1,5 \cdot EI/E_g} \text{ depending on the model (} K \text{ and } E_g \text{, see figure 6; } EI \text{, see 3.2).}$$

The stiffness radius primarily influences the distribution of the ground pressure, which in turn influences the bending moment, figure 6. From this it follows that it is important to define the stiffnesses, both for the subgrade and the slab.

This gives rise to some questions, which are discussed in the following.

Figure 6.
Illustration of the effect of stiffness relations on ground pressure distribution and moments.



3.2 Stiffness of slab

Models for reinforced concrete in [1] are based on slab stiffness for *fully cracked section*. This corresponds to elastic behaviour between cracking and yielding, neglecting any contribution from concrete in tension between cracks (tension stiffening). A low stiffness is favourable, cf. figure 6, which could lead to the conclusion that it is unsafe to ignore tension stiffening. However, on the way to a fully developed yield line pattern, the stiffness in the first yield lines will become *lower* than the assumed value, due to plastic rotations. Therefore, on the whole it is probably safe to use the stiffness for fully cracked section.

For fibre concrete the cracking moment is normally the *highest* moment that can be taken, and there is nothing like a “cracked elastic stage”. Therefore, the *stiffness for uncracked section* is normally used. However, before cracking for negative moment, the stiffness in the positive “yield lines” will be reduced due to rotations beyond cracking. Questions are then:

*Is it unnecessarily conservative to use the stiffness for uncracked section?
Would it be justified to use a somewhat reduced stiffness?*

3.3 Effect of long-term deformations

The effect of long-term deformations is closely related to the above discussion of stiffness. Concrete and most types of subgrade are characterized by time-dependent deformations under sustained load. (For convenience, the term *creep* is used here for both concrete and subgrade.)

The effect of creep on the flexural stiffness of the *slab* is very different for uncracked sections (plain, or with fibres) compared to that of cracked, reinforced sections, see figure 7. The stiffness of the *cracked reinforced section* is not very sensitive to creep, see figure 8. For long-term load, it is then essential to consider creep *at least in the stiffness values for the subgrade*, otherwise the result will be unsafe due to underestimation of bending moments; cf. 3.1.

The stiffness of the *uncracked section* is on the other hand very sensitive to creep. In principle, a creep factor $(1 + \varphi)$ will now appear on *both* sides of the fraction line in the expression for r :

$$r = \sqrt[3]{1,5 \cdot \frac{E_c I_c / (1 + \varphi_c)}{E_g / (1 + \varphi_g)}}$$

If the φ -values do not differ too much they will have little effect on r , and thereby on the bending moment. The important thing is then to use the *same type* of stiffness values for both concrete and subgrade; whether they are long-term or short-term values is less important.

Stiffness values for the subgrade, given in handbooks and codes, are often long-term values intended for calculation of settlements. If they are used in the present application, together with a short-term modulus for the concrete, bending moments will be overestimated, i.e. the error is on the *safe* side. In the opposite case, the error would be on the *unsafe* side. Thus, a warning is due:

Do not combine short-term values for the subgrade with long-term values for concrete.

Cracked section with ordinary reinforcement:

$$EI = E_s A_s (d - x)(d - x/3)$$

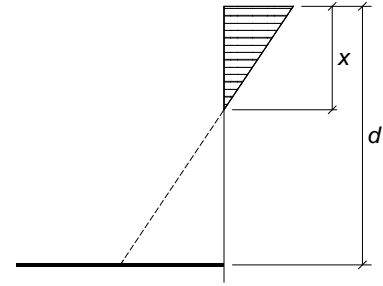
$$= E_s A_s d^2 (1 - \xi)(1 - \xi/3)$$

where $\xi = \alpha\rho(\sqrt{1 + 2/\alpha\rho} - 1)$

$$\alpha\rho = A_s E_s / A_c E_{ef}$$

$$E_{ef} = E_c (1 + \varphi_c)$$

φ_c = creep coefficient for concrete



Uncracked section (with or without fibres):

$$EI = E_{ef} h^3 / 12$$

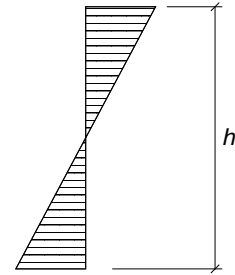
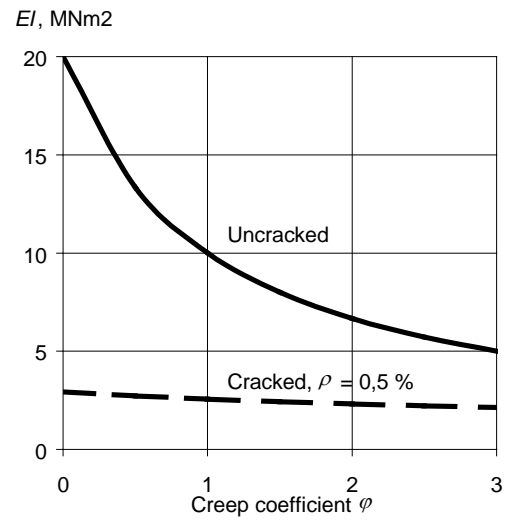


Figure 7. Flexural stiffness of cracked reinforced and uncracked section respectively.

Figure 8.

Example of the effect of creep in a cracked reinforced section and an uncracked section respectively.



4. RESTRAINED IMPOSED DEFORMATIONS

4.1 General

Concrete shrinks and a slab (at least outdoors) can be subjected to temperature changes. These effects cause the slab to move, or at least “try to”, figure 9.

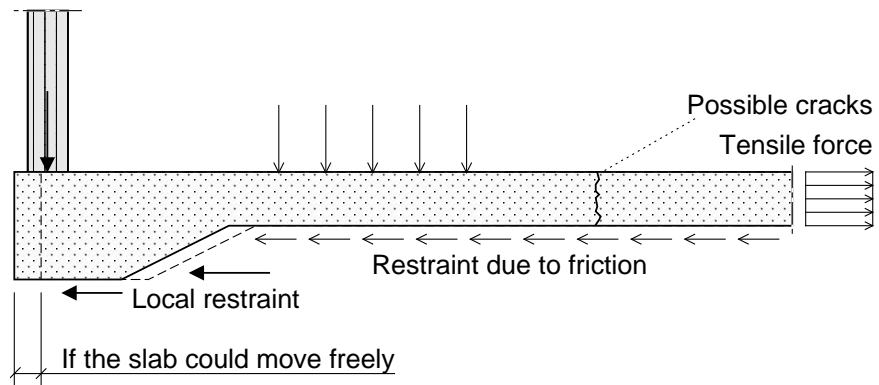


Figure 9.
The effect of imposed deformations.

4.2 Taking into account restraint in design

With elastic analysis (normally used in SLS and in certain cases in ULS), stresses due to restraint are simply added to those due to external load, figure 10.

The total stress should normally not exceed the cracking stress. It can be discussed, however, whether it would be possible to allow some cracking in SLS, and in that case, whether one could use plastic analysis to some extent also in SLS.

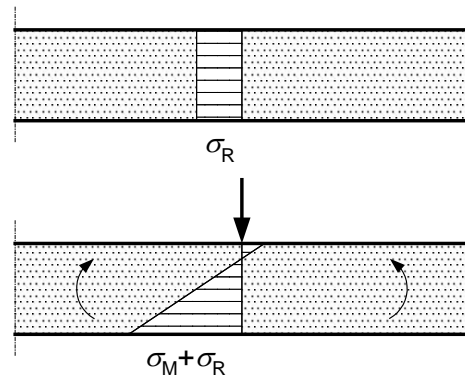


Figure 10. *Stresses due to restraint added to those from bending moment due to external load.*

In ULS design of reinforced concrete, the effect of imposed deformations can be ignored, *if* the increased plastic rotation is covered by the rotation capacity.

A similar approach can be used for fibre concrete in connection with ULS design. Thus, instead of adding stresses from restraint to those from external load, deformations are taken into account, e.g. in the form of increased crack widths, see figure 11.

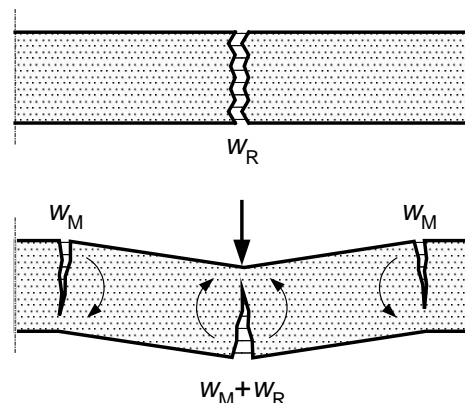


Figure 11. *Crack width from restraint added to that from load.*

This can be done by defining the residual strength for a deformation interval, which includes the effect of *both load and imposed deformation*, cf. figure 12.

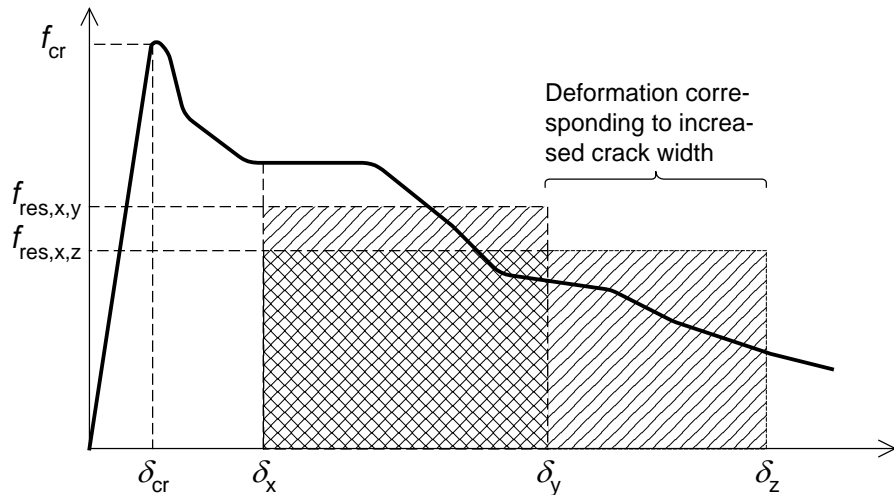


Figure 12.
Increased deformation capacity to cover increased crack width due to imposed deformation.

4.3 Relation between residual strength and crack width

The residual strength can be related to crack widths with a simple model. Consider a test beam with one crack, located in the middle, figure 13:

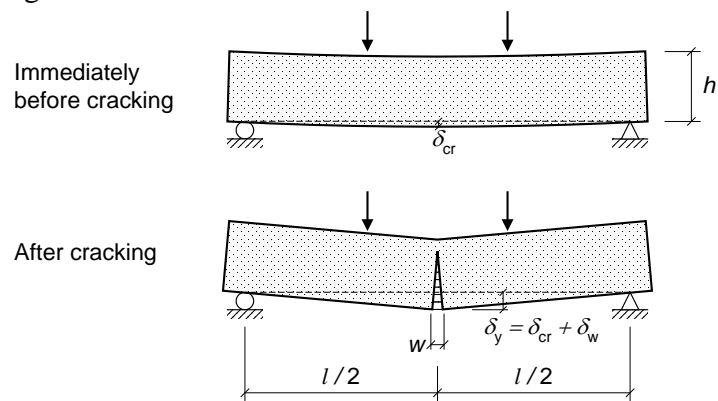


Figure 13.
Deflection and crack opening.

The opening of the crack gives the whole increase of deflection after cracking:

$$\delta_w = w \cdot (l/4h) \quad \text{For test beams often } l/h = 6 \Rightarrow \delta_w = (6/4) \cdot w = 1,5 \cdot w$$

$$\delta_y = \delta_{cr} + \delta_w = \delta_{cr}(y+1)/2 \quad (\text{total deflection; see 2.2}) \Rightarrow y = 1 + 2 \delta_w / \delta_{cr}$$

Certain dimensions and a certain flexural strength will give a certain cracking deflection δ_{cr} . Example: cracking deflection $\delta_{cr} = 0,15 \text{ mm} \Rightarrow y = 1 + 2 \cdot 1,5 \cdot w / 0,15 = 1 + 20 w$.

Thus, a residual strength based on $R_{10,20}$ would cover a crack width $w \approx 1 \text{ mm}$. To cover 2 mm, e.g. to include an imposed deformation, $R_{10,40}$ should be used. However, these figures are only examples, based on $\delta_{cr} = 0,15 \text{ mm}$. Other beam sizes and/or concrete strengths will give other values. Example: if $\delta_{cr} = 0,05 \text{ mm}$, $R_{10,20}$ would cover only $w = 0,3 \text{ mm}$. Different beam sizes are used in different standards, and test beams do not always represent the dimensions of a slab. Therefore, this model is, although logical and simple, to some extent built on sand.

5. PUNCHING

For reinforced concrete, design is based on a nominal shear stress in a cylindrical control section at a certain distance outside the loaded area. In e.g. the Swedish code this distance is $d/2$ (d is effective depth), and the nominal shear strength is 1,5 times that in “ordinary shear”. In EC2 (prEN-version), the distance is $2d$ but the shear strength is the same as in ordinary shear. Neither model has anything to do with the real mechanisms of failure, but both are claimed to give good agreement with test results, of which large amount exists.

There are few test results for fibre concrete, and the failure mechanism can be different. Despite this, and in the absence of better alternatives, models for reinforced concrete are often used. A model based on the Swedish code for reinforced concrete will be described as an example of this; see figure 14. With the control perimeter at distance $h/2$, the punching load can be written

$$P_u = h \cdot u \cdot f_{pd} + A_p \cdot p = 2\pi c \cdot h \cdot f_{pd} + \pi c^2 \cdot p$$

where

- p average ground pressure within A_p
- f_{pd} punching strength $\approx k \cdot 0,45 \cdot f_t / \gamma_M$
- f_t axial tensile strength $\approx 0,6 \cdot f_{cr}$
- f_{cr} flexural strength

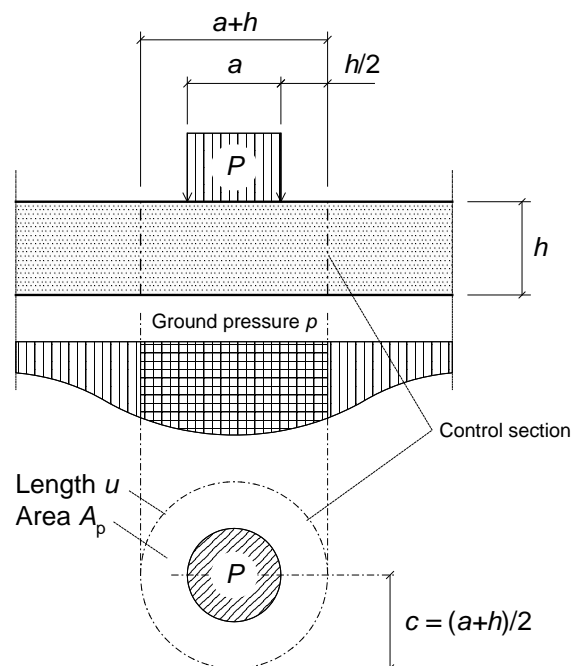
$$k = 1,4$$

The punching stress becomes

$$f_{pd} = 1,4 \cdot 0,45 \cdot 0,6 \cdot f_{cr} / \gamma_M \approx 0,4 \cdot f_{cr} / \gamma_M$$

Figure 14.

Example of model for punching design, based on the Swedish code for reinforced concrete.



The models in [1] include the pressure distribution under the slab, but based on *flexural failure*, with a corresponding (large) deflection. In punching the deflection prior to failure is much less, and so is the ground pressure. On the other hand, a high pressure may be compensated by a small area; the “real” area is probably much larger than the area within control perimeter $h/2$.

Figure 15 illustrates some of the uncertainties related to punching.

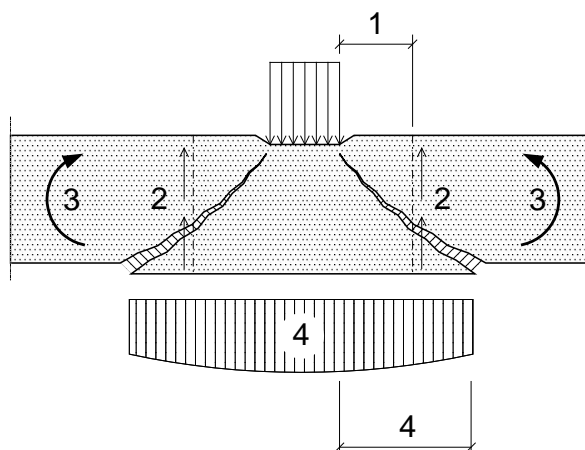


Figure 15.

Uncertainties related to punching design of fibre concrete slabs on ground.

1. Location of control section?
2. Shear strength in control section?
3. Effect of bending moment?
4. Effect of ground pressure?

Some of the questions around punching may be answered in a research project at KTH (see separate contribution to this seminar by Ulf Nilsson). However, ground pressure is not relevant in that project and this question will therefore remain on the table.

6. DOME ACTION

Tests to study the applicability of yield line theory are reported in [3] (without elastic subgrade). Load capacities were found to be high above those predicted by the theory, and fibres made little difference. This is attributed to *dome action*, possible by axial restraint along the periphery of slabs and activated by rotation of parts between cracks, see figure 16. The effect is similar to that of reinforcement, but in the case of external restraint, the lever arm z is reduced with increasing deflection; this is not the case with reinforcement.

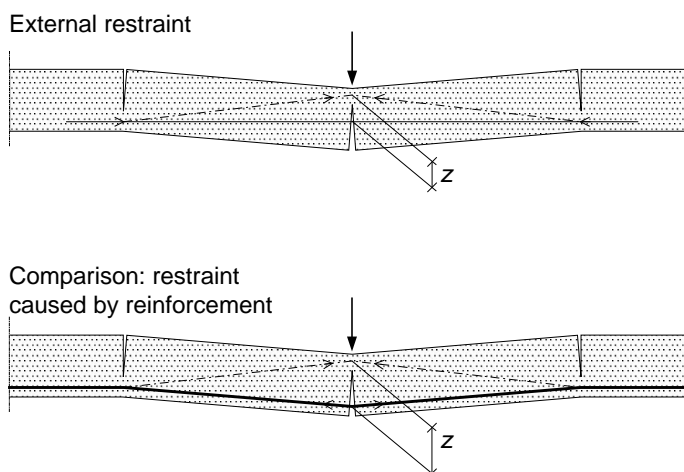


Figure 16.

Illustration of dome action.

The following is worth noticing

- In [3] there was a considerable dome effect even in thin slabs (30-40 mm)
- Slabs on ground are usually much thicker, e.g. 100-200 mm
- Good possibilities for restraint in slabs on ground can be expected, at least for interior loads

The following questions arise:

- *Is flexural design at all relevant for interior loads on slabs on ground?*
- *Will instead punching be the governing criterion?*

REFERENCES

- [1] Losberg A: “Design methods for structurally reinforced concrete pavements”. *Transactions of Chalmers University of Technology*. Gothenburg 1961
- [2] Svenska Betongföreningen (Swedish Concrete Association): “Stålfiberbetong – rekommendationer för konstruktion, utförande och provning” (Steel fibre concrete – recommendations for design, execution and testing). *Betongrapport nr 4*, utgåva 2, 1997
- [3] Nilsson U: “Load bearing capacity of steel fibre reinforced shotcrete linings”. *Royal Institute of Technology, Department of Structural Engineering, Bulletin 56*, 2000.

Improvements of the Swedish Concrete Association's Method for Design of SFRC Slabs on Grade



Prof. J. Silfwerbrand, Ph.D.
johan.silfwerbrand@struct.kth.se

Royal Institute of Technology (KTH)
Dept. of Structural Engineering
SE-100 44 Stockholm, Sweden

ABSTRACT

The use of steel fibres in concrete slabs on grade has several advantages over conventional welded fabrics: (i) absence of labour intensive reinforcement work, (ii) a reinforcement type that is less sensitive to construction variations, and (iii) a probable improvement of shrinkage crack control. The Swedish Concrete Association developed design guidelines in 1995. They are summarised here. The guidelines deal mainly with flexural loading. Additional details on the estimation of the degree of restraint to shrinkage movements are given in this paper. This paper describes also how to handle punching loads.

Key words: SFRC, slabs on grade, flexure, punching, restraint loading, design.

1. INTRODUCTION

The use of steel fibre reinforcement has increased in concrete slabs on grade, especially in industrial floors. By choosing steel fibre reinforcement instead of conventional reinforcement, it is possible to save the labour-intensive and expensive reinforcing work. Most likely, the use of steel fibre reinforced concrete (SFRC) slabs on grade would increase further if reliable, approved, and simple design methods were available. In traditional design methods for slabs on grade, the estimation of mechanical stresses, e.g., truck traffic stresses, is fairly good, whereas stresses due to restrained shrinkage or thermal movements are either neglected or considered very roughly. This might be acceptable for conventionally reinforced slabs with sufficient reinforcement area and large ductility, but will not be suitable for SFRC slabs.

The international engineering society has not established any design methods for SFRC slabs on grade yet, but several design proposals exist, see, e.g., *Falkner et al.* [1], *Bischoff & Valsangkar* [2], and *Skarendahl & Westerberg* [3]. Most of these proposals deal solely with mechanical loading. *Bischoff & Valsangkar* discern between two design approaches: (i) providing the slab with a minimum reinforcement sufficient to carry the mechanical load after cracking and (ii) ensuring that the slab does not crack under the combined action of mechanical load and restraint load. A similar approach was used by the *Swedish Concrete Association* in 1995 [4]. It will be described briefly below.

Traditional design methods for slabs on grade cover the flexural failure due to mechanical loading, e.g., truck traffic, in a fairly straightforward way, whereas the punching failure is either neglected or considered very roughly. For large concentrated loads, e.g., stacked containers supported by small feet, the punching load may constitute the design load. In this paper, a method on punching design of SFRC slabs on grade is described. It has recently been used for developing design charts for industrial SFRC pavements, see *Silfwerbrand* [5].

2. THE SWEDISH DESIGN PHILOSOPHY

The Swedish design method for SFRC slabs on grade was established by the *Swedish Concrete Association* in 1995 [4]. The method covers both ultimate limit state and serviceability limit state. For the ultimate limit state, the designer might select either the uncracked or the cracked state (Figure 1). In the uncracked state, the concrete slab has to carry both external loads and restraining loads. In the cracked state, it only needs to carry external loads. The ductility of the SFRC is assumed to contain any effects of restraint. This assumption is an adoption of *Losberg’s* statement concerning reinforced concrete pavements: “...temperature and shrinkage do not influence the ... ultimate moment...” [6]. *Losberg’s* explanation is that stresses caused by temperature and shrinkage (restraint stresses) disappear as soon as the reinforcement stress has reached the yield point (i.e., after cracking). It is obvious that SFRC with sufficient ductility can be treated in a similar way. Experimental evidence for this statement has been provided by tests by *Alavizadeh-Farhang* [7].

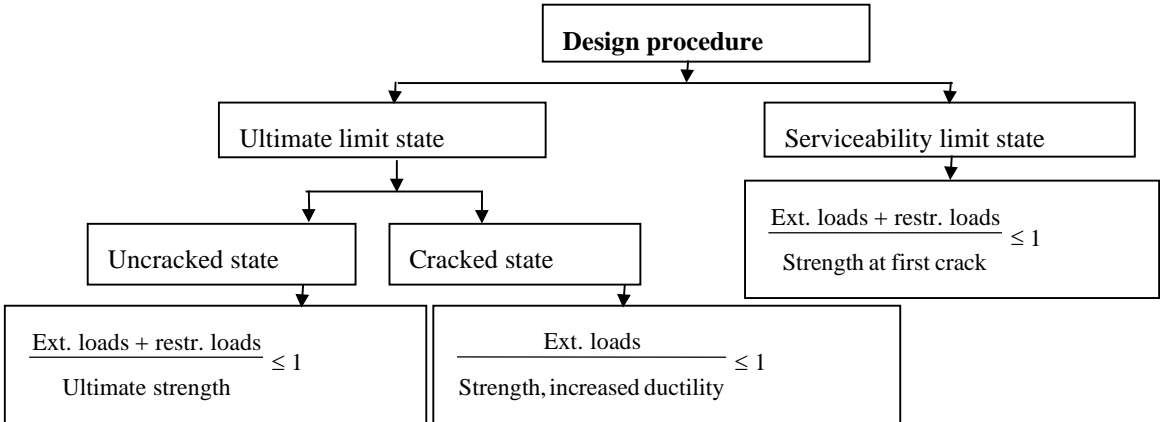


Figure 1 – Design procedure according to the Swedish Concrete Association [4].

3. FLEXURAL DESIGN

3.1 Loads and Stresses

Slabs on grade are subjected to external loads from, e.g., lorries and fork-lift trucks and from the storage of goods. Restraining loads may originate from restrained thermal or shrinkage movements. Most industrial floors have a fairly constant indoor climate. For such slabs, concentrated loads and loads due to restrained shrinkage are the most important ones.

For the uncracked state, the stresses due to concentrated loads could either be computed by using Westergaard's theory of elastic slab on a dense liquid (resilient or Winkler) foundation or the theory of a multi-layered elastic half-space. It is without the scope of this paper to report the comprehensive research that has been devoted to this area.

For the uncracked state, the tensile stress σ_t due to restrained shrinkage (for simplicity: called shrinkage stress below) may be computed by the following simple equation:

$$\sigma_t = \psi \cdot \frac{E \varepsilon_{cs}}{1 + \phi} \quad (1)$$

where, ψ = degree of restraint ($0 \leq \psi \leq 1$), E = modulus of elasticity of the concrete slab, ε_{cs} = free concrete shrinkage, ϕ = concrete creep coefficient.

Eq. (1) is valid for the uniform shrinkage distribution. In reality, the shrinkage distribution is non-uniform with higher values at the top than at the bottom due to drying mainly upwards. The uniform assumption is, however, conservative and is therefore used for simplicity.

The degree of restraint ψ vanishes if the slab may shrink completely freely and equals unity for complete restraint. It is fairly difficult to determine. It is, however, known to be dependent on the following factors:

1. Slab length or distance between joints
2. Slab thickness
3. Distributed load in addition to the dead load of the slab
4. Friction between slab and subgrade
5. Presence of haunches or tapered cross section
6. Locking or bond to adjacent structures or construction elements

Haunches and locking to adjacent structures, e.g., walls, columns, foundations, previously cast floor slabs, should be avoided. If so, the degree of restraint is mainly dependent on the friction and the ratio between slab size and slab thickness. Based on the *Swedish Concrete Association* [4], the following simplified table may be used to roughly estimate the degree of restraint:

Table 1 – Estimation of the degree of restraint ψ at slab centre

Subgrade	Ratio between slab length (joint spacing) and slab thickness, L/h				
	10	20	30	50	> 100
Even subgrade + two sheets of cling film	0.05	0.15	0.25	0.5	1
Compacted gravel	0.1	0.3	0.5	1	1
Macadam without levelling	0.2	0.6	1	1	1

These values are valid in the interior parts of the slab. At free slab edges and undowelled joints, there is no restraint against the shrinkage, i.e., the degree of restraint vanishes (Figure 2).

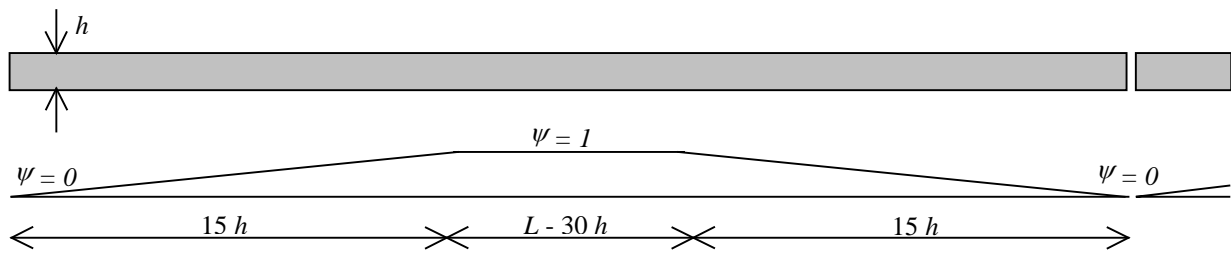


Figure 2 – The degree of restraint ψ may be assumed to vary linearly from $\psi = 0$ at slab edges or undowelled joints and $\psi = 1$ in an interior part. The figure shows an example of a concrete slab resting on macadam without levelling.

Recently, a new production method has been developed making it possible to reduce the degree of restraint further. It uses evenly spaced airbag lifting the slab temporarily during the first couple of weeks after casting and initial curing enabling free shrinkage and bilateral drying, see *Silfwerbrand & Paulsson* [8].

For the cracked state, the yield line theory is used. Consequently, it is not meaningful to compute stresses. Instead, design load is compared with the load carrying capacity discussed in the following subsection.

3.2 Material Strength and Load Carrying Capacity

The material strength is evaluated through flexural tests on beam specimens. According to the *Swedish Concrete Association* [4], the beam is tested in four point bending (Figure 3). Recommended measures are beam height $h = 75$ mm, beam width $b = 125$ mm, and span length $l = 6h = 450$ mm.

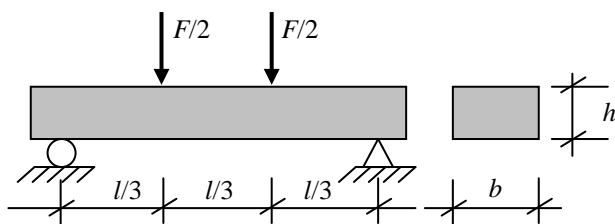


Figure 3 – Beam tests according to the Swedish Concrete Association [4].

From the relationship between computed maximum flexural stress at midspan and midspan deflection δ , the following three strength measures are derived:

- First crack strength f_{flcr}
- Ultimate strength f_{flu}
- Residual strength f_{flres}

Characteristic strength values can either be determined by testing several beams and using statistics or estimated by testing three beams and defining the characteristic value as 90 % of

the lowest value. Design values for flexural and tensile strength may subsequently be determined by using the following table:

Table 2 – Design values for flexural f_{fl} and tensile strength f_t

	Ultimate limit state		Serviceability limit state
	Uncracked state	Cracked state	Uncracked state
Flexural strength f_{fl}	$\frac{f_{fluk}}{\eta \cdot \gamma_m \cdot \gamma_n}$	$\frac{f_{flresk}}{\eta \cdot \gamma_m \cdot \gamma_n}$	f_{flcrk}
Tensile strength f_t	$0.6 \cdot \frac{f_{flcrk}}{\eta \cdot \gamma_m \cdot \gamma_n}$	$0.37 \cdot \frac{f_{flresk}}{\eta \cdot \gamma_m \cdot \gamma_n}$	$0.6 \cdot f_{flcrk}$

Note. For slabs on grade, the partial coefficient for material $\eta \cdot \gamma_m = 1.2$ and the partial coefficient for security class $\gamma_n = 1.0$. The coefficient 0.6 is based on unpublished Finnish test results and the coefficient 0.37 is based on a theoretical discussion in DBV [9].

As stated above, design loads are to be compared directly with the load carrying capacity in the cracked state. *Losberg* applied the yield line theory on concrete slabs (pavements) on both a resilient foundation and an elastic half-space [6]. The load carrying capacity F could be given by the following principal function:

$$F = g(m, m', a/l) \quad (2)$$

where, g is a function, m and m' are the ultimate bending moment per unit width for positive (slab bottom) and negative (top) yield lines, respectively, a is the radius of the loaded circular area, and l is the radius of relative stiffness defined as follows:

$$l = \sqrt[4]{D/k} \quad (3)$$

where, $D = Eh^3/[12(1-\nu^2)]$ is the flexural rigidity of the slab and k the modulus of subgrade reaction. In a homogeneous SFRC slab, there is no difference between the ultimate moments in bottom and top, hence

$$m = m' = \frac{f_{fl} h^2}{6} \quad (4)$$

where, f_{fl} is the design value of the flexural strength according to Table 2.

Losberg [6] presents solution to several loading cases, e.g., interior, edge, and corner loading for single and twin wheels.

3.3 Design Criteria for Ultimate Limit State

For the uncracked state, the following two design criteria should be fulfilled:

$$\frac{\sigma_{fl}}{f_{fl}} + \frac{\sigma_t}{f_t} \leq 1 \quad (5)$$

$$1.3 \cdot \frac{\sigma_{fl}}{f_{fl}} \leq 1 \quad (6)$$

where, σ_{fl} is the flexural stress due to external load, σ_t is the tensile stress due to restrained shrinkage, and f_{fl} and f_t are the design values of the flexural and tensile strength according to Table 2, respectively.

For the cracked state, the following design criteria should be fulfilled:

$$1.3 \cdot \frac{P}{F} \leq 1 \quad (7)$$

where, P is the design value of the external load and F is the design value of the load carrying capacity according to Eq. (2). Any effect of restraint, e.g., restrained shrinkage, should be regarded by increasing the ductility demand when using the residual strength f_{flres} for computing flexural strength f_{fl} , ultimate moment m , and load carrying capacity F .

4. PUNCHING SHEAR DESIGN

4.1 Derivation of the failure load

If a small area, e.g., a small square with side length b , of a slab on grade is loaded by a large concentrated force F , there is a risk for a punching shear failure. A frustum of a cone is assumed to be punched out of the slab. The slope between the envelope surface and the slab plane is assumed to be 45° . It means that only a tensile stress σ acts in the failure surface. At failure, $\sigma = f_v$, where f_v is the shear strength of the concrete slab.

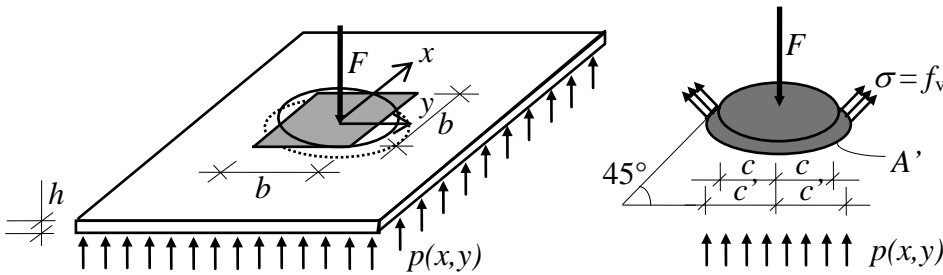


Figure 4 – Assumed failure mode at punching shear failure.

Vertical force equilibrium for the frustum leads to the following equation:

$$F = \frac{1}{\sqrt{2}} f_v \cdot 2\pi(c + h/2)\sqrt{2} \cdot h + \iint_{A'} p(x, y) dx dy \quad (8)$$

or

$$F = \frac{2\pi \cdot f_v \left(1 + \frac{h}{2c}\right) ch}{1 - Q'/F} \quad (9)$$

where,

- c = radius of a circle with equal perimeter as the loaded square, i.e., $c = 2b/\pi$
- h = slab thickness
- A' = area of the bottom side of the frustum, $A' = \pi(c')^2$
- c' = radius of the bottom side of the frustum, $c' = c + h$
- Q' = $\iint_{A'} p(x, y) dx dy$ = resultant to the subgrade reaction within the area A' (For simplification, Q' may be approximated as the resultant to the subgrade reaction within a centrally located square with side length $b' = \sqrt{\pi \cdot c'}$.)

In many practical cases, the ratio Q'/F is so small that the denominator in Eq. (9) might be put to unity. However, for small slabs, the subgrade reaction on the bottom side of the frustum might have a considerable influence on the failure load. In these cases, the distribution of the subgrade reaction needs to be estimated.

4.2 Estimation of the shear strength of concrete

According to Eq. (9), there is a linear relationship between the failure load F and the shear strength of concrete, f_v . Since the shear strength is impossible to measure directly, it has to be derived from other properties. Even the existence of a shear strength is questioned. However, it is often used in design. The *Swedish Concrete Association* [4] proposed the following relationships between shear strength, pure tensile strength f_{ct} , and flexural strength f_{cfl} :

$$f_v = \xi \cdot 0.45 \cdot f_{ct} \quad (10)$$

where,

$$\begin{aligned} \xi &= 1.4 \text{ if } h \leq 0.2 \text{ m} \\ \xi &= 1.6 - h(\text{m}) \text{ if } 0.2 \text{ m} < h \leq 0.5 \text{ m} \\ \xi &= 1.3 - 0.4 \cdot h(\text{m}) \text{ if } 0.5 \text{ m} < h \leq 1.0 \text{ m} \\ \xi &= 0.9 \text{ if } h > 1.0 \text{ m} \end{aligned} \quad (11)$$

and

$$f_{ct} = 0.37 \cdot f_{cfl} \quad (12)$$

Eq. (10) is originally based on a relationship for RC slabs in the *Swedish Handbook for Concrete Structures* (BBK 94) [10] and Eq. (12) is adopted from *DBV* [9]. The flexural strength is a residual strength considering the load carrying capacity after cracking. Eqs. (10) and (12) lead to a fairly low shear strength. Consider a SFRC slab with $h = 0.2$ m, fibre content = 40 kg/m³, flexural strength at cracking = 5.0 MPa. The residual flexural strength might be 60 % of

the cracking strength or 3.0 MPa, $f_{ct} = 1.11$ MPa, and $f_v = 0.70$ MPa or only 14 % of the flexural strength at cracking. Are such values likely to be representative in a real case? Available test results in the literature show that such low shear strength values are too far on the conservative side.

4.3 Proposed Design Method

Based on the test results reported by *Westin et al.* [11], *Beckett & Humphreys* [12], *Beckett* [13], *Falkner & Teutsch* [14], and *Barros & Figueiras* [15] evaluated in *Silfwerbrand* [16] and the *Swedish Concrete Association's* guidelines [4], the following design equations are proposed:

$$F_d = \frac{2\pi \cdot f_{vd} \left(1 + \frac{h}{2c}\right) ch}{1 - Q'/F_d} \quad (13)$$

where, F_d = design load and f_{vd} = design value of the shear strength according to

$$f_{vd} = \frac{C \cdot f_{cfl}}{\zeta \cdot \eta \gamma_m \cdot \gamma_n} \cdot \frac{\xi}{1,4} \quad (14)$$

where, $C = 0.45$, $\eta \gamma_m$ = partial coefficient for material uncertainties (often $\eta \gamma_m = 1.2$), γ_n = partial coefficient for security class ($\gamma_n = 1.0$ for slabs on grade), ξ = factor dependent on slab thickness according to Eq. (11) and ζ = crack security coefficient, given by

$$\zeta = 2 - R/100 \quad (15)$$

where, R = residual strength factor (in %) defined as ratio between the average load carrying capacity between certain displacements after cracking and the load at first crack for a standard test beam loaded in four point bending, see [4]. Unfortunately, the residual strength factor was not measured in the referred tests. However, it has been experimentally found that for common concrete strength values, common fibre types, and common fibre contents one may use $R = 0$ for $\rho = 0$ and R (%) = ρ (kg/m³) + 20 for $\rho > 15$ kg/m³. This has been done here. The relationship between design loads and observed failure loads (Figure 5) is fairly good.

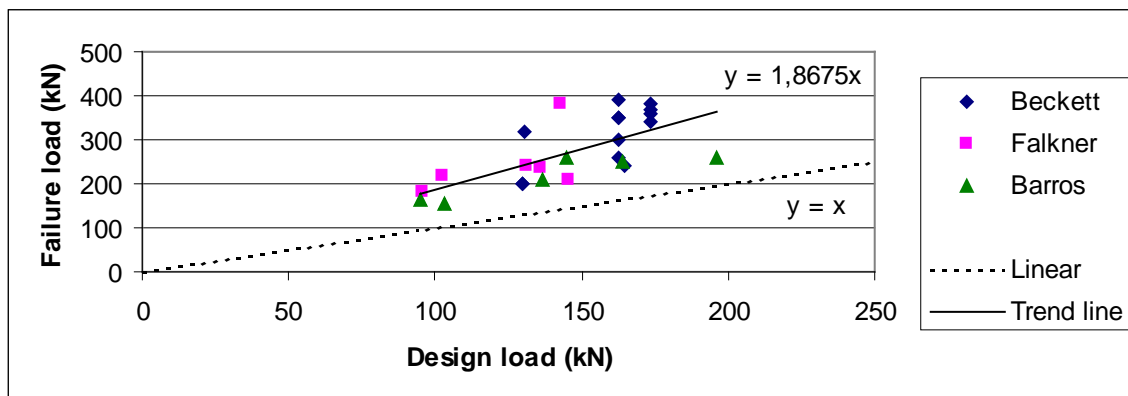


Figure 5 – Relationship between design loads and observed punching failure loads.

CONCLUDING REMARKS

SFRC slabs on grade have several advantages over both RC slabs and jointed plain concrete slabs on grade. According to the *Swedish Concrete Association's* design method for SFRC slabs on grade, the designer has two options, either for the uncracked state or for the cracked state. Swedish tests show that thermally precracked SFRC structures have a considerable load carrying capacity. For the uncracked state, restraint stresses have to be superposed the mechanical stresses. The designer might, however, consider the beneficial circumstance that the highest mechanical stresses arise in slab parts (edges, corners) where the restraint stresses vanish.

The risk of punching failures must be considered in cases with heavy concentrated loads. The paper proposes a design method for this loading case. Comparisons with test results presented in the literature show a decent agreement between the computed loads and obtained failure loads.

REFERENCES

1. Falkner, H., Huang, Z., & Teutsch, "Comparative Study of Plain and Steel Fibre Reinforced Concrete Ground Slabs", *Concrete International*, Vol. 17, No. 1, January 1995, pp. 45-51.
2. Bischoff, P.H., & Valsangkar, A.J., "Assessment of Slab-on-Grade Design and Comparison with Model Slab Behaviour", *Proceedings*, 4th International Colloquium on Industrial Floors, Ostfildern, Germany, January 1999, Vol. I, pp. 153-158.
3. Skarendahl, Å., & Westerberg, B., "Guide for Designing Fibre Concrete Floors", *CBI Report 1:89*, Swedish Cement and Concrete Research Institute, Stockholm, Sweden, 1989. (In Swedish).
4. Swedish Concrete Association, "Steel Fibre Reinforced Concrete – Recommendations for Design, Construction, and Testing", *Concrete Report* No. 4, 2nd Edn, Stockholm, Sweden, 1997. (In Swedish).
5. Silfwerbrand, J., "Design of Industrial Concrete Pavements" (Preliminary title), *Report*, Dept. of Structural Engineering, Royal Institute of Technology, Stockholm, Sweden, 2001. (In Swedish).
6. Losberg, A., "Design Methods for Structurally Reinforced Concrete Pavements", *Bulletin* No. 250, Chalmers University of Technology, Göteborg, Sweden, 1961, 143 pp.
7. Alavizadeh-Farhang, A., "Concrete Structures Subjected to Combined Mechanical and Thermal Loading". *Bulletin* No. 60 (*Ph.D. Thesis*), Dept. of Structural Engineering, Royal Institute of Technology, Stockholm, Sweden, 294 pp.
8. Silfwerbrand, J., & Paulsson-Tralla, J., "Reducing Shrinkage Cracking and Curling in Slabs on Grade". *Concrete International*, Vol. 22, No. 1, January 2000, pp. 69-72.
9. DBV. "Technology of Steel Fibre Reinforced Concrete and Steel Fibre Reinforced Shotcrete", Deutscher Beton-Verein (German Concrete Society) E.V. DBV-Merkblätter Faserbeton, Fassung, 1992. (In German).
10. BBK 94. Swedish Board of Housing, Building and Planning, "Handbook for Concrete Structures", Karlskrona, Sweden, 1994, 185 pp. (In Swedish).
11. Westin, I., Petersson, Ö., & Nordin, A., "Steel Fibre Reinforced Industrial Floors", *CBI Report* No. 6:92, Swedish Cement and Concrete Research Institute, Stockholm, Sweden, 1993, 55 pp. (In Swedish).
12. Beckett, D., & Humphreys, J., "Comparative Tests on Plain, Fabric Reinforced & Steel Fibre Reinforced Concrete Ground Slabs". *Report* No. TP/B/1, Thames Polytechnic, School of Civil Engineering, Dartford, Kent, UK, 1989.
13. Beckett, D., "A Comparison of Thickness Design Methods for Concrete Industrial Ground Floors". *Proceedings*, 4th International Colloquium on Industrial Floors, Ostfildern, Germany, January 1999, Vol. I, pp. 159-170.
14. Falkner, H., & Teutsch, M., "Comparative Investigations of Plain and Steel Fiber Reinforced Industrial Ground Slabs". *Report* No. 102, Institute for Building Materials, Concrete Structures and Fire Protection, Technical University of Brunswick, Brunswick, Germany, 1993, 70 pp.

15. Barros, J.A.O., & Figueiras, J.A., "Experimental Behaviour of Fibre Concrete Slabs on Soil", *Mechanics of Cohesive-Frictional Materials*, Vol. 3, No. 3, July 1998, pp. 277-290.
16. Silfwerbrand, J., "Punching Shear Capacity of SFRC Slabs on Grade". Proceedings, International Workshop on Punching Shear Capacity of RC Slabs, Dept. of Structural Engineering, Royal Institute of Technology (Bulletin No. 57), Stockholm, June 2000, pp. 485-493.

Competitive Concrete Solutions for Industrial and Residential Buildings



Tor K. Sandaker
M.Sc.
e-mail: tk@norconsult.no

Norconsult AS
Vestfjordgaten 4
1338 Sandvika
Norway

Author of chapter 5:
M. Sc. Arne Vatnar, Norcem AS, FoU
e-mail: arne.vatnar@norcem.no

Author of chapter 6:
M. Sc. Øyvind Bjøntegaard, post doc, NTNU
e-mail: oyvind.bjontegaard@bygg.ntnu.no ,

ABSTRACT

Within the ongoing research project 'Competitive concrete solutions for industrial- and residential buildings', a main goal is to establish a design guide for fibre reinforced concrete floors applicable for the Norwegian market. Up till now, such a publication has not been performed in this country, even though the method has been practiced for a long period. Due to the economical limitations within the project, the work has been limited to a literature study where the authors have tried to summarize the calculation methods used in different countries establishing a design guide applicable for the Norwegian market.

In addition to be a design guide, the publication will contain advices and experience related to practical execution of typical fibre reinforced concrete floors.

Key words: fibre reinforced concrete floors, design guide, competitive concrete solutions

1 INTRODUCTION

In 1998 Norcem performed a study about the customers and clients view on the concrete line challenge in the future. Two main aspects were found and performed the main supposition for an application to the Research Council of Norway in the autumn of 1998:

- There is a too big gap between the research activities and the viewable practical utility
- Focus within concrete research should be concentrated to practical use in typical buildings

The main goal for the initial application was defined:

To develop the concrete material and systems for concrete solutions with respect to improved competitive strength through election of solutions in future industrial- and residential buildings

The main aspect was to develop concrete solutions to take care of coming requirements to environment, aesthetics and effective execution. The following activities were defined:

- DP1: Self compacting concrete
- DP2: Environment and aesthetics
- DP3: Concrete floors

Norcem AS performed the project administration. The research and development activities in laboratory should be done at Norcem and Sintef/NTNU. All the participants were obligated to contribute partly to the project through cash or by self-work. The project was started in 1999 and will end within 2001.

Within the DP3 group it was decided to concentrate the research to the following different aspects:

Shrinkage and curl
RH-measurements
Design with respect to humidity
Subgrade friction
On-site experiments related to construction
Design guide for fibre reinforced concrete floors

It was decided within the DP3 project to derive a design guide related to fibre reinforced concrete floors. The main goal was to develop a publication named 'Philosophy and design guide to fibre reinforced concrete floors'.

Within the DP3 partial project, the following departments and companies contributes:

Norcem

Norwegian Public Road Administration
Selmer Skanska (previous Selmer)
Skedsmo betong
Norbetong
Unicon (previous Stange betong)
Scancem Chemicals
Veidekke ASA
SINTEF
Tiller Vimek AS
Norconsult AS

So far 11 project meetings has been held in the DP3 group in addition to 2 information seminars for the entire project. The group performing the publication related to the 'Fibre reinforced concrete floor' has met in typical working groups in a tight relation.

In total, the estimate of cost for entire project is about 8-10 mill. NOK. The dispose of the partial project DP3 is about 5 mill. NOK.

2 DESIGN GUIDE TO FIBRE REINFORCED CONCRETE FLOORS

The main aspect has been to develop a design guide applicable for use when designing a concrete floor including fibre reinforcement. Up till now, such a publication has not been performed in this country, even though the method has been practiced for a long period. In design, engineers have used recommendations given by the fibre fabricators and suppliers. Standards and design guides have been available from other countries; a common Norwegian guide has therefore been requested for a period of time.

The following design guides and specifications have mainly been used when performing the document:

ASTM C1018, Standard Test Method for Flexural Toughness and First-Crack Strength of Fibre-Reinforced Concrete, 1992.

Cement och Betong Institutet, CBI rapport nr. 1:89, Åke Skarendahl og Bo Westerberg,Handledning för dimensjonering av fiberbetonggolv, Stockholm 1989.

Svenska Betongföreningen, Betongrapport nr. 4, Stålfiberbetong, rekommendationer för konstruksjon, utförande och provning, 1997

Concrete Society, Technical report 34, Concrete Industrial Ground Floors, - A guide to their design and construction, second edition 1994.

NS 3473 Concrete structures, Design rules, 5th edition, Nov. 1998

2.1 Partial coefficient method

Typical Norwegian design guides follows the partial coefficient method utilizing material factors and load coefficients. The authors have tried to establish a calculation method following

these principles based on the limit state consideration in design. The design method is therefore performed considering the requirements in the following limit states:

- serviceability limit state
- ultimate limit state

Accidental limit state and fatigue limit state have not been considered due to economical limitations within the project.

Following these principles, the authors have tried to evaluate different well known calculation methods to fit into the partial coefficient method related to an un-reinforced concrete floor (ordinary longitudinal reinforcement bars are not used). The following simple consideration derived:

Serviceability limit state:	Design based on elasticity theory
Ultimate limit state:	Design based on yield line theory

The yield or first cracking load under a typical out-of-plane load can be determined from elastic theory, while the ultimate load-carrying capacity is established from plastic theory. As concluded in [1], this proposed method of analysis is in fair agreement with field observations on plain and reinforced concrete.

2.2 Calculation according to elastic theory

The classical calculation formulas for a typical concrete floor are based on work performed by Westergaard in the 1920's. S.P. Timoshenko modified the theory. In the calculation of the elastic formulas, the uncracked stiffness of the plate is used. The capacity of the concrete section is defined, based on the assumption that the calculated tension stress in the plate should be equal to or below the flexural tension strength. Considering a concrete plate including a concentrated vertical lateral load, internal or at the edge, the maximum tension stress will act just below the load at the lower face of the plate. In case of a vertical concentrated load acting at the corner of the rectangular plate, the maximum tension stress will be at the upper face of the plate.

Considering concrete floors on an elastic subgrade calculated based on the elasticity theory, the load bearing capacity will be lower than when utilizing plasticity theory.

Both TR 34 [2] and BR4 [3] follow this philosophy in the elastic theory consideration. According to Meyerhof [1], plasticity theory might be used considering concrete plates free of traditional longitudinal reinforcement.

2.3 Calculation according to plasticity theory

Considerations based on elasticity theory show fair agreement compared to observed deformations and measured stresses at lower load levels. During the 50'ties and 60'ties plasticity theory considerations were developed. The main reason was to achieve a calculation model that showed a better agreement to ultimate loads.

Plasticity models include possibility of stress distribution including increased load bearing capacity of the concrete plate. This statement requires a ductile behaviour at collapse, i.e. the plate has to be reinforced (including fibre or longitudinal reinforcement). The entire capacity of the plate will then be the sum of capacities along typical yield lines.

Considering a load increase for an internal load, the concrete section will first reach a capacity in accordance to elasticity theory where the flexural tension stress is equal to the tension stress capacity f_{tbd} at the lower face of the plate. This load is defined to P_e . At further load increase, the cross section will crack. Due to the ductile behaviour of the plate, the plate will still have a load bearing capacity for an increased load. A modified stress level is defined, as a percentage part R of the maximum tensile stress capacity f_{tbd} . The final rupture will first take place when the tension stresses at the upper face of the plate are equal to f_{tbd} . This load level is denoted P_1 .

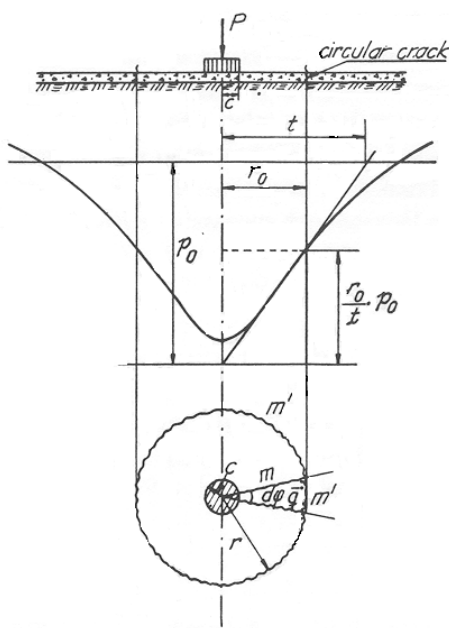


Figure 1- Yield line theory of a plate

Considering a load level below P_1 , the upper face of the plate will not crack, and the concrete floor will appear free of cracks (cracks might occur due to shrinkage, temperature, imposed deformations etc.). When the load level P_1 is exceeded, the capacity of the plate is given taking into account the load capacity of the upper face of the plate is similarly considered as a percentage part R of the capacity of the maximum tension stress level.

The number R is in the range of 30-80 % of f_{tbd} depending of the chosen fibre type and dosage. The factor R is in general given by the fibre producers and is defined in accordance to the Japanese standard JSCE-SF4 or according to the American standard ASTM C 1018.

Technical Report no. 34 (UK) uses the notation "flexural ratio", $R_{e,3}$ to state the maximum tensile strength to be used in the calculations in relation to the flexural tensile strength of a concrete section. "Betongrapport no. 4" (Sweden) uses an equivalent notation defining the factor $R_{10,x}$ ("residualhållfasthetsfaktoren") where X is a strain index often defined to 20, 30 or 50.

2.4 Loading conditions

The publication concentrates about typical load actions out-of-plane. In general this includes point loads, line-loads and locally distributed loads. In addition, groups of loads are considered related to the elastic length parameter of the concrete floor with respect to the stiffness of the subgrade material.

Other typical load effects acting on floors are static membrane tension. Pure tension and combination of tension and bending due to gradients will always represent a necessary load action to consider. Such load effects might be due to temperature (curing and exposed to exterior effects), shrinkage and different types of rigid or fixed points that contribute to an unfavourable controlled deformation.

3 FIELD MEASUREMENTS

During the project period, focus has been put on execution of typical fibre reinforced concrete floors. Different ongoing projects have been used as references focusing into typical well-known problem areas related to concrete floors to achieve and improve the construction methods. One typical project is a depot at Langhus close to Oslo where Veidekke ASA was a contractor for COOP Norway, casting in total 28.350 m² of a fibre reinforced concrete floor.

Based on the calculations, the following main dimensions were chosen:

Concrete grade:	C35 NA
Floor thickness:	150 mm
Steel fibre dosage:	33 kg/m ³ Dramix RC65/60 BN

Typical joint areas were up till 30 x 50 m. A smooth planning machine including a laser screed planed the floor. A high strength concrete (type Herkulit) improved the surface as a dry mortar and was littered in wet concrete and finally rubbed down by a flat steel trowel. Finally, the jointing was performed 19 months after the curing.

Measurements and behaviour of the finite floor shows the following quality goals:

- tolerances of the even surface within ± 1 mm equal 74.3 % and ± 2 mm equal 92.3 %
- documented resistance to wear
- in practice no cracks in spite of large contraction joint distances
- contraction joint openings as expected in the range of 5-10 mm depending of the joint distance
- limitation of curl to about 2.5-5 mm

The experience achieved at Langhus will be available through a publication.

4 SUBGRADE FRICTION

A literature study has been performed at SINTEF to summarise the main aspects and results from international literature concerning friction coefficients between the concrete floors and the subgrade.

Cracks in concrete floors are a well-known problem, however still efficient solutions are wanted. Such cracks often occur due to certain degree of fixing between the floor and the subgrade. Increased tension stresses develop due to the friction related to horizontal movements in the layer.

The literature does not give any unique answer to the best method in use to avoid or reduce the friction problem between concrete and the subgrade. Depending of the chosen technical solution, the literature does not either give any exact answer to the expected friction coefficient related to a chosen solution. However, it is stated that i.e. sand gives a lower friction coefficient compared to broken stone. Use of plastic membrane gives the lowest friction. Including one layer of plastic between the sand layer and the concrete, the friction coefficient is reduced by about 50 %.

5 MATERIAL PROPERTIES FOR CONCRETE USED IN FLOORS

Perfect concrete floors requires a combination of fair design and understanding of behaviour of “floating floors” together with right execution and “good” enough concrete mixture, that means concrete having proper material properties. The definition of good enough concrete mixture for floors depends of whom you are talking to. The contractor wants a concrete including a very high slump that can be smoothed just after casting. The opposite person is the concrete technologist, who wants a mix with minimum shrinkage. This concrete often requires hard work for the contractor. A mix design halfway between the two concrete’s is probably a good starting point.

Concrete is shrinking when drying and will give cracks if the floor is not framed to handle these movements. The most important material property to control is then the potential of shrinkage, and when we talk about floors, plastic shrinkage and drying shrinkage in particular.

5.1 Plastic shrinkage

It appears when we still can work with the concrete, i. e 1-3 hours after casting. The shrinkage appears due to evaporation of water from the surface. When the evaporation is larger than the transport of water in the concrete, there will be tensile forces working on the particles as a consequence of underpressure in the concrete` s pore-water. If these forces are greater than the tensile strength, cracks appear and these are often continuous.

Wind and low relative humidity (RH-%) increases the plastic shrinkage dramatically. Covering the floor is therefore the most efficient way to prevent plastic shrinkage. Concrete with high initial temperature combined with cold weather increases the plastic shrinkage due to the difference in temperature and high evaporation. High content of silica fume and higher concrete

quality are unfavourable because the concrete is more compact and reduces the possibility of water transport.

5.2 Drying shrinkage

The drying shrinkage appears months and years after casting and reduces the volume due to evaporation of water from the capillary pores. Figure 1 shows the mechanism for drying shrinkage. While drying, a meniscus waterfront appears in the pores. The meniscus adds tensile forces to the concrete skeleton. These forces make the concrete shrinking. The form of the meniscus is getting sharper (short radius curve) when the concrete is drying more and more. Higher forces appear and the concrete shrinks even more. If the floor is not built and act as a floating floor, cracks will appear due to this drying shrinkage for a long period.

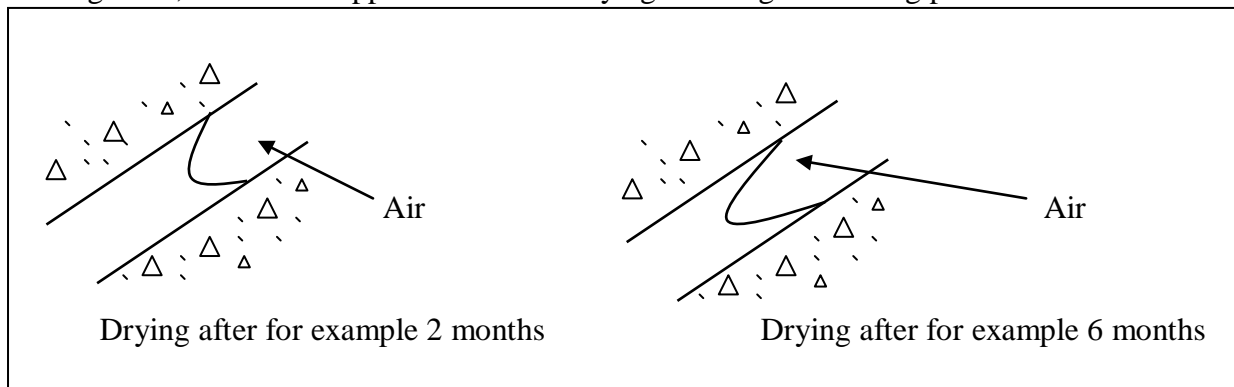


Figure 2- Mechanism for drying shrinkage.

The size of the drying shrinkage varies but is often 0,3 – 0,6 ‰ (mm/m). It is largest at the surface where the toughest drying appears. Drying shrinkage is consequently depending of the dimension, floors with higher thickness gives a slower shrinkage progress.

The material parameters that control the drying shrinkage are mainly the properties of the cement paste. Rapid cement gives a larger drying shrinkage because this cement is extremely finely ground and then gives a larger number of fine pores described above. There are more meniscuses adding tensile forces on the concrete. Larger drying shrinkage appears. The cement's chemical composition also affects the size of drying shrinkage.

Concerning drying shrinkage, the water content of the concrete is the parameter that has been focused most. The drying shrinkage is generally reduced when reducing the water content. If you reduce just the water content, then you of course achieve a higher concrete quality and the minimum reinforcement must be calculated according to this. To obtain the same w/c-ratio, the cement content also has to be reduced. This reduced paste volume contributes to lower drying shrinkage in general.

The reduction in cement paste described above leads to concrete with lower slump (consistency). If the same slump is needed, you get this by using larger content of P- or SP-admixture. This increased content can lead to concrete with higher drying shrinkage. The positive contribution from the paste reduction is neutralised due to higher content of admixtures.

Use of P- and/or SP-admixture can influence the size of drying shrinkage in both directions, as shown above. The admixtures generally reduce the drying shrinkage due to its water reducing effect. This effect can, as already mentioned, be destroyed because the cement grains are much more dispersed and give a larger number of capillary pores and meniscuses mentioned earlier.

Aggregates influence the size of drying shrinkage indirectly by the change of water demand. Coarse aggregate reduces the water demand and then also the drying shrinkage. Larger content of coarse aggregate give increased rigidity and larger resistance against shrinkage.

6 SHRINKAGE- AND SELF-INDUCED STRESS GENERATION IN STEEL FIBRE REINFORCED CONCRETE

This is a short note on the experience at NTNU on the shrinkage- and stress development in steel fibre reinforced concrete. *The experience is based on some tests performed in two experimental rigs measuring free deformation and 100% restraint stresses, respectively, from the time of setting and the next few weeks.* The topic has been investigated only in two test series, and the two test series are very different both in terms of concrete composition and curing conditions.

6.1 Test series and results

Test series 1 [4, 5], consisting of two tests, was performed with a special very high strength concrete ($f_{c28} = 140$ MPa) made with $w/b=0.23$ and a paste volume of 37%. One concrete was made without fibre and one concrete was made with 77 kg of 12.5 mm long steel fibres (1% of concrete volume, 2.7% of paste volume). The concretes were subjected to identical test conditions: The concretes were cured under sealed conditions (i.e. no drying shrinkage) and imposed to a realistic temperature history with 60°C as maximum. Figure 3 shows the free deformation results (total deformation) from setting and the first week, where the measured deformation reflects the sum of thermal expansion and autogenous shrinkage. As can be seen, there is no effect of the fibres on the measured deformation. Note that the net shrinkage of around 800×10^{-6} after 1 week (168 h) is caused by autogenous shrinkage (which is extremely high), since the temperature is approaching the initial temperature of 20 °C at that time (i.e. no net temperature change). The parallel stress measurements were in good agreement with Figure 1 in that there was no effect of the fibre addition on the stress development.

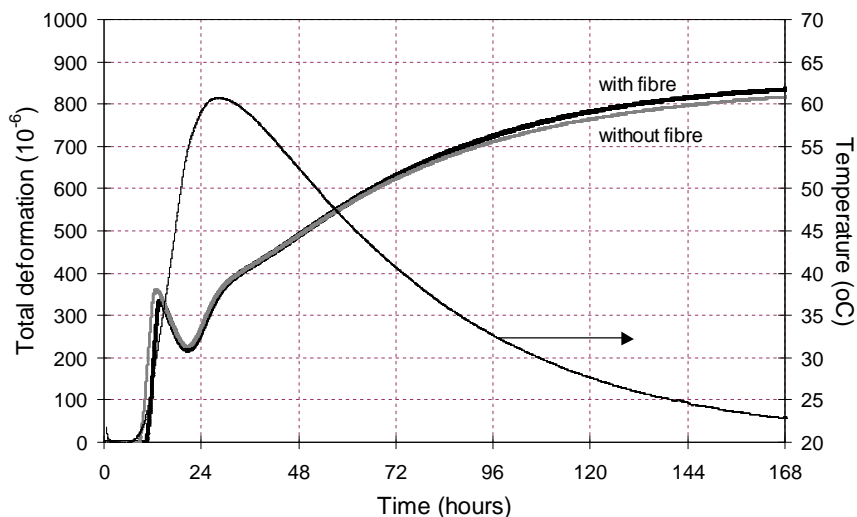


Figure 3. Free deformation results of thermal and autogenous shrinkage

Test series 2 [6], consisting also of two tests, was performed with a normal strength concrete ($f_{c28} = 50$ MPa) made with $w/b=0.57$ and a paste volume of 25%. One concrete was made without fibre and one concrete was made with 32 kg of 60 mm long steel fibres (0.4% of concrete volume, 1.7% of paste volume). The concretes were subjected to identical test conditions: 20 °C constant temperature the entire test, sealed curing the first day and exposure to 50% RH beyond that. Hence, the results from this series are caused by shrinkage (mostly drying shrinkage, but also a small component of autogenous shrinkage), since there is no thermal component. The results from this series also showed that there were no significant effect of the fibre addition on drying shrinkage and the subsequent stress development (and time of cracking) in the restraint stress rig.

6.2 Final comments

In the case where temperature is the dominating mechanism (often the case in hardening concrete) it could be expected that fibre additions have no clear effect on the free deformation and subsequent stress development, since the coefficient of thermal expansion of steel is rather close to concrete. The NTNU-results supports this assumption.

The amount of work reported on the effect of fibres on shrinkage in concrete from very early on is, to my knowledge, quite limited. It is, however, likely to expect that fibre addition will reduce shrinkage, since in this case there are differential strains between the steel fibres and the active matrix phase (restraining effect). However, it is likely that the effect is marginal, see the following simple calculation: A fibre content of 1% of concrete volume corresponds to an area of steel of $1\%/3 = 0.33\%$ in a cross section of the concrete (one dimension). Assuming that that the long term E-modulus of steel is 20 times that of concrete, the ratio between the effective stiffness of the two phases is $20 \times 0.33\% = 7\%$. Hence, the maximum potential for the steel fibres to restrain shrinkage is 7% - provided perfect bond between steel and concrete. As discussed above, the NTNU-results showed no clear effect of the fibre addition on the shrinkage.

Hence, the few preliminary results from NTNU (and some theoretical considerations), dealing with the hardening phase of concrete, imply that fibre addition may be a better measure for

improved post-cracking behaviour rather than a measure to reduce shrinkage and stress development before cracking.

REFERENCES

- 1 Journal of the Soil Mechanics and foundations division, 'Load-carrying capacity of concrete pavements' by G. G. Meyerhof, June 1962.
- 2 Concrete Society, Technical report 34, Concrete Industrial Ground Floors, - A guide to their design and construction, second edition 1994.
- 3 Svenska Betongföreningen, Betongrapport nr. 4, Stålfiberbetong, rekommendationer för konstruktion, utförande och provning, 1997.
- 4 Bjøntegaard, Ø. (1999), Thermal Dilation and Autogenous Deformation as Driving Forces to Self-Induced Stresses in High Performance Concrete, *Doctoral thesis*, NTNU, Dept. of Structural Eng., ISBN 82-7984-002-8.
- 5 Bjøntegaard, Ø. (2000), High strength concrete for military use: Volume changes and stress development (in Norwegian), NTNU-report, Division of Structural Engineering.
- 6 Bjøntegaard Ø. (2001), w/b = 0.57 floor concrete: Effect of shrinkage reducing admixture and steel fibre addition on the shrinkage and stress development in the hardening phase (in Norwegian), NTNU-report, Division of Structural Engineering.

Design of Fibre Reinforced Floors – Practical Experiences



Bo Malmberg
M Sc Civ eng
AB Jacobson & Widmark
Box 446
651 10 Karlstad
E-mail: bo.malmberg@jw.se

ABSTRACT

The design of fibre reinforced floors must be done very carefully in order to take care of all functional requirements as durability, abrasion resistance, moisture protection, crack width limitation etc as well as the specific loads and relevant properties of the sub-base.

The designer has to select the type of floor, closely jointed or “joint-free”, according to the functional requirements.

To be able to do this in a proper way there is a demand for more practically applicable guidance than there are at the moment.

Key words: fibres, concrete floor, design, joints.

1. INTRODUCTION

Concrete floors and especially industrial floors are very important parts of a building. If, for some reasons, there are any problems with the floor it can have a very substantial influence on the productivity and thus on the economic result of the industrial activity. Other structures as walls and roofs can often be repaired or adjusted without major influence on the production. Accordingly it is very essential to be very careful and systematic when designing a floor in order to fulfil all demands, static as well as more functional. This is, of course, valid for conventional reinforced as well as for fibre reinforced floors.

The design of fibre reinforced floors are, however, not always done in a proper systematic way. The design often starts with design of a conventional reinforced floor which is then, just before the performance, transferred to a fibre reinforced one after proposals from a contractor or a ready mix concrete supplier. The transformation is often based only on a comparison of the possibility to fulfil the bearing capacity of the floor, thus maybe neglecting many other important functional requirements. This may end up in:

- not desired joints
- unacceptable cracking
- unacceptable surface properties

Our experiences within J&W are that there are a lot of uncertainties especially regarding the design and performance of concrete industrial floors. In order to increase the knowledge of the basis for floor design we have made a concrete floor design guide. The guide focus on conventional reinforced floors but this paper presents the principal steps in the guide though focussing on the use of fibre reinforcement and gives practical experiences from design of a lot of fibre reinforced floors.

2. DETERMINATION OF ESSENTIAL DESIGN PARAMETERS.

2.1 Durability

For floors as well as other concrete structures the expected influence of the environment should be considered, that is, in terms of resistance against action of

- Freeze/thaw attacks
- Corrosion attack on reinforcement
- Chemical attacks

Frost/thaw attacks are never a problem in tempered buildings and attack on reinforcement, in this case steel fibres, gives in moist environment discoloration on the concrete surface. This may, of course, be a disadvantage in certain situations and may call for applying a separate surface layer as flow-applied flooring, granolithic concrete or polymer based coatings.

In moist environment with presence of chloride ions it can be expected that fibres bridging cracks will break due to corrosion rather soon. This is normally no problem when the objective with fibres primary is to distribute cracks, a mechanism that normally is fulfilled within a rather short time of the life time of a floor. However, when fibres bridging cracks are supposed to contribute to the bearing capacity of the floor it is of course essential that the durability of the fibres are guaranteed during the expected life time for instance by minimising the crack widths.

A recommended principle regarding design to resist chemical attacks is to apply suitable surface layers or surface treatments when the chemical environment, otherwise, should call for lower w/c-ratios of the concrete than 0,55, which normally corresponds to a strength class K40. For fibre reinforced floors it is recommended to use surface layers such as

- thick (≥ 10 mm) granolithic concrete layers
- thick (3-15 mm) polymer based coatings

The use of thick layers mean that you become both protections from chemical attack on the concrete surfaces as well a minimum risk for fibres protruding the concrete surface.

2.2 Abrasion resistance

The requirements regarding abrasion resistance shall be determined in relation to the utilisation of the floor and the requirements are often expressed as demands on the surface strength.

The use of fibre reinforcement is sometimes supposed to improve the abrasion resistance of concrete, probably due to the secondary effect of less aggregate separation in the concrete mass. For most floor applications the primary objective is to minimise dust formation in the upper surface layer, which is taken care of in a better way by other measures. Though floors exposed for heavy impact and wear loads could get an increased abrasion resistance by fibre reinforcement. That is, the same measures as for conventionally reinforced concrete has to be taken to fulfil requirements on abrasion resistance. For fibre reinforced floors the preferred methods are

- application of granolithic concrete by dry topping material or wet-in wet materials
- application of appropriate flow-applied flooring.
- application of polymer based layer

2.3 Moisture precautions

A very essential question to be answered in the design work is whether a dense layer is supposed to be applied to the floor surface at the moment or in the future. That is, layer such as glued PVC-carpets or polymer-based layers.

In order to avoid moisture-related problems, measures have to be made to protect the surface layer. These measures include the use of moisture protecting sheets under the concrete slab to prevent the moisture in the ground to reach the floor surface as well as minimising the thickness of the slab and decreasing the w/c-ratio to prevent the build in moisture in the concrete to cause problems. Figure 1.

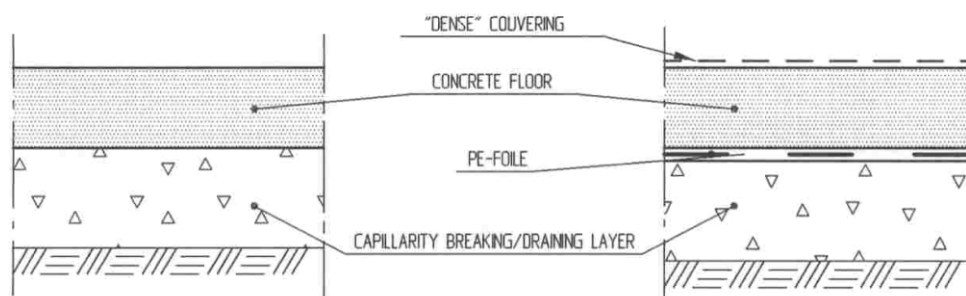


Figure 1. Principal sub base details for concrete floor on ground.

Left: For floors without covering or with vapour proof cover.

Right: For floors with dense covering.

These measures are the same whether the concrete is reinforced by conventional reinforcement or by fibres. For fibre reinforced jointed floors it should, however, be noticed that the measures may have an important influence on the shrinkage of the concrete and the friction properties under the slab, which influence the magnitude of joint movements and the ability for the fibres to bridge the joints. If the movements in the joint increase there is also an increased tendency for crawling, which has to be handled, especially if a moisture-protecting sheet is placed under the slab.

2.4 Crack width limitation and joints.

The issues above lead naturally to the most important questions to be solved when designing a concrete floor. That is

- is it possible to design the floor with shrinkage joints?
- what is the maximum number of joints allowable and what is the maximum joint width allowed
- should the joint be filled with joint material.

The acceptable crack widths or joint widths should be determined in relation to requirements on

- the utilisation of the floor.
- durability
- protection from radon gas
- the appearance of the floor surface
- hygienic aspects

It is also essential to determine whether the floor slab can be designed separated from surrounding walls or necessarily designed with edge beams.

To be noticed is that the user of the floor often can accept cracks with limited crack widths but do not prefer wide joints that could cause maintenance problems.

The normal design principal in Sweden and a technique that most designers are used to apply are floors without shrinkage joints reinforced with continuous bar reinforcement. That is, he do not have to bother very much about where and how to form joints.

The fibre reinforcement technique, on the other hand, force him to make considerations whether he should design a floor with low amount of reinforcement and closely spaced shrinkage joints, a floor with greater amount of fibres and a large distance between the joints or perhaps, if the floor shall be covered by a carpet etc, without joints and allowing “wild” cracking of the floor. These are considerations that most designers not are used to and therefore need proper guidance to carry out the design.

One specific issue that needs certain consideration when applying fibre reinforcement technique is when designing a floor on ground where there is a risk for ingress of radon gas to the building. The protection is normally secured by designing a “crack free” continuous floor where the concrete slab form the primary protection. In order to compensate this function when using jointed fibre reinforced floors it is recommended to place a single or double layer of plastic sheet under the slab as a gas proof layer.

2.5 Evenness, Flatness and Inclination

Requirements on the evenness of the floor surface is related to what kind of surface layer that is intended for the floor or if the surface is intended to be the wear surface. If the surface is intended to be a base for plastic sheeting etc the surface should be steel trowelled or levelled by

flow-applied flooring. For steel fibre reinforced floors the latter method is to be recommended in order to minimise the risk of fibres protruding the floor surface.

The possibilities to fulfil different requirements on flatness mean no difference whether the floor is reinforced by bar reinforcement or by fibres. When the utilization of the floor call for tolerances lower than $\pm 1,5$ mm over 2m length a special levelling layer of granolithic concrete or flow-applied flooring is to be recommended. This is also in good agreement with what is preferred for fibre-reinforced floors.

2.6 Installations and embedded items

In floors, and especially industrial floors, there are often different kind of installations and embedded items that influence the minimum or maximum dimensions of the floor as well as possibilities to arrange the reinforcement. For instance

- **Embedded positioning control coils**

While the embedment of position control coils may cause restrictions on the distance to normal bar reinforcement the use of fibres does not seem to influence the performance of the coils.

- **Heating- or cooling coils or hoses**

When using plastic hoses for heating the risk for penetration of the hoses by the needle like fibres during placing and compacting the concrete has been expressed.

- **Fixing screws**

The use of fibre reinforcement could be expected to be beneficial for the anchorage of expanding screws, for instance, by decreasing the risk of spalling and thus allowing closer distances between screws in a group and less distance to the concrete surface.

2.7 Load situation

The considerations regarding the expected load situation are the same whether the floor is reinforced with bars or with fibres. It is primary point loads from storage handling devices and wheel pressure from trucks that are of interest.

Besides the magnitude of the loads it is very important to consider the duration of the loads.

The expected load situation is preferably to be found in the specifications for the floor or in general reports concerning characteristic loads for different kind of industries.

2.8 Sub base

Important properties of the sub base are the evenness and the stiffness.

The evenness is of very great importance in the design of “joint-free fibre reinforced floors” but should be considered also in design of other fibre reinforced floors in order to avoid unfavourable constrain situations.

Guidance on how to regulate this property in design is indistinct in Swedish regulations but can be found more stringent in other countries.

The stiffness of the sub-base can be characterized in different ways, which often causes confusion to the designer. It can be expressed as

- Elastic (Young’s) modulus
- Modulus of sub grade reaction
- CBR-value (California Bearing Ring)

The choice of way to characterize the sub-base is related to the design method applied.

As well as for load considerations it is of the same importance to consider the duration of loads when applying a value for the stiffness of the sub-base in design. Our experience is that this has not been done in a proper way when comparing different kinds of floor types.

Floors constructed as unreinforced roller compacted slabs have been designed using values for the stiffness of the sub-base related to short duration of truck traffic, though storage racks with considerable static point loads have been placed on the floor.

3. SELECTION OF FLOOR TYPE

After considering the aspects according to 2.1-2.8 the limiting requirements on the floor can be listed according to table 1.

Table 1. Limiting design parameters for a concrete floor.

Parameter	Design value	
W/C	Min:	Max:
Freeze/Thaw resistance:	Class:	
Strength class	Min:	Max:
Floor thickness:	Min:	Max:
Max crack width:		
Continuity in joints required?:	Yes:	No:
Max joint movement:		

The first selection to make is to determine weather the floor shall be reinforced by bars or if it is possible or preferable to use fibre reinforcement.

If the decision is to design a fibre reinforced floor three main types can be distinguished characterized according to table 2.

Table 2. Characteristics for some major types of fibre reinforced floors. [Translation from 1]

Characteristic	Type A	Type B	Type C
Joint distance	20-30x h	20-30 m	40-50 m
Slab geometry	Preferably quadratic	quadratic	quadratic
Friction to sub-base	Low	Great	Very low
Working characteristics	Crack arresting	Preferably hardening	strain Preferably hardening
Fibre content	Low	Great	Moderate
Other			Low shrinkage Careful quality control Prolonged curing Late loading
Surface movements	Some mm	Some mm	Some cm

Type A: Floor with closely spaced saw cut as shrinkage joints.

Normal maximum joint distance: 4-6 m

The floor is only reinforced according to requirements on load capacity. That is, normally a rather low amount of fibres and thus economically beneficial.

Many joints could cause maintenance problems and the type should normally be limited for use when the contact pressure from wheels are less than 5 MPa.

Type B: Floor with intermediate joint spaces.

The joint space is often enough to allow a small floor to be made without joints or only with some transversal joints in long and narrow buildings.

A presupposition is that the friction to the foundation is high which must be considered when combined with measures related to moisture precautions for the floor. A low friction will result in large movements by the joints.

The toughness properties of the material should be characterized as “strain-hardening” which, in practice, very seldom is fulfilled. One reason for this is that there are no practically applied measures to specify this property. An other reason is that there are difficulties to get a strain-hardening load-deflection curve with the fibre types and the fibre contents that are used, normally maximum 40 kg/m³.

An alternative type between type A and B is floor jointed by saw cuts about every 10 m in two directions. This type, which has been common in Sweden, will also result in rather large joint widths if the friction under the slab is low. Fibres bridging the crack will tend to be pulled out to a considerable extent that may spoil the load transfer possibility over the crack and also cause tendency for carving.

Since this joint spacing often mean that joints have to be cut in the working area of the floor it may cause maintenance problems unless much care are taken to protect the joints in traffic zones.

Type C. “Joint-free floor”

This floor type is, in reality, not joint-free though the distances between the joints are of the magnitude that it is possible to make floors, up to 2000-3000 m² in one pour. When applied to larger floor areas very stiff shrinkage joints are formed using steel profiles.

It is very important that the friction to the base is low and that tolerance for the evenness of the base is restricted.

Additionally, it is important to isolate the slab from adjacent structures that could cause constraint and also add conventional bar reinforcement at points where peak strengths can be expected.

The shrinkage potential of the concrete should be minimised by restrictions on the added water content and great care shall be taken for curing of the floor.

If all these measures are taken the amount of fibres does not have to be extremely high.

4. DESIGN

The design of a floor should preferably be done according to the principals in the Swedish Concrete Associations' Concrete Report 4. This is at least possible for a "general" designer if there is a reliable computer program to utilize. Otherwise it is rather difficult to realize the principals and, thus mainly used by well-informed persons such as researchers, fibre suppliers and a few consulting engineers.

The design that results in specifications of the requirements on the concrete in terms of residual strength, $f_{flcr} \times R_{10,x} / 100$, or residual factors $R_{10,x}$ (%), are not well understood by designing engineers nor by contractors who are going to buy the fibre reinforced concrete from a concrete supplier. Although the objective has been to express the requirement on the fibre reinforced concrete in "functional" terms we still have to translate these to specified fibre types and fibre contents in kg/m^3 .

Basically it is a good principle to specify the requirements on the fibre reinforced concrete in functional terms. This allow for engineering skills in the proportioning of the concrete to find an optimum combination of the matrix properties and the fibre properties to fulfil the requirements on the composite material. However, it is not unusual that the fibre type that the concrete supplier has stored and the concrete recipe he has programmed in his computer determines the "optimum" combination of fibres and concrete.

This may end up in improper fibre types in relation to the floor dimensions, for instance too short fibres in a thick floor which means that the fibres gets an unfavourable orientation.

It also happens that the design of the floor thickness only is based on load situations with the design loads placed in the middle of the slab. That is, without considering load situation over saw cuts, formed joints or edges. This may result in a economic favourable slab but not always fulfilling all functional requirements.

The design of the load bearing capacity of fibre-reinforced floors is seldom a problem. The problem is how to design the floor in the serviceability limit state, that is, how to determine the proper measures to guaranty a certain maximum crack width. Although the Concrete Report 4 gives principals even how to treat this problem it has happened that the designer strictly follow what can be seen in figures like figure 2. That is, it is enough to use about 0,2 vol-% fibres or less than $20 kg/m^3$ to reduce the crack widths to less than 0,2 mm, which never is the fact in reality

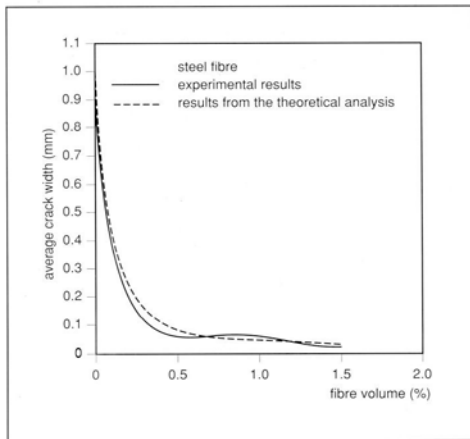


Figure 2. Average crack width versus fibre volume according to [2]

The development of design principles for fibre reinforced concrete has mainly been focused on methods that take into account different ways to describe the toughness behaviour of the concrete. These methods has, thus, encouraged the use of fibres witch gives high ductility to the concrete by plastic deformation of the fibres and decreased friction between the fibre and the matrix when the fibres are pulled out of the matrix. (Curve B in figure 3).

Not all fibres act, however, like this. For example milled fibres have a very high tensile strength and an excellent bond to the matrix but the ductility of the fibre material itself is low, which may be noticed as curves between curve A and B in figure 3.

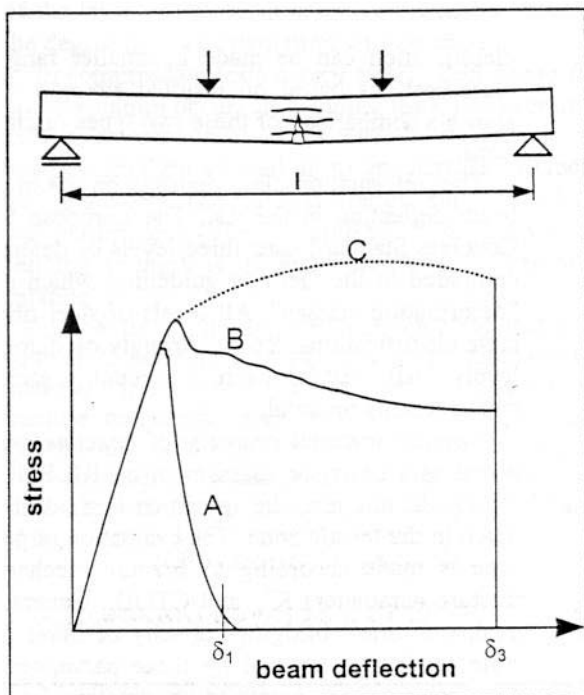


Figure 3. Bending stress-deformation curves for steel fibre reinforced concrete compared to plain concrete [3]

Those fibres are not sufficient for applications with high requirements on ductility as required for many shotcrete applications but they could be very useful for industrial floor applications. This is a fact that should be more considered when methods for design in the serviceability limit state are developed.

It is also important to consider the possibility to combine different kinds of fibres, steel fibres as well as polymer fibres, to reach the optimum requirements although this may be contradictory to what has been said above concerning the practical limitations for the concrete supplier to handle many constituent materials in an economic way.

5. CONCLUSION

The technique to reinforce concrete with fibres has been used in Sweden for about 25 years. In many other countries the application for concrete floors has increased to a great extent and the question has often been raised why the application in Sweden does not develop in a similar way. The primary reason for this is that there still is a lack of guidance for design and performance that are applicable in practice for a “normal” designer. In particular there is a demand for guidance for design in the serviceability limit state, that is how to handle requirements on crack widths and joints for different kinds of floor types. Additionally there is a demand for guidance how to handle other types of functional requirements or how these are influenced by the fibre reinforcement technique.

REFERENCES

1. Silfwerbrand J. Att kontrollera sprickbildningen i betonggolv. Bygg & Teknik 7/96.
2. Vanderwalle M. Tunnelling the World. N.V Bekaert 1991.
3. Schorn H. Classification of steel fibre reinforced shotcrete according to recent European standards. Proceedings from conference “Shotcrete: engineering Developments”. Hobart. 2001.

Yield and Failure Criteria of Fibrous Cement Based Composites



Lutfi Ay
Ph.Lic. C.E., Bridge Designer
Royal Institute of Technology
Department of Structural Engineering
Stockholm, SE-10044, Sweden
E-mail: Lutfi.Ay@struct.kth.se

ABSTRACT

Behaviour of Fibrous Cement Based Composites (FCBC) has been investigated since last four decays. Although, there are a lot of research on modelling of FCBC for different mechanical characteristics, there is no constitutive yield and failure criterion for this material.

A constitutive yield and failure criterion has been researched in this investigation by the help of the theory of plasticity.

Key words: Fibrous Cement Based Composites, Fiber Reinforced Concrete, Modelling, Yield and Failure Criteria of Composite Materials.

1. INTRODUCTION

Fibers are spread out in the concrete matrix in contrast to reinforcement bars in Ordinary Concrete (OC). This makes the resulting performances of FCBC more sensitive to matrix characteristics. The main factors affecting the matrix characteristics can be grouped as in Tab.1. These groups can be divided into subgroups, which results in a large number of variables.

The approaches to modelling of FCBC depend mainly on fiber characteristics and bonding strength between fiber and matrix interface. Experimental investigations have showed that the parameters for defining the FCBC have large scatter. The formulations in the fiber level may either overestimate or underestimate the capacity of FCBC strongly [1]. Another way of looking at the FCBC may be seeing it from a larger scale. By means of this way those micromechanical parameter which have been mentioned above can be included in the final formulation. A yield and failure criterion which assumes the concrete as a homogeneous material but precise enough is needed for designing and engineering applications.

Table 1 – Main parameters affecting the performance of FCBC

Fibers	Amount
	Number
	Length
	Aspect ratio
	Tensile strength
	Shape
	Dispersion
	Orientation
Water	Bond strength
	Amount
Cement	Amount
	Type
	Particle size
Aggregates	Amount
	Max. size
	Size distribution
	Strength
	Surface structure
	Shape
	Chemical composition
	Mica content
Microfiller content	
Supplementary cementitious additives	Amount
	Type
	Dispersion
Superplasticizer and other admixtures	Amount
	Type
	Compatibility
Mixing order	All ingredients
Vibration	Type
	Duration
Curing	Type
	Duration

2 RESULTS AND DISCUSSIONS

A stress tensor, σ_{ij} can be divided into hydrostatic and deviatoric stresses as given in Eq. (1) and Fig.1 [2].

$$\sigma_{ij} = \mathbf{S}_{ij} + \sigma_m \delta_{ij} \quad (1)$$

Where, \mathbf{S}_{ij} is *stress deviator tensor*, $\sigma_m = \frac{1}{3}(\sigma_1 + \sigma_2 + \sigma_3)$ is *hydrostatic stress tensor* and δ_{ij} is Kronecker delta ($\delta_{ij} = 1$ if $i = j$, otherwise $\delta_{ij} = 0$).

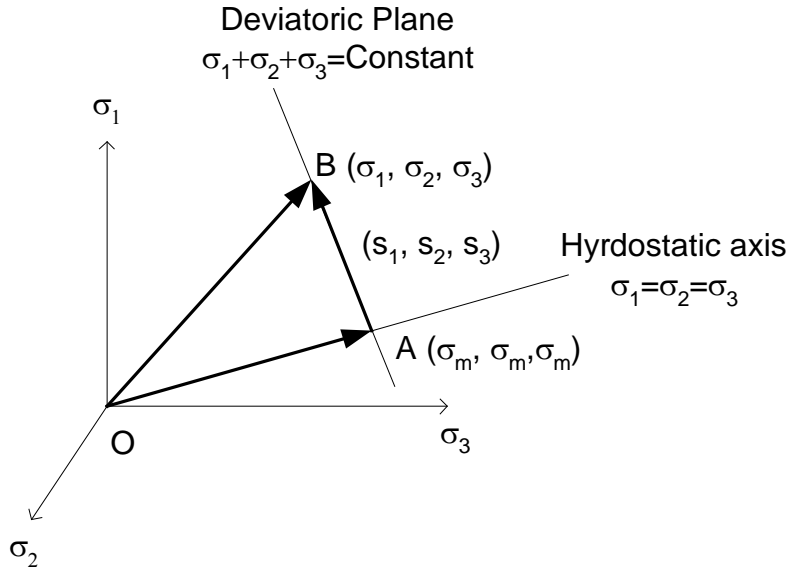


Figure 1 - Stress tensor in principal stress space

Experimental investigations have showed that the influence of hydrostatic pressure on yielding for ductile materials, such as metals, is not appreciable [3]. In contrast, the stresses, which cause yielding of the brittle materials, are mainly not stress deviator tensor. In other words, the yield criteria for ductile materials are independent of the hydrostatic pressure and for the brittle materials the yield criteria are independent of the stress deviator tensor.

OC is generally assumed as brittle material and the Mohr-Coulomb yield criterion which, accounts for the hydrostatic pressure effect is used widely. The yield surface in three-dimensional stress space is as in Fig. 2 and given in the following form in Eq. (2) [2].

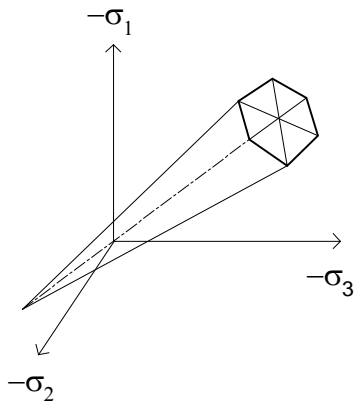


Figure 2 - Mohr-Coulomb failure surface in the principal stress space

$$\begin{aligned}
 f(I_1, J_2, \theta) = & \frac{1}{3} I_1 \sin \phi + \sqrt{J_2} \sin \left(\theta + \frac{\pi}{3} \right) \\
 & + \frac{\sqrt{J_2}}{\sqrt{3}} \cos \left(\theta + \frac{\pi}{3} \right) \sin \phi - c \cos \phi = 0
 \end{aligned} \tag{2}$$

where,

$$\theta = \frac{1}{3} a \cos \left(\frac{3\sqrt{3} J_3}{2 J^{3/2}} \right) \text{ is the angle of similarity}$$

$$I_1 = \sigma_{ii} \text{ is the first invariant of stress tensor}$$

$$J_2 = \frac{1}{2} s_{ij} s_{ij} \text{ is the second invariant of stress deviator tensor}$$

$$J_3 = \left| s_{ij} \right| \text{ is the third invariant of stress deviator}$$

ϕ is the angle of friction

c is cohesion coefficient

The von Mises yield criterion which is used for pressure-independent isotropic materials is given in Eq. (3). This equation represents a circular cylinder as in Fig. 3 with radius

$$\rho = \sqrt{\frac{2}{3}} \sigma_0, \text{ where } \sigma_0 \text{ is the yield stress in simple tension.}$$

$$f(J_2) = J_2 - \frac{\sigma_0^2}{3} \quad (3)$$

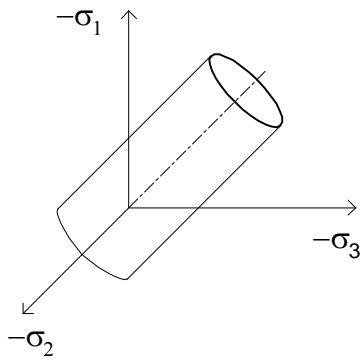


Figure 3 - Yield surface of von Mises criterion in principal stress space

Fibers increase the toughness and the ductility is a known phenomenon. FCBC can behave like a brittle or a ductile material depending on volume fraction of fibers, V_f . The same matrix with different amount of fibers can have different yield and failure stresses. Fig.4 shows plain concrete and FCBC with $V_f = 5\%$.

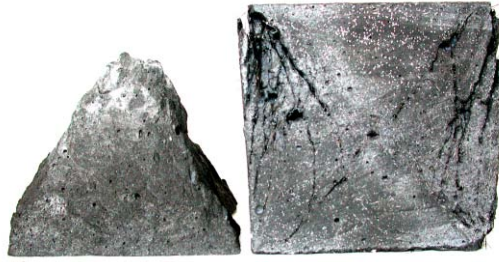


Figure 4 - Plain concrete (on the left) and FCBC (on the right) cubes after compressive strength test [4].

The stress-strain response under compressive stress of both concretes is shown in Fig. 5.

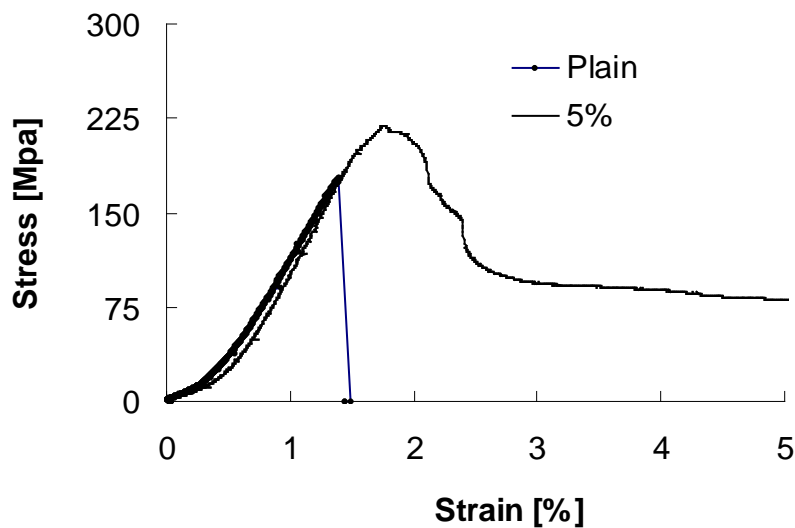


Figure 5 - Stress-strain curves of plain concrete and FCBC of $V_f = 5\%$ [4].

The plain concrete has $f_c = 178$ MPa and FCBC has $f_c = 219$ MPa . The plain concrete shows a very brittle character while FCBC has very large ductility compared to the plain concrete. Any mechanical behavior of the plain concrete can be modeled by Mohr-Columb criterion. However, FCBC has metallic character, which is similar to von Mises model. The most important question is the failure of the FCBC between these two concretes. These two constitute the upper limit (ductility) and lower limit (brittleness) character of the concrete as a material. An important hypothesis can be done such as the yield stresses of all other FCBC of different classes and of different fiber types are within these two limits. The FCBC with low fiber content may be assumed as Mohr-Coulomb material and the FCBC with higher fiber content approaches to von Mises yield surface which is a circle. This assumption is represented in Fig. 6.

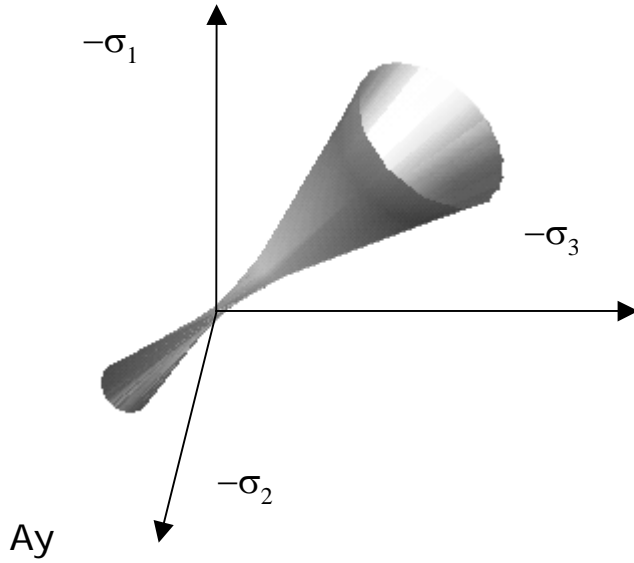


Figure 6 – Proposed yield surface of FCBC in principal stress space

The failure criteria of FCBC may have the form as in Eq. (4).

$$f(I_1, J_1, m) = m I_1 + (1 - m) J_1 - k^\alpha \quad (4)$$

where, m is a material parameter and function of $m = f(V_f, C_f, C_m, M)$. V_f, C_f, C_m, M are volume fraction of fibers, stiffness of fibers, stiffness of matrix and coupling modulus between fibers and matrix, respectively. Finally, k^α represents the yield stress.

The theoretical and experimental investigations in form of three-axial compression and tension tests etc. are still being conducted by the author. The results will be published as a Ph.D. Thesis as a continuation of reference [1].

REFERENCES

1. Ay, L., "Using Prestressed Steel Fiber Reinforced High Performance Concrete in the Industrialization of Bridge Structures," *Licenciate Thesis*, Department of Structural Engineering, Royal Institute of Technology, Bulletin 49, December 1999.
2. Chen, W.F., D.J.Han., "Plasticity for Structural Engineers", Purdue University, West Lafayette, Indiana 47907, USA, April 1995, pp. 77-95.
3. Hill, R., *The mathematical Theory of plasticity*, Oxford University Press, London, 1950.
4. Ay, L., *Ph.D. Thesis* which will be published in 2002, Department of Structural Engineering, Royal Institute of Technology.

Determination of Fracture Mechanical Properties for FRC



Henrik Stang
Ph.D., Associate Professor
Department of Civil Engineering
Building 118, Technical University of
Denmark,
DK-2800 Lyngby, Denmark
E-mail: hs@byg.dtu.dk

ABSTRACT

The present paper discusses the applicability of fracture mechanical properties in the design of fibre reinforced concrete structures and places special emphasis on the possibilities of determination of such properties. It reviews recently proposed methods and point out the possibility of using the 3 point bending beam proposed by RILEM in order to verify fracture mechanical properties used in design.

Key words: Fibre reinforced concrete, fracture mechanics, testing, design.

1. INTRODUCTION

The use of Fibre Reinforced Concrete, FRC, today is typically limited to non-structural applications or in secondary elements, where the fibres are employed to serve functions such as minimizing shrinkage cracking and limit crack widths due to mechanical loading. Structural use of FRC is scarce, and attempts to use fibre reinforcement as structural reinforcement has so far been concentrated on replacement of shear reinforcing stirrups in structural members such as beams as well as replacement of complicated reinforcement arrangements in areas where concentrated loading is applied to the structure.

While extensive amounts of research have been carried out in FRC, the expected pervasive use of FRC in the construction industry has not materialized. There are a number of possible reasons for this phenomenon. Conceptually, while FRC is generally recognized as tougher than concrete, a logical and systematic translation of this property into structural performance is all but absent. On a practical level, current design codes for structures do not usually cover FRC materials. Without design guidelines, engineers find it difficult to incorporate this material into their structural design. Secondly, test methods that are robust and at the same time properly characterize FRC are still under debate. Thirdly, without a rational methodology for selection of fiber, matrix and control of interface, the resulting composite usually does not achieve optimal behavior, thus negatively affecting the performance to cost ratio.

2. ON THE USE OF FRACTURE MECHANICS IN DESIGN OF FRC

Traditional design of concrete and reinforced concrete structures typically involve a very few material parameters describing the mechanical behaviour of concrete, typically only the compressive strength and the Young's modulus. Tensile strength is – if applied – typically deduced from compressive strength. Alternatively, design formulae take tensile strength into account in an implicit way. To the author's knowledge, no design formulae contain explicit information about fracture toughness, even though it is recognized that toughness plays a significant role for the structural behaviour, both in the serviceability and in the ultimate limit state. To take the influence of toughness in design into account implicitly is permissible only if the ratio between strength parameters, typically the compressive strength, and toughness is more or less constant in the materials under consideration. For special types of concrete such as high strength concrete and fibre reinforced concrete this turns out not to be the case.

Recently, much focus has been put on the use of fracture mechanical concepts in testing and design of FRC, [1,2,3]. This has been done in recognition of the fact that fibres in conventional concrete primarily have a toughening effect while fibres play little or no role with respect to stiffness and strength. Thus, the effect of the fibres is a pronounced change in ratio between the (compressive) strength and the toughness. As a consequence the use of standard design tools for concrete structures in the design of FRC becomes questionable.

The basic fracture mechanical concept suggested to be applied in FRC design is the stress-crack opening relationship, which is associated with the so-called fictitious crack model. The model was originally suggested by Hillerborg to be used in concrete and FRC, [4] and [5], and in recent years its applicability in FRC design has been demonstrated in a number of different contexts. The fictitious crack model can be thought of as a cohesive crack model relating the cohesive stress on the surface of the fictitious crack, σ_w , with the crack opening, w . This relation is called the stress-crack opening relationship. For $w=0$, $\sigma_w(0)=f_t$.

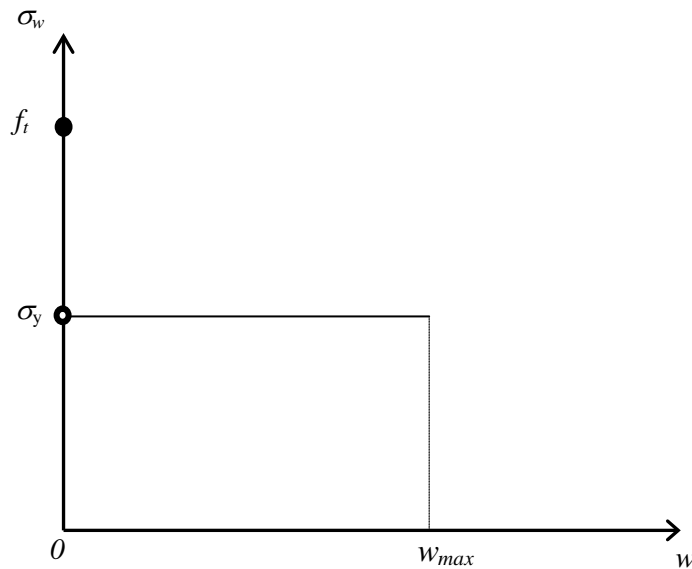


Figure 1. Simplified stress-crack opening relationship suggested for design purpose, the drop-constant relationship, characterized by a tensile strength f_t and a constant stress σ_y , called the residual stress, acting on the fictitious crack for crack openings less than a maximum crack opening w_{max}

There are a number of advantages associated with the use of a fracture mechanical approach in the design of FRC. Several micro-mechanical models are available in order to provide understanding of the connection between material composition and stress-crack opening relationship. When failure is not pure compression failure it is well known that there are significant size effects associated with the failure stress. These size effects originate for a large part in the fracture process, thus design formulae based on fracture mechanics automatically takes the structural size into account. Design formulae based on fracture mechanical concepts typically contain information on crack widths inherently.

The disadvantages of applying fracture mechanics in design are that fracture mechanics concepts are not very well known in civil engineering community, and that the stress-crack opening relationship is not a property very well suited for design, especially since the relationship is highly non-linear and since the stress level as well as the shape depend on concrete, fibre type, and amount of fibre. To overcome this problem a number of different simplified stress-crack opening relationships have been suggested, [1], among which the bi-linear and the drop-constant relationships seem to be the most operational. The simplest, the drop-constant relationship is shown in Fig. 1. This relationship prescribes a tensile strength f_t and constant stress, σ_y , called the residual stress up to a maximum crack opening w_{max} .

3. ON TESTING OF FRC FOR FRACTURE MECHANICAL PROPERTIES

3.1 General

Determination of fracture mechanical properties of FRC is done via testing. The testing can typically have two objectives.

One objective is to obtain as detailed information as possible about the stress-crack opening relationship using testing designed for detailed investigations. The principles of this type of testing are outlined in Fig. 2.

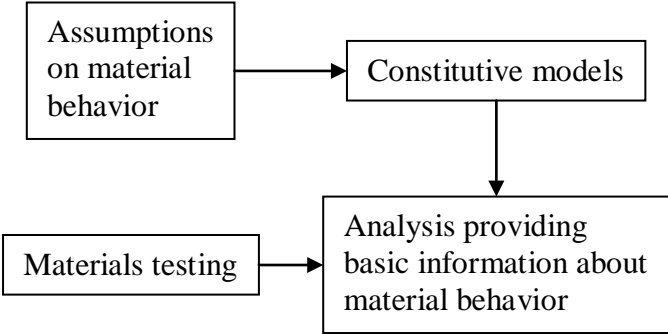


Figure 2. Principles of laboratory testing carried out in order to derive basic information about material behaviour. After basic assumptions about the material behaviour have been formulated in terms of a constitutive model the testing results are analysed using this model. In this way the analysis provides information about the validity of the constitutive model or provides numerical values for the parameters in the constitutive model.

This kind of testing requires basic assumptions about the material behaviour, i.e. a constitutive model. In the case of a fracture mechanical approach to FRC this would be the assumption of the validity of the fictitious crack model. After the testing has been carried out the constitutive model is used to interpret the results of the testing. The interpretation of the test often requires structural analysis of the test specimen and loading configuration. The interpretation will help to shed further light on the assumptions initially made about the material behaviour i.e. of the validity of the constitutive model. Furthermore, numerical values for the parameters in the constitutive model are provided, in this case detailed information about the stress-crack opening relationship, which is the fundamental property in the fictitious crack model. The testing procedure is often fairly complicated and is typically carried out only in research laboratories.

Another objective for the testing could be determination or verification of the material parameters introduced in the simplified stress-crack opening relationships introduced in design. Application of Fiber Reinforced Concrete (FRC) in structural applications requires testing methods, which are comparable to testing methods applied for conventional concrete with regards to simplicity and reliability. Furthermore, it is a requirement that the parameters determined in the testing have a direct link to material properties used by the structural designer. In Fig. 3., the typical relationship between design and testing is outlined. Design is carried out under the assumption of certain material parameters. In the case of a fracture mechanical approach to FRC these parameters would be the material parameters associated with the drop-constant stress-crack opening relationship outlined in Fig. 1. Subsequent testing of the materials applied should be able to determine or verify the material parameters used in design through simple means of interpretation of the test results.

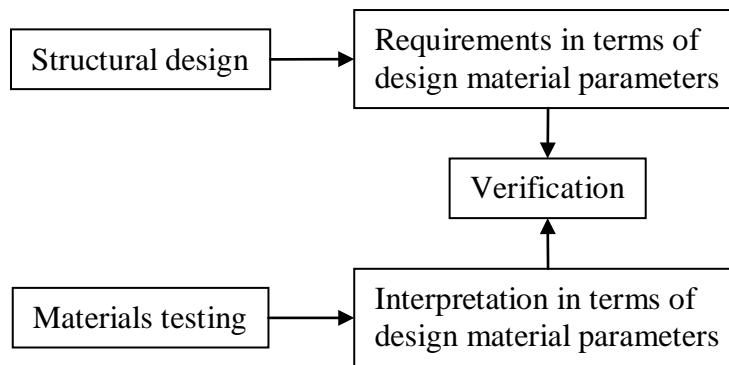


Figure 3. The typical relationship between design and testing for material parameters: the structure in question is designed assuming or requiring certain material parameters. When the structure is build, it should be varified that the design requirements are in fact meet. The test should be simple and reliable and a simple interpretation should be available to indicate whether the material used meets the requirements in terms of the design material parameters.

3.2 The uniaxial tensile test

The uniaxial tensile test seems the most direct and logical way of determining the stress-crack opening relationship. Recently, RILEM technical committee TC 162-TDF, “Test and design methods for steel fibre reinforced concrete” published a recommendation for uniaxial testing of FRC with the aim of determining the stress-crack opening relationship directly [6]. The test rely on the assumption that it is possible to restrain rotation of the crack surfaces in order to make it possible obtain more or less uniform crack opening over the whole specimen.

The test is conducted as a displacement controlled tensile test on a notched specimen as shown in Fig. 4. The specimen can be either cast or cored from an existing structure or structural element, which is one of the attractions of the method. The test is conducted in a closed loop mechanical testing machine using the average measurement of the displacement over the notch as the feed back signal or in another test setup which ensures stable post cracking response such as placing the specimen in parallel with steel bars in the testing machine. Both ends of the testing specimen shall be clamped to the testing machine and fixed with respect to rotation in such a way that rotation is sufficiently eliminated. At the same time care shall be taken not to introduce pre-stressing of the specimen. This can, for example, be achieved by providing special fixtures, which allow the test specimen to be glued directly into the test machine. Fixing of the ends of the specimen is a slightly controversial point, since it has been shown that when testing plain concrete for fracture energy in tension, the fracture energy is over-estimated when a fixed specimen is used compared to the situation where the ends of the specimen is allowed to rotate [7]. However, the test proposed by RILEM is intended not for investigation of the crack propagation but rather the crack opening process after a certain minimum crack opening has been achieved. During testing the load and corresponding displacement is recorded digitally.

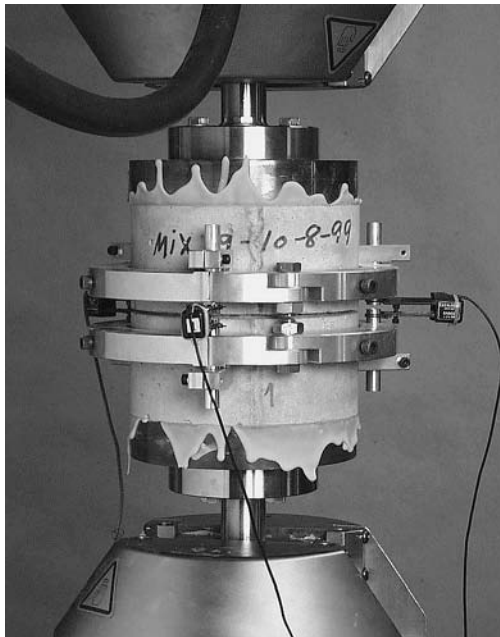


Figure 4 The uniaxial tensile test specimen and arrangement according to the recent RILEM recommendation [6]. The specimen is glued directly into the testing machine resulting in fixing of both ends of the specimen with respect to rotation. The specimen is instrumented with clip gauges and/or LVDTs in order to measure crack opening and to check rotation of the crack faces.

The recommendation specifies a method for interpretation of a single test to obtain the stress-crack opening relationship between two crack openings: a minimum crack opening w_i and the maximum crack opening applied in the test w_m . The recommendation also defines an average as well as a characteristic stress-crack opening curve.

The method determines the stress-crack opening curve directly, in the sense that no structural model is necessary for the interpretation of the results. The stress is determined on the basis of the load by direct calculation and the crack opening is determined directly from the average reading of the clip gauges measuring the crack opening apart from a small correction due to the elastic deformation of the material next to the crack surfaces. Consequently the test method can be used both to obtain detailed information about material behaviour and to determine or verify simplified stress-crack opening relationships used for design. However, the test method is demanding both with respect to time and laboratory equipment.

3.3 The beam test

The beam test is well known as a tool for the determination of fracture energy G_F of concrete [8]. Recently, a method was proposed by the RILEM technical committee TC162 “Test and Design Methods for Steel Fibre Reinforced Concrete” [9]. This method proposes a 3 point bending test on a test specimen with a notch, see Fig. 5. The standard specimens proposed has a span l of 500 mm, a height h of 150 mm, a width, b , of 150 mm and a notch depth a_0 of 25 mm. The load P as well as the deflection δ is measured. Optionally, the Crack Mouth Opening

Displacement, CMOD, can be measured at a distance d from the bottom of the beam. Overall the beam test is less demanding with respect to time and laboratory work than the uniaxial test, however it should be emphasised that the test is significantly more demanding than e.g. a standard compression test.

The beam test is intended for use in a design method based on a non-linear stress-strain relationship. The result of the bending test is interpreted in way that yields so-called equivalent flexural strengths, which can subsequently be applied in design according to recommendations by the same committee [10]. The design is based on a non-linear stress-strain relationship in which key elements are determined by the equivalent flexural strengths determined in the test. However, it has been shown recently that it is possible to model the behaviour of an FRC beam with or without a notch with good results using a fracture mechanical approach. This can be done both using non-linear finite elements and an analytical approach introducing a non-linear hinge, where the crack is propagating, in an otherwise elastic beam. The approach is discussed at some length in a paper on structural analysis of FRC structures based on fracture mechanics from RILEM technical committee TC162, [1].

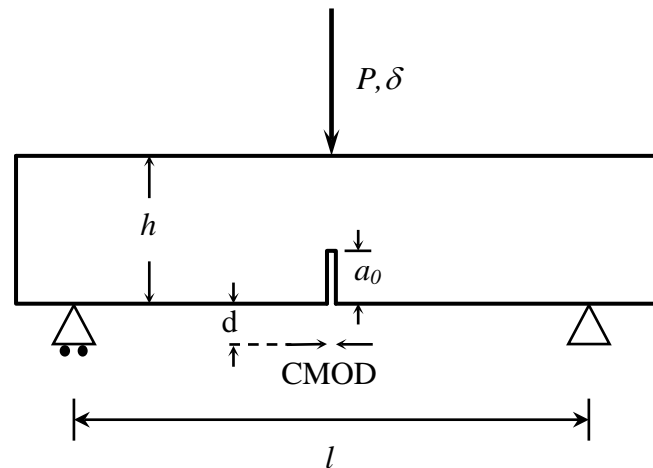


Figure 5. The principal test configuration suggested by the RILEM technical committee TC162 [9]. The standard specimen proposed has a span l of 500 mm, a height h of 150 mm, a width, b , of 150 mm and a notch depth a_0 of 25 mm. The load P as well as the deflection δ is measured. Optionally, the Crack Mouth Opening Displacement, CMOD, can be measured at a distance d from the bottom of the beam.

The analytical analysis can be based on analytical solutions for the non-linear hinge in terms of moment versus angular deformation relations. Closed form solutions are available for both the bi-linear as well as the drop-constant stress-crack opening relationship [11].

The existence of such relative simple solutions for the beam test based on fracture mechanics obviously opens up for using the beam test for determination of the fracture mechanical properties, i.e. the stress-crack opening relationship.

When detailed information about the stress-crack opening relationship is required a so-called back analysis is needed, because it is not possible based on knowledge of the beam response (load-deflection or load-CMOD) to solve directly for the underlying stress-crack opening relationship. Back analysis is based on a comparison between the observed response and the

response calculated with a certain choice of stress-crack opening relationship. This comparison is quantified in terms of an error. The best choice of stress-crack opening relationship can now be determined by minimizing the error. Back analysis for the beam test has been studied extensively for concrete and FRC [12], [13]. However, it was shown in [14] that it is very difficult with this method to distinguish between tensile strength and the initial part of the stress-crack opening relationship which seems to indicate that back analysis should not be attempted unless independent information about the tensile strength exist, especially in the case of FRC, where the ratio between strength and toughness can vary significantly.

The beam test is suitable for determination or verification of the fracture parameters in the simplified stress-crack opening relations applied in design, such as the bi-linear or the drop-constant relationship.

In the case where the simple drop-constant stress-crack opening relationship has been applied the expected beam response in terms of either a load-deformation or a load-CMOD relation can be calculated using the analytical model outlined above. For a given test specimen geometry, this calculation can be based on the assumption of vanishing tensile strength and a certain value σ_y of the residual stress. Choosing different values for the residual stress, σ_y , a series of curves is produced which can be interpreted as a verification chart. Since the influence of the Young's modulus is very weak for practical purposes only a single verification chart is needed for each type of test specimen. In Fig. 6 a verification chart for the beam suggested by RILEM technical committee TC 162-TDF [9] is shown together with the relationship between the deflection and the crack opening displacement, COD, at the bottom of the ligament.

A given test result obtained using a certain test specimen geometry and instrumentation (e.g. according to [9]) can be compared with the corresponding verification chart. A certain assumed design value σ_y , valid up to a certain maximum crack opening w_{max} is verified if the measured load-deflection or load-CMOD curve lies above the curve in the verification chart corresponding to the same value of σ_y for all deflections or CMODs less than certain values, δ_{max} or $CMOD_{max}$. It can be shown that deflection, δ , and CMOD are approximately linearly related to COD (see Fig. 6), which again can be related to w_{max} in design guidelines. This makes use of the verification charts particularly simple. The use of the verification charts does not involve tensile strength and again the tensile strength should be determined/verified independently from the beam test.

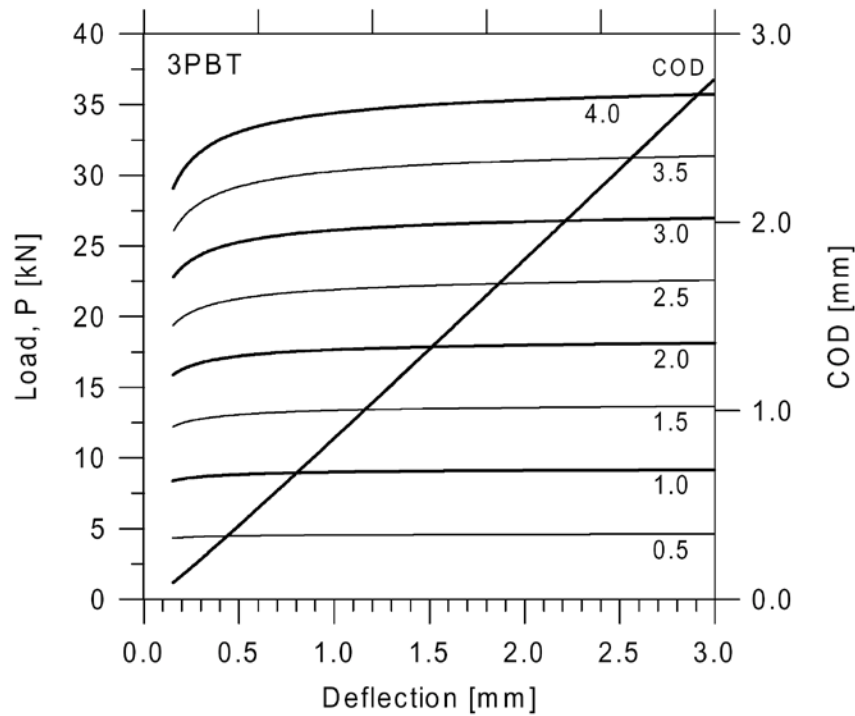


Figure 6. Verification chart for the RILEM 3 point bending test (3PBT), proposed for steel fibre reinforced concrete by the technical committee TC 162-TDF. The verification charts can be used to verify or determine the residual stress σ_y used in the drop-constant stress-crack opening relationship. The numbers next to the curves refer to the residual stress σ_y . The left axis is load, the right axis is the COD and the almost straight line represents the relationship between deflection and COD.

3. CONCLUSIONS

A fracture mechanical approach to design of FRC structures is gradually becoming more and more realistic, also from a practical point of view. A sound basis for such an approach seems to be the so-called fictitious crack model, which uses the stress-crack opening relationship as a basic input. Advantages connected to a fracture mechanical approach include: micro-mechanical models are available in order to provide understanding of the connection between material composition and stress-crack opening relationship, design formulae based on fracture mechanics automatically takes the structural size into account and design formulae based on fracture mechanical concepts typically contain information on crack widths inherently. A number of standards for test specimens have now been recommended by RILEM. These specimens include a uniaxial and a bending test specimen. The results of both tests can be interpreted in terms of fracture mechanical properties. This can be done either in order to get detailed information about the fracture mechanical parameters or in order to determine or verify simpler stress-crack opening relationships applied in design. A simple method for determining the residual stress σ_y in the drop-constant stress-crack opening relationship is suggested.

REFERENCES

1. "Test and Design Methods for Steel Fiber Reinforced Concrete. Design of Steel Fibre Reinforced Concrete using the $\sigma-w$ Method: Principles and Applications". Prepared by RILEM-Committee-TDF-162, Chairlady L. Vandewalle. Submitted for publication in *Mat. Struc.* 2001.
2. Rossi, P.: "Les Betons de Fibres Metalliques". Final report on Betons de Fibres Metalliques, elemets de structure fonctionnant comme des poutres by AFREM. 1995.
3. Stang, H. and Olesen J.F.: "A Fracture Mechanics Based Design Approach to FRC". In: *Fibre-Reinforced Concretes FRC, BEFIB' 2000*. (Eds. P. Rossi and G. Chanvillard). RILEM Publications S.A.R.L. ENS - 61 Av. Pdt. Wilson, F-94235 Cachan Cedex, France. 2000. 315-324.
4. Hillerborg, A., Modeer, M. and Petersson, P.E.: Analysis of Crack Formation and Crack Growth in Concrete by Means of Fracture Mechanics and Finite Elements. *Cem. Concr. Res.* 1976, **6**, 773-782.
5. Hillerborg, A.: Analysis of Fracture by Means of the Fictitious Crack Model, Particularly for Fibre Reinforced Concrete. *The Int. J. Cem. Comp.* 1980. 2. 177-184.
6. "Test and Design Methods for Steel Fiber Reinforced Concrete. Recommendations for Uni-axial Tension Test." Prepared by RILEM-Committee-TDF-162, Chairlady L. Vandewalle. *Mat. Struc.* 2001, **34**, 3-6.
7. Van Mier, J. G. M., Schlangen, E. and Vervuurt, A.: Tensile Cracking in Concrete and Sandstone: Part 2 - Effect of Boundary Rotations. *Mat. Struc.* 1996, **29**, 87-96.
8. RILEM Committee FMC 50. "Determination of the Fracture Energy of Mortar and Concrete by Means of the Three-point Bend Tests on Notched Beams. *Mat. Struc.* 1985, **18**, 285-290.
9. "Test and Design Methods for Steel Fiber Reinforced Concrete. Recommendations for Bending Test". Prepared by RILEM-Committee-TDF-162, Chairlady L. Vandewalle. *Mat. Struc.* 2000, **33**, 3-5.
10. "Test and Design Methods for Steel Fiber Reinforced Concrete. Recommendations for $\sigma-\epsilon$ Design Method." Prepared by RILEM-Committee-TDF-162, Chairlady L. Vandewalle. *Mat. Struc.* 2000, **33**, 75-81.
11. Olesen, J.F.: "Fictitious Crack Propagation in Fiber-reinforced Concrete Beams". *J. Eng. Mech.* 2001, **127**, 272-280.
12. Nanakorn, P. and Horii, H.: "Back Analysis of Tension-Softening Relationship of Concrete". *J. Materials, Conc. Struc., Pavements, JSCE.* 1996, **32**, 265-275.
13. Kitsutaka, Y.: "Fracture Parameters by Polylinear Tension-Softening Analysis". *J. Eng. Mech.* 1997, **123**, 444-450.
14. Stang, H. and Olesen, J.F.: "On the Interpretation of Bending Tests on FRC-Materials". In: *Fracture Mechanics of Concrete Structures, Proceedings FRAMCOS-3*. (Eds. H. Mihashi and K. Rokugo). Aedificatio Publishers, D-79104 Freiburg, Germany. 1998, 511-520.

A Test Method for Studying Crack Development in Steel Fibre Reinforced Concrete Overlays Due to Restrained Deformation



Jonas Carlswård
M.Sc. Doctoral Student
Betongindustri AB
Box 47 312 Stockholm
E-mail: jonas.carlsward@betongindustri.se

ABSTRACT

A test method for studying the formation of cracks in restrained concrete overlays has been developed. The set-up consists of 15 cm thick concrete toppings that are placed on the surface of a bottom slab constituting a stiff foundation. By exposing the overlays to a temperature gradient of considerable magnitude, tensile stresses, gradually leading to the formation of cracks, develop in the concrete. In this way a total of six overlays have been tested. Three of the specimens were produced with plain concrete while steel fibre reinforced concrete was used for the other specimens. Results show that there was no distinct difference in cracking behaviour for the fibre reinforced specimens as compared to the plain concrete specimens. More tests will be performed to further examine the phenomenon.

Keywords: Temperature load, Restraint, Cracks, Steel fibres.

1. INTRODUCTION

An area of application where steel fibres are frequently used today is as crack distribution reinforcement in thin ground supported concrete structures such as slabs cast on grade, repairs, overlays etc. It is quite clear that the major concern for such structures is related to stresses arising due to restrained deformation. Nevertheless, there is, to the author's knowledge, no generally accepted methodology available that enables a designer to predict crack spacing and widths based on the material properties of steel fibre reinforced concrete. In order to find such methods of design it is necessary to learn more about the behaviour of concrete structures subjected to restrained deformation. To develop such a method has been the main objective of this study.

Most often, imposed deformations in concrete overlays are connected to the process of drying shrinkage. However, in this case it was decided to apply a temperature differential as a load rather than a humidity gradient. The main reason for this choice was that drying shrinkage is a

long-term process that takes several months to develop fully. As a consequence, restrained shrinkage tests require lots of time to perform. Even so, the outcome of such tests is to a high degree uncertain. Thus, although it may not represent the actual load case for such applications in reality the use of temperature loads offers a number of benefits. Amongst other things it makes it possible to perform a test within a much shorter period of time. This provides a possibility to develop and refine a test method through a series of rather quick tests before finding a procedure that works satisfactorily. The test set-up and procedure that was eventually decided for in this study are described in more details below.

2. TEST PROGRAM

The test methodology described here was developed under a relatively long period of time, during which several tests were performed in order to refine the technique. For various reasons, the early tests did not provide information regarding the cracking behaviour of restrained concrete overlays. Thus, it was decided not to include these tests here. Instead, this report focuses on the last three tests that have been performed within the frames of a research program.

2.1 Specimen Details

The aim of the present study was to develop a test procedure that, in a realistic way, simulates the behaviour of concrete overlays exposed to restraint stresses. To fulfil this objective a test set-up was developed, see Figure 1 and Figure 2, consisting of a 200x1200x4200 mm bottom slab (1), constituting the substrate material. In order to be able to control the temperature in the substrate two coils of heating cables were embedded close to the top and bottom surfaces (2). Each coil produced a total effect of about 1,6 kW. Furthermore, the slab was prepared with Ø80 mm holes with an individual distance of 1 m along each side where Ø50 mm restraining ties were fitted (3). This made it possible to fasten the slab rigidly to the floor, to simulate a very stiff sub-grade.

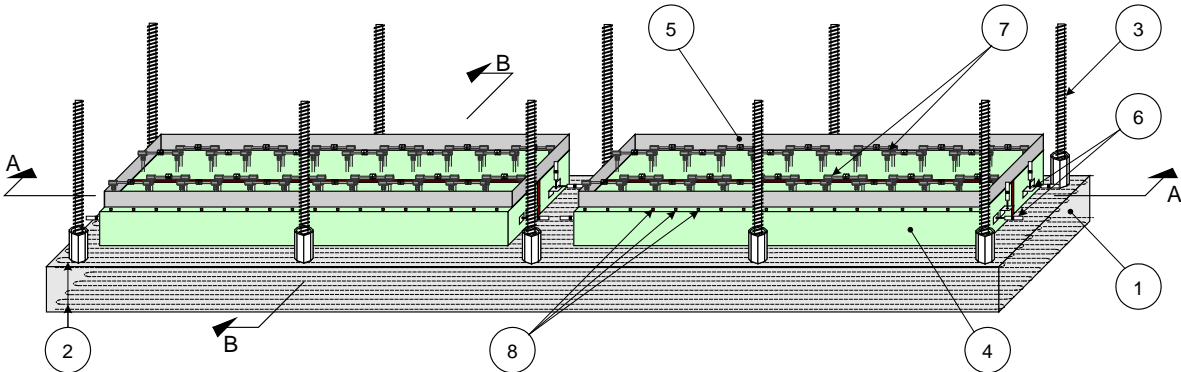


Figure 1 – Principle illustration of the test set-up used in the study.

Concrete toppings (4) with a depth of 150 mm, a width of 300 mm and a length of 1800 mm were then placed on top of the substrate, which had been previously cleaned and wetted 24 hours in advance in order to enhance the bond properties. At each test occasion two such specimens were cast side each other, one with plain and one with steel fibre reinforced concrete. More

details regarding the material properties of the concrete and fibres used at each test occasion can be found in Table 1. As can be seen in Figure 1 and Figure 2 the upper surfaces of the overlays were also provided with borders of sheet metal (5). The reason for this was to prevent the cold water, which was used to create the temperature gradient, from running off the upper surface of the overlays in an uncontrolled fashion. Also shown are the different gauges for measuring deformations (6, 7 and 8). These are described in more detail in section 2.3.

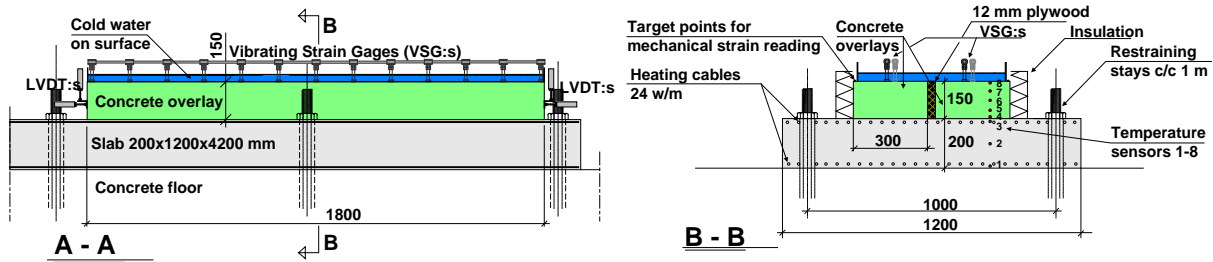


Figure 2 – Sections through the test set-up showing some measures and instrumentation.

2.2 Test Procedure

In order to reach a state of stress in the concrete overlays that would lead to cracking one of the main issues was to create as large temperature difference between the top and bottom faces of the test specimens as possible. At the same time it was necessary to restrain the specimens to avoid free deformation. The testing technique that was adopted to fulfil these requirements is schematically presented in Figure 3.

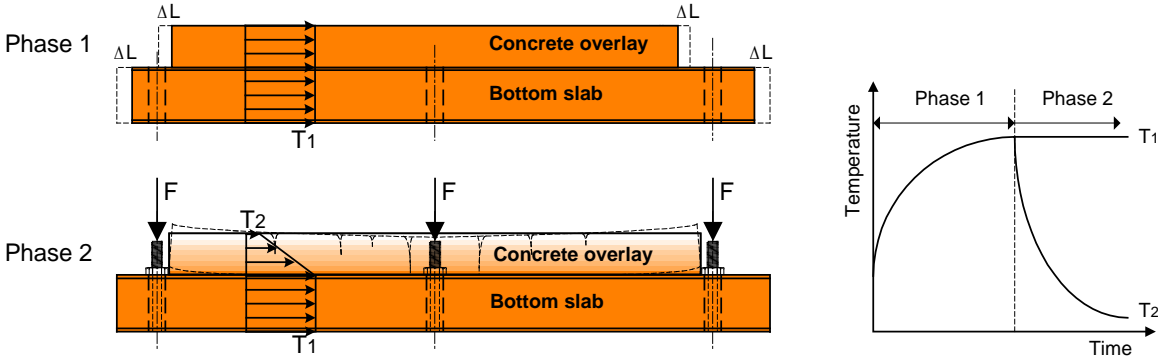


Figure 3 – Schematic illustration showing the different phases of the test procedure.

Each test was initiated by heating up the specimens to a certain temperature using the embedded heating cables, phase 1 in Figure 3. During the heating process the slab was free to move in order to avoid pre-stressing the specimens. Also, in order to avoid too great differences in temperature between the various parts of the test set-up the overlays were covered with a layer of insulation, see section B-B in Figure 2. After reaching a maximum temperature the bottom slab was fastened to the floor by applying loads to the restraining ties. By doing so further movements of the test set-up could be avoided and the bottom slab could be seen as a stiff sub-grade. At this point, corresponding to the initiation of phase 2, cold water was distributed on the upper surface of the

concrete overlays, which lead to a rather steep temperature decrease. At the same time the heating cables in the slab made it possible to maintain a fairly high temperature in the sub-grade. In this way temperature gradients of substantial magnitude rapidly developed over the depth of the overlays. As a consequence tensile stresses, that gradually lead to the formation of cracks, were created in the concrete toppings.

2.3 Instrumentation

The instrumentation that was used in the tests to provide information about temperature distribution and deformations is evident from Figure 1 and Figure 2. As can be seen thermocouples were embedded at different levels both in the bottom slab and in the overlays, sensors 1 to 3 in the slab and 4 to 8 in the concrete overlays. This made it possible to follow the temperature development throughout the different phases of the testing procedure. Expected deformations that are valuable to follow for the type of structure studied here are longitudinal strains in the concrete overlays and the relative movements between slab and toppings at the ends. For reasons of verification, it was decided to use two different types of strain reading devices to measure longitudinal deformations on the upper surfaces of the specimens, Vibrating Wire Strain Gauges (VSG:s) and target points for mechanical measurements, see (7) and (8) in Figure 1 and Figure 4. As is evident from the name the VSG:s use the vibrating wire principle when measuring strains. The implication of this is further developed in [1]. Manual measurements were performed using a mechanical reader of the type Staeger, which was positioned between two succeeding target points.

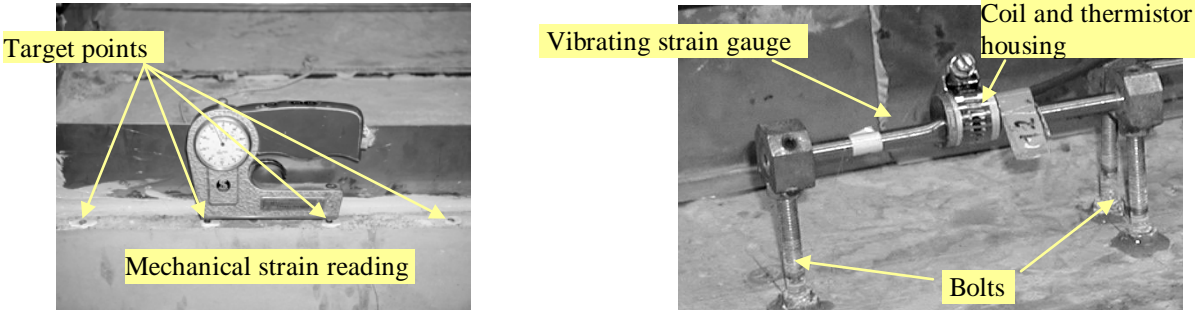


Figure 4 – Strain measurement devices used in the study. A mechanical strain reading device to the left (Staeger) and a Vibrating Wire Strain Gauge (VSG) to the right.

Horizontal and vertical displacements of the ends of the overlays were measured by means of Linear Voltage Differential Transducers (LVDT:s) as can be seen in Figure 1 and Figure 2. At one end the displacements were measured relative to the floor while the displacements at the other end were measured relative to the bottom slab. The reason for this was mainly a shortage of available gauges but also the lack of space around the end zones of the overlays. Naturally, to enable measurements of end lifting and slipping in a correct way it would have been more reasonable to conduct the measurements relative the slab at both ends. However, measuring deformations relative to the floor at one end provided valuable information regarding the displacement of the complete set-up during the heating process. Also, this way of measuring made it possible to control that the bottom slab would not move during the cooling process.

2.4 Material Details

As the primary objective was to develop a test procedure that gave reliable results no predefined test program was followed in which a certain mix design was used. Thus, the concrete composition changed each time as is evident from Table 1. As can be seen a total of three recipes were designed, one for each test. In each case one mix was produced with steel fibres and one without. The amount of steel fibres, that were of the type DRAMIX[®] RC-65/35-BN from Bekaert, varied from 30 kg/m³ for the first test, 40 for the second and 20 for the last test.

Table 1 – Mix proportions and material properties.

Material	Test 1		Test 2		Test 3	
	Kg/m ³		kg/m ³		kg/m ³	
	PC:1	FRC:1	PC:2	FRC:2	PC:3	FRC:3
Cement type Slite Bygg	350	350	360	360	350	350
Limestone filler type Köping 500	150	150	180	180	150	150
Fine aggregate 0 – 8	1010	1010	968	968	1172	1172
Coarse aggregate 8 - 16	673	673	645	645	631	631
Superplasticizer Type Glenium 51	3,5	3,5	2,9	2,9	2,8	2,8
Water	178	178	190	190	192	192
Dramix [®] RC-65/35-BN	0	30	0	40	0	20
Water / Cement ratio (w/c)	0.51	0.51	0.53	0.53	0.55	0.55
Compressive strength, f_{cc} (MPa)	43,7	53,0	46,0	39,3	- ^{*)}	- ^{*)}
Uniaxial tensile strength, f_{ct} (MPa)	3,34	3,35	2,72	2,55	- ^{*)}	- ^{*)}
Ultimate flexural strength, f_{flu} (MPa)	5,63	6,32	5,46	5,46	- ^{*)}	- ^{*)}

^{*)} No values available.

The type of concrete that was composed was a self compacting one (SCC) with an intended cube compressive strength of 40 MPa after 28 days. To enhance the stability of the mix limestone filler, of the type Köping 500, in amounts of 150 and 180 kg/m³ were used. The cement was of type CEM I 42,5 R (Slite Bygg). Both coarse and fine aggregates used in the concrete were natural rounded materials from Riksten.

3 TEST RESULTS

3.1 Material properties

Material properties obtained from compressive, tensile and four point flexural tests are summarised in Table 1. The compressive strength was measured on 150 mm cubes while the tensile strength was obtained from uniaxial tests on Ø94 mm cylinders. In order to enable measurements of the crack width during the process of a tensile test the specimens were prepared with a notch giving a waist diameter of about 74 mm. This made it possible to conduct the tests under displacement control, which gave valuable information regarding the post cracking behaviour. A diagram showing the post cracking response of the plain and fibre reinforced concrete used in the first two tests, test 1 and 2, are shown in Figure 5 (a). Interesting to see is that the fibre reinforced concrete produced for the second test, FRC:2, exhibits about the same, if not poorer, performance as compared to the one produced in the first test, FRC:1. This is somewhat strange considering that the amount of fibres was less for FRC:1 than for FRC:2, 30

compared to 40 kg/m^3 . One explanation for this may have been that the number of fibres positioned in the actual fracture zone was greater for FRC:1 than for FRC:2. In a way this demonstrates the sensitivity of such test methods. On the other hand, both the compressive as well as the uniaxial and flexural tensile strengths were lower for FRC:2 which indicates that the concrete had a somewhat lower quality. This makes comparisons arguable.

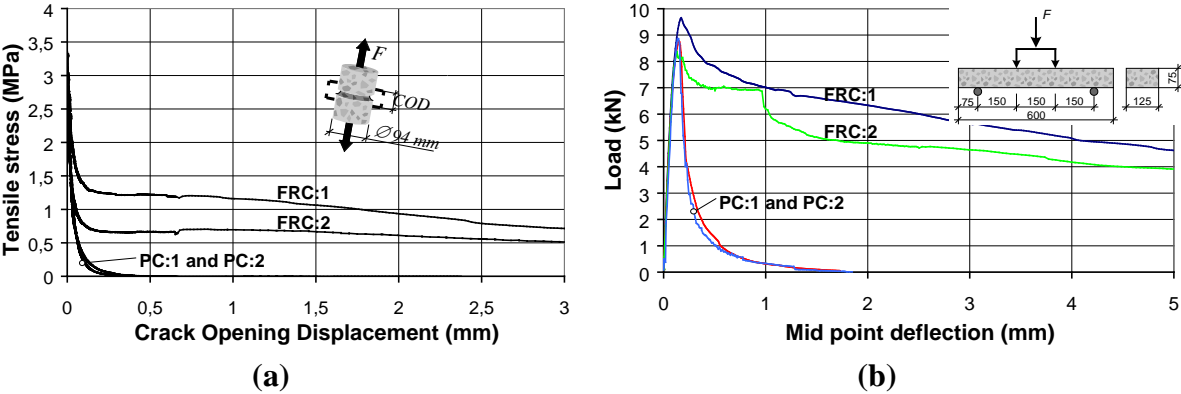


Figure 5 – The diagrams show results from uniaxial tensile tests in (a) and from four point flexural tests in (b). The reason why only results from tests 1 and 2 are presented here is that the results from the third test were not available at the time.

Flexural tensile tests were performed on $75 \times 125 \times 450 \text{ mm}$ beams in accordance with the ASTM C1018 standard, see e.g. [2] for a more detailed description. Results from tests on the plain and fibre reinforced concrete used in the first two tests are presented in Figure 5 (b). Similar to the results of the uniaxial tensile tests the fibre reinforced concrete showed a considerably better post cracking response as compared to the plain concrete.

3.2 Temperature development

An example of the temperature development during the different phases of the testing procedure for the first test, test 1, is shown in Figure 6. As can be seen there was a temperature difference, ΔT_1 , of maximum $13 \text{ }^\circ\text{C}$ between the slab and the overlays during the heating process. Generally, this is not good considering that a temperature difference equals a difference in expansion, which most certainly will create unintentional stresses in the system. However, as the slab was free to move during this phase of the procedure this was considered to have less significance for the final results. Also, prior to fastening the slab to the floor, the heating was turned off so that the temperature distribution would be more even. Accordingly, as can be seen in Figure 6, there was only a minor temperature difference, about $3 \text{ }^\circ\text{C}$, at this stage.

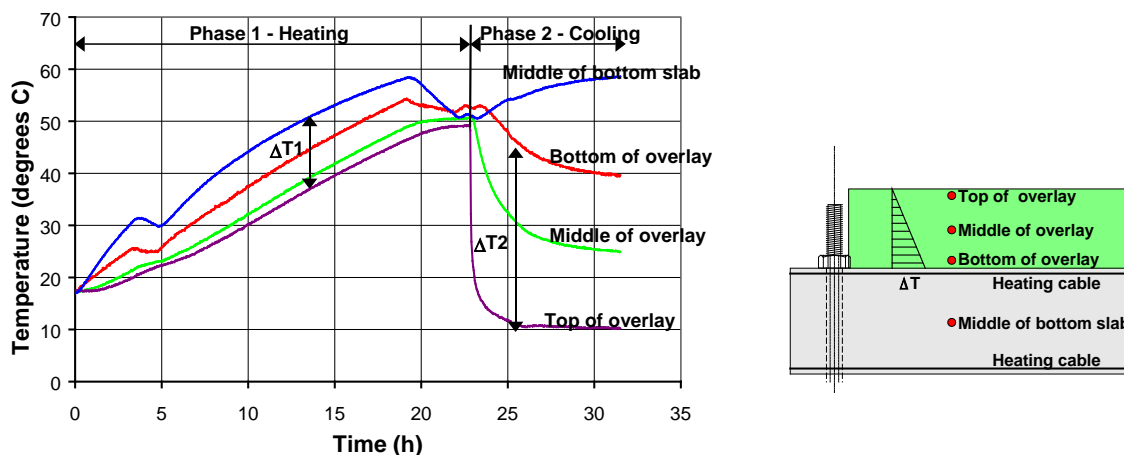


Figure 6 – Development of temperatures in the first test, test 1, during the different phases of the testing procedure in accordance with Fig. 3. Also, illustrated to the right are the positions of the thermocouples shown in the diagram.

The cooling process was then initiated by flushing cold water on the upper surface of the overlays. As is quite clear from the diagram this lead to a rather steep temperature fall at the top of the section, while the temperature close to the bottom of the overlays could be kept on a rather high level by restarting the heating of the bottom slab. In this way a temperature gradient, ΔT_2 , of up to a maximum of about 34 °C was reached. Evidently, this was enough to create tensile stresses that exceeded the strength of the overlay material, see Figure 7 and Figure 8. As the temperature developments for tests 2 and 3 were rather similar they will not be presented here.

3.3 Development of longitudinal strains

Longitudinal strains were measured using two different systems, Staeger and VSG:s, as shown in Figure 4. A comparison of the strain readings obtained with the different methods in the third test is shown in Figure 7 (a) and (b). It is quite clear that both methods of measuring gave reasonable results. The reason for the differences in magnitude of the readings, that are particularly conspicuous on the positive side, is that the measuring lengths are different, 150 mm for the VSG:s and 100 mm for the Staeger.

If the actual results are looked upon it can be seen that a dominating crack has formed approximately in mid section for both the fibre reinforced (FRC:3) and plain concrete (PC:3) specimens. In this case the crack width was less for FRC:3 than for PC:3, about 0,15 compared to 0,25 mm. Also, only two cracks were visible for FRC:3 compared to three for PC:3, which indicates that there may have been a slight contribution of the small amount of fibres used, only 20 kg/m³.

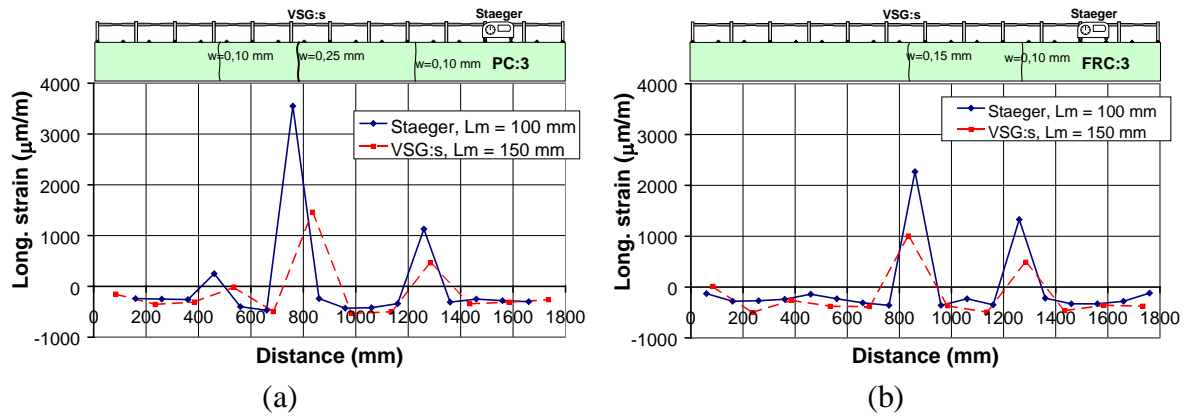


Figure 7 – Results from longitudinal strain measurements and some illustrations showing the visual cracks in the overlays from the third test, plain concrete in (a) and fibre reinforced in (b).

Longitudinal strain readings from the other tests, tests 1 and 2, are shown in Figure 8. The reason why only the Staeger readings are presented here is that there were some practical problems with the VSG:s which made the results a bit unreliable. Another problem, that becomes evident when trying to compare the results from the three tests, is that the measuring length of the Staeger readings, L_m , used in test 1 was 200 mm while only 100 mm in test 2 and 3. As a consequence the level of the measured strains over appearing cracks was substantially lower for test 1.

As was the case for the third test, a few dominating cracks with a rather extensive width formed in the overlays of tests 1 and 2 as well. From the diagrams shown in Figure 8 it is quite clear that the differences in cracking behaviour between the fibre reinforced and the plain concrete specimens were not striking. An explanation for this may be that the amount of fibres, 20 - 40 kg/m^3 , was too low to enable a good crack distribution. Especially when considering the rather abrupt load that was put on the overlays. Another possible reason may have been that the surface of the bottom slab was very rough, thus implying that the bond properties between the overlays and the substrate were exceptional. Naturally, this has also had a certain amount of influence on the resulting crack pattern.

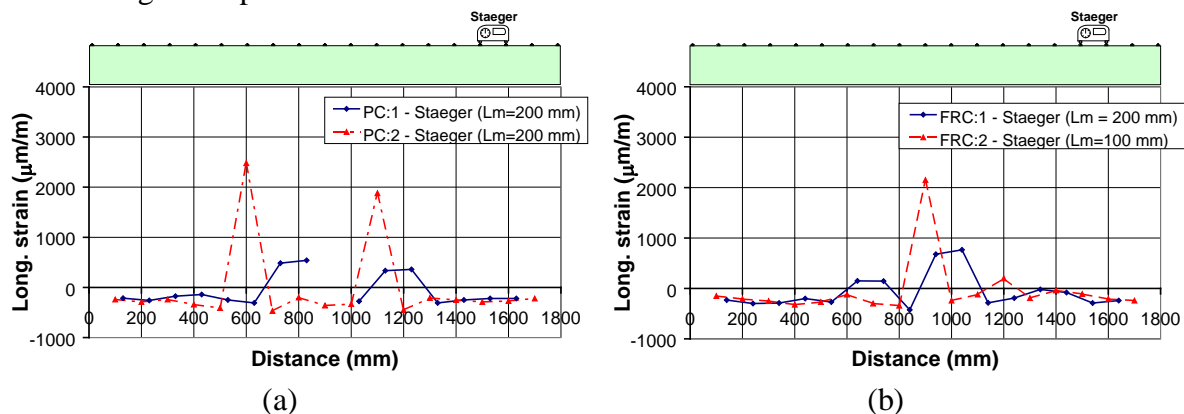


Figure 8 – Development of longitudinal strains measured with the Staeger device on the upper face of the overlays. Notice that the measuring length, L_m , was 200 mm for test 1 while only 100 mm for tests 2 and 3, which explains the rather big strain difference.

4 CONCLUSIONS

The principle aim of the presented study was to develop a test method for studying the crack distributing ability of steel fibres in restrained concrete overlays. Accordingly, a test methodology, where temperature gradients were used as loads, was developed and tested. Results show that, although there are still some problems that need to be solved, in particular regarding the way of creating the temperature gradient, it is possible to use the suggested method for studying the formation and propagation of cracks. Regarding the effect of steel fibres the tests that have been performed so far have not indicated any distinct differences in cracking behaviour between fibre reinforced and plain concrete specimens. However, a reason for this may have been that the amounts that have been used here, 20 – 40 kg/m³, were too low to give a sufficient contribution to the crack distribution. In particular considering that the temperature load was applied in a rather abrupt way.

REFERENCES

1. Geokon. "Instruction Manual Model VSM-4000 Vibrating Wire Strain Gage" Lebanon, USA: Geokon Inc., Geotechnical Instrumentation.1996.
2. Groth, P. "Fibre Reinforced Concrete – Fracture mechanics methods applied on self-compacting concrete and energetically modified binders," Doctoral Thesis 2000:04,Luleå University of Technology, Division of Structural Engineering. ISSN: 1402-1544. 2000.

Properties and Use of the Round, Determinately Supported Concrete Panel for Testing of Fibre Reinforced Concrete.



Jonas Holmgren
PhD, professor in Concrete Structures
Dept. of Structural Engineering (Byggkonstruktion)
Royal Institute of Technology (KTH)
SE-100 44 Stockholm
SWEDEN
E-mail: Jonas.Holmgren@struct.kth.se



Bert Norlin
PhD, senior lecturer in Steel Structures
Dept. of Structural Engineering (Byggkonstruktion)
Royal Institute of Technology (KTH)
SE-100 44 Stockholm
SWEDEN
E-mail: Bert.Norlin@struct.kth.se

ABSTRACT

The paper deals with a test specimen for steel fibre reinforced concrete suggested by Dr Stefan Bernard, Dept. of Civic and Environmental Engineering, Univ. of Western Sydney, Nepean, Australia. The test slab is analysed in the elastic state using FEM and in the plastic state using the yield line theory. Suggestions for how to replace certain beam test methods with the slab test are also made.

Key words: Concrete, fibres, slab, test method.

1. INTRODUCTION

1.1 General

One of the most important properties of fibre reinforced concrete is its ability to resist loading after cracking. This property is normally defined as the load carrying capacity of a certain type of test beam measured at a specified deflection. In most cases such tests exhibit large variations. Dr Stefan Bernard, Dept. of Civic and Environmental Engineering, Univ. of Western Sydney, Nepean, Australia, has invented a test specimen that gives very small variation in the recorded property. The test specimen is a circular slab, which is supported at three points and loaded at the centre. See Figure 1.

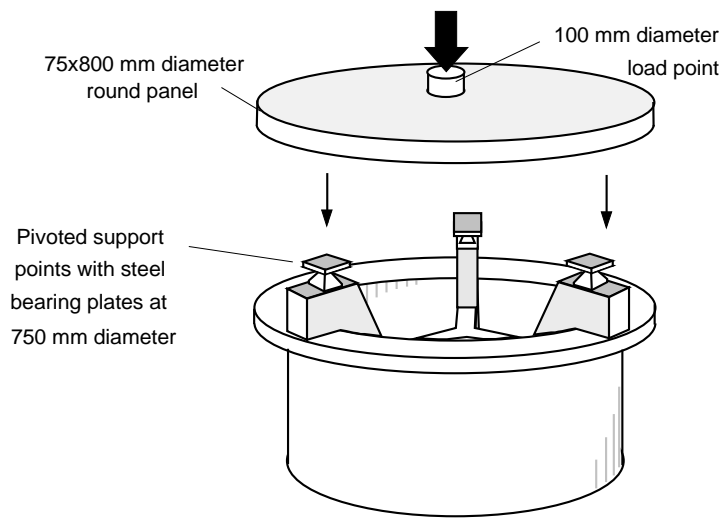


Figure 1 - The round, determinately supported concrete panel for testing of fibre reinforced concrete.

1.2 Other test methods

The most common test methods of today are the EFNARC beam test which is used in Norway and the modified ASTM C1018 beam test which is used in Sweden.

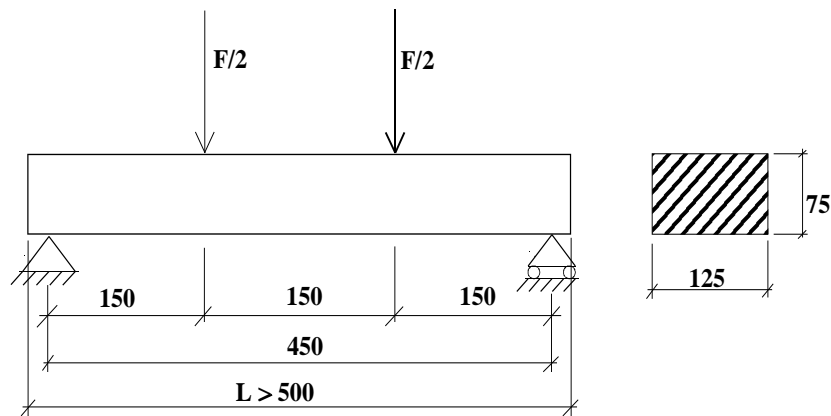


Figure 2 – Modified ASTM C1018 test beam used in Sweden

2. THEORETICAL ANALYSIS

2.1 Analysis according to theory of elasticity

The circular slab was analysed using linear elastic Finite Element analysis under small displacement conditions. The used mesh is shown in Figure 3 where some calculation results also are shown. The analysis was carried out using the ABAQUS 5.8 software. Eight node isoparametric shell elements were used (S8R) except at the centre where six node triangular shell elements (S3R) were used. Proper Multi Point constraints (MPCs) were applied at all

locations where mesh refinements or a change of element type was made, see Figure 3. This was done to secure continuity between elements.

Figure 4 shows the tangential stresses in the soffit along radii located in different angles from the radius where the support is situated. The curves show that the variation of the tangential stress is small when moving from the "support radius" and outwards.

The conclusion of this study is that a radial failure crack might fall anywhere within a large sector because of the natural variation of the failure strength of the concrete in the slab. The analysis of the slab according to the yield line theory must therefore take into consideration that the locations of the radial yield lines are highly arbitrary.

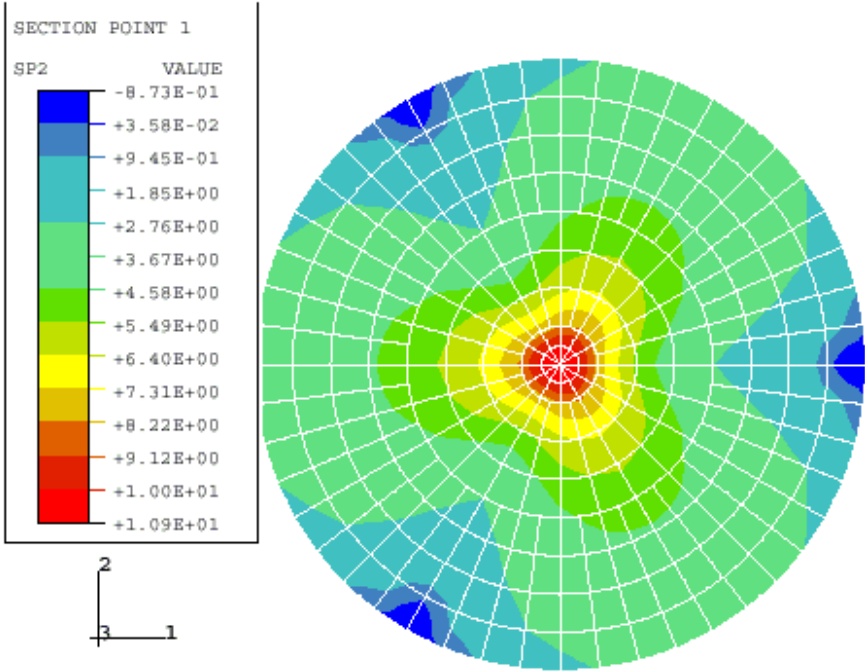


Figure 3 – Used mesh and principal stresses in the soffit of the slab. $P = 30 \text{ kN}$, $E = 34 \text{ GPa}$, $\nu = 0,2$.

Tangential stresses along a radius at 5 different angles to the intended crack direction

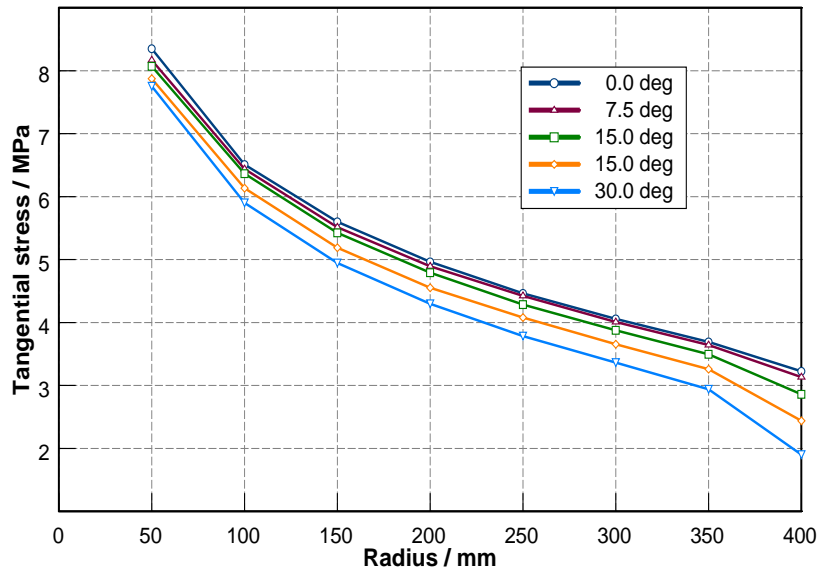


Figure 4 – Variation of tangential stresses in the soffit of the slab.

2.2 Analysis according to yield line theory

Geometrical relationships

In the yield line analysis it is assumed that the radial yield lines lie in angles α_A , α_B and α_C from one of the support radii which is defined as the x-axis in a rectilinear co-ordinate system. The supports have the co-ordinates $(x_1, y_1, 0)$, $(x_2, y_2, 0)$ and $(x_3, y_3, 0)$. The points of intersection between the yield lines and the periphery of the slab have the co-ordinates (x_A, y_A, δ_A) , (x_B, y_B, δ_B) and (x_C, y_C, δ_C) . The co-ordinates of the midpoint of the slab are $(0, 0, \delta_0)$. See Figure 5.

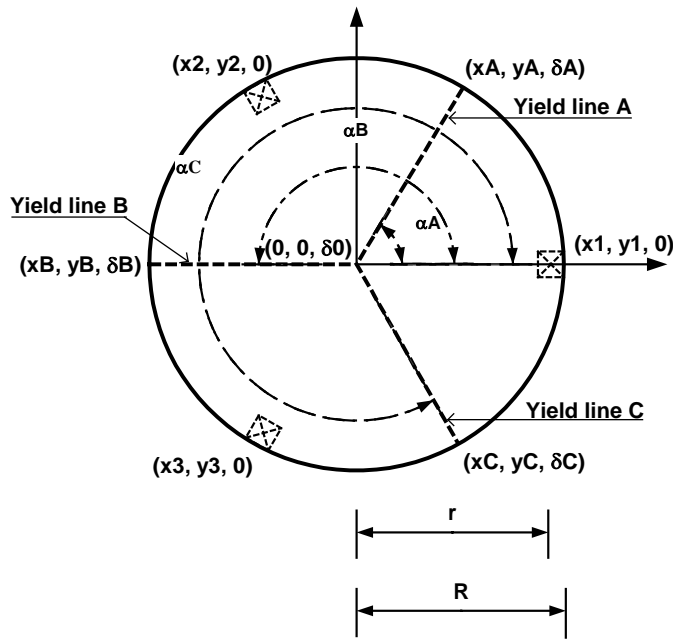


Figure 5 – Notations for yield line analysis.

The equations for the three planes that are formed when the mechanism is deflected are used for solving δA , δB and δC when $\delta 0$ is given. See Eqs. 1, 2, 3. The values for δA , δB and δC are then used for the calculation of the angles between the three planes. The type of formula used is shown in Eq. 4. Thus the relationship between the midpoint deflection and the angular deflection in the yield lines is established.

$$\begin{pmatrix} 0 & \delta 0 & 1 \\ 0 & 0 & 1 \\ y_A & \delta A & 1 \end{pmatrix} \cdot (x_C - 0) + \begin{pmatrix} \delta 0 & 0 & 1 \\ 0 & r & 1 \\ \delta A & x_A & 1 \end{pmatrix} \cdot (y_C - 0) + \begin{pmatrix} 0 & 0 & 1 \\ r & 0 & 1 \\ x_A & y_A & 1 \end{pmatrix} \cdot (\delta C - \delta 0) = 0 \quad (1)$$

$$\begin{pmatrix} 0 & \delta 0 & 1 \\ \frac{r\sqrt{3}}{2} & 0 & 1 \\ y_B & \delta B & 1 \end{pmatrix} \cdot (x_A - 0) + \begin{pmatrix} \delta 0 & 0 & 1 \\ 0 & \frac{-r}{2} & 1 \\ \delta B & x_B & 1 \end{pmatrix} \cdot (y_A - 0) + \begin{pmatrix} 0 & 0 & 1 \\ \frac{-r}{2} & \frac{r\sqrt{3}}{2} & 1 \\ x_B & y_B & 1 \end{pmatrix} \cdot (\delta A - \delta 0) = 0 \quad (2)$$

$$\begin{pmatrix} 0 & \delta 0 & 1 \\ \frac{-r\sqrt{3}}{2} & 0 & 1 \\ y_C & \delta C & 1 \end{pmatrix} \cdot (x_B - 0) + \begin{pmatrix} \delta 0 & 0 & 1 \\ 0 & \frac{-r}{2} & 1 \\ \delta C & x_C & 1 \end{pmatrix} \cdot (y_B - 0) + \begin{pmatrix} 0 & 0 & 1 \\ \frac{-r}{2} & \frac{-r\sqrt{3}}{2} & 1 \\ x_C & y_C & 1 \end{pmatrix} \cdot (\delta B - \delta 0) = 0 \quad (3)$$

$$\arccos(\theta_{12}) = \frac{\begin{pmatrix} 0 & \delta 0 & 1 \\ 0 & 0 & 1 \\ y_A & \delta A & 1 \end{pmatrix} \cdot \begin{pmatrix} 0 & \delta 0 & 1 \\ \frac{r\sqrt{3}}{2} & 0 & 1 \\ y_B & \delta B & 1 \end{pmatrix} + \begin{pmatrix} \delta 0 & 0 & 1 \\ 0 & r & 1 \\ \delta A & x_A & 1 \end{pmatrix} \cdot \begin{pmatrix} \delta 0 & 0 & 1 \\ 0 & \frac{-r}{2} & 1 \\ \delta B & x_B & 1 \end{pmatrix} + \begin{pmatrix} 0 & 0 & 1 \\ r & 0 & 1 \\ x_A & y_A & 1 \end{pmatrix} \cdot \begin{pmatrix} 0 & 0 & 1 \\ \frac{-r}{2} & \frac{r\sqrt{3}}{2} & 1 \\ x_B & y_B & 1 \end{pmatrix}}{\sqrt{\left[\begin{pmatrix} 0 & \delta 0 & 1 \\ 0 & 0 & 1 \\ y_A & \delta A & 1 \end{pmatrix} \right]^2 + \left[\begin{pmatrix} \delta 0 & 0 & 1 \\ 0 & r & 1 \\ \delta A & x_A & 1 \end{pmatrix} \right]^2 + \left[\begin{pmatrix} 0 & 0 & 1 \\ r & 0 & 1 \\ x_A & y_A & 1 \end{pmatrix} \right]^2 + \left[\begin{pmatrix} 0 & \delta 0 & 1 \\ \frac{r\sqrt{3}}{2} & 0 & 1 \\ y_B & \delta B & 1 \end{pmatrix} \right]^2 + \left[\begin{pmatrix} \delta 0 & 0 & 1 \\ 0 & \frac{-r}{2} & 1 \\ \delta B & x_B & 1 \end{pmatrix} \right]^2 + \left[\begin{pmatrix} 0 & 0 & 1 \\ \frac{-r}{2} & \frac{r\sqrt{3}}{2} & 1 \\ x_B & y_B & 1 \end{pmatrix} \right]^2}} \quad (4)$$

Some numerical studies of the effect of deviation of the yield line from its theoretical position have been made. In short they showed that a deviation of 10° gave a variation in the angular displacement of approximately 10%. The study also showed that an increase of the angular displacement of one yield line was combined with a decrease for another yield line. See Figure 6.

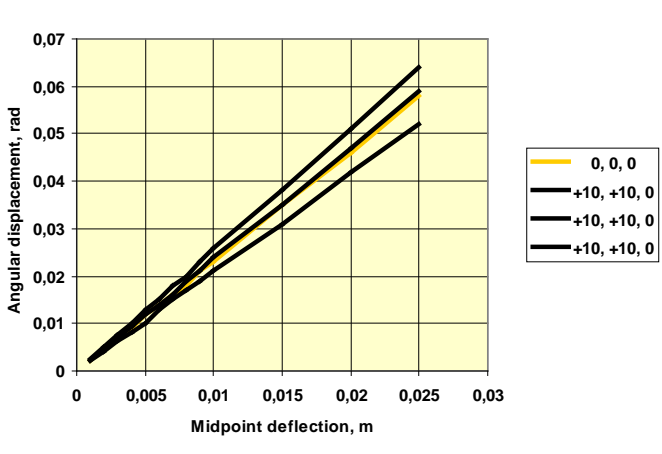


Figure 6 – Angular displacement in yield lines as a function of midpoint deflection. Curve 0, 0, 0 represents the theoretical position of all three yield lines. Curves +10, +10, 0 represents the case when the two "first" yield lines deviate 10° in positive direction and the "last" one does not deviate.

Force relationships

As it cannot be assumed that the three slab sectors carry their part of the total load independently of each other, nodal forces at the points of intersection between the yield lines and the periphery of the slab are assumed. These are denoted KA, KB and KC. The portion of the total load which is carried by each sector is denoted P1, P2 and P3, respectively. Since the angular displacement of each yield line cannot be assumed to be equal, three moment capacities – one of each yield line has to be assumed: mA, mB and mC. Angles between yield lines and the x-axis as well as some help angles are defined in Figure 7. A variable of the type d0LAB denotes the distance between point 0 (the midpoint) and the line between points A and B.

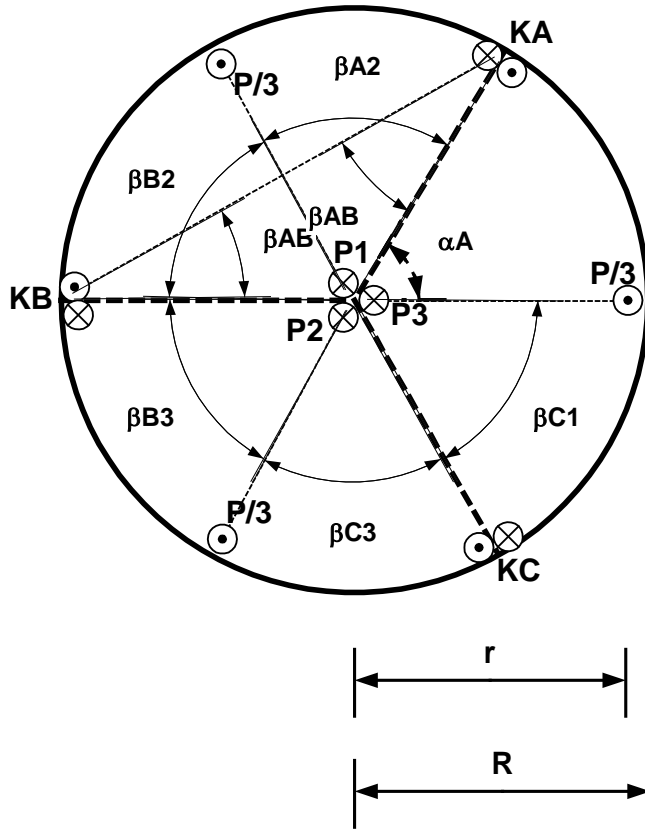


Figure 7 – Notation for forces and angles.

The system of equations for solving the unknowns is shown below.

$$KA \cdot \sin(\beta A2) - mA \cdot \cos(\beta A2) + mB \cdot \cos(\beta B2) + KB \cdot \sin(\beta B2) = 0 \quad (5)$$

$$KB \cdot \sin(\beta B3) - mB \cdot \cos(\beta B3) + mC \cdot \cos(\beta C3) + KC \cdot \sin(\beta C3) = 0 \quad (6)$$

$$KC \cdot \sin(\beta C1) - mC \cdot \cos(\beta C1) + mA \cdot \cos(\alpha A) + KA \cdot \sin(\alpha A) = 0 \quad (7)$$

$$mA \cdot R \cdot \cos(\beta AB) + mB \cdot R \cdot \cos(\beta AB) - \frac{P}{3} \cdot d2LAB - P1 \cdot d0LAB = 0 \quad (8)$$

$$mB \cdot R \cdot \cos(\beta BC) + mC \cdot R \cdot \cos(\beta BC) - \frac{P}{3} \cdot d3LBC - P2 \cdot d0LBC = 0 \quad (9)$$

$$mC \cdot R \cdot \cos(\beta CA) + mA \cdot R \cdot \cos(\beta CA) - \frac{P}{3} \cdot d1LCA - P3 \cdot d0LCA = 0 \quad (10)$$

$$P1 + P2 + P3 - P = 0 \quad (11)$$

If the angles between the yield lines and the moments are known then the applied load, the nodal forces and the portions of the total load carried by each slab sector can be solved. It is not, however, possible to solve the moments when the angles between the yield lines and the applied load are known!

Constitutive relationship

In order to study the effect of variations in the angles between the yield lines which in turn gives a variation in the angular displacement in the yield lines a rather extreme relationship between the moment and the angular displacement of a yield line is chosen. See Figure 8.

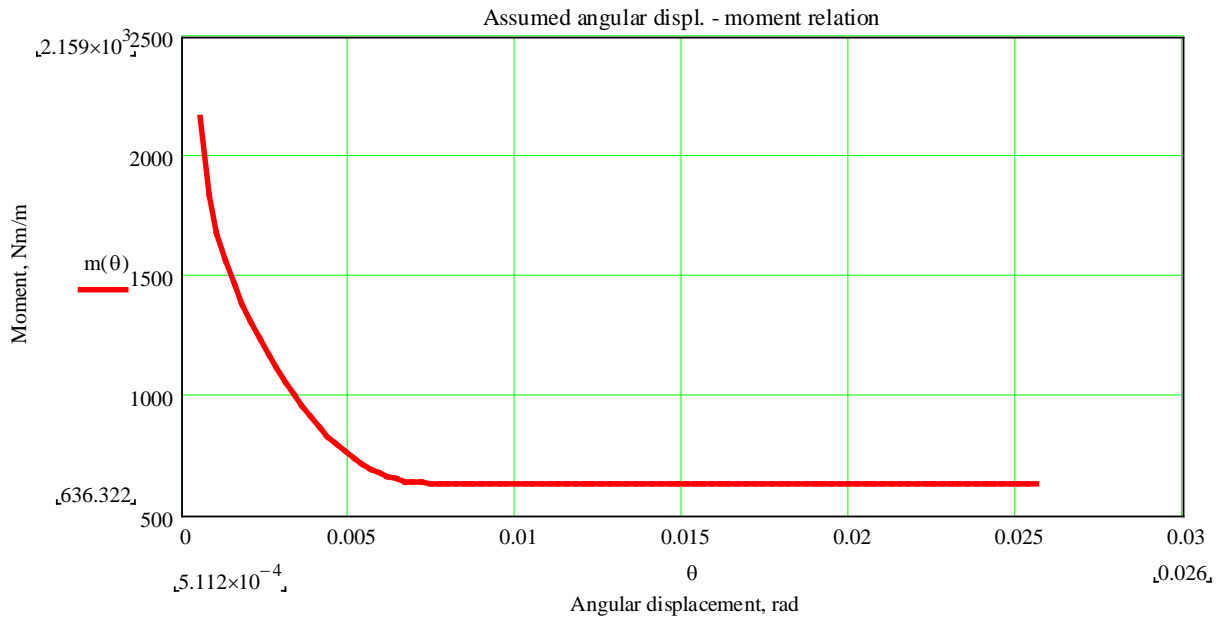


Figure 8 – Chosen relationship between angular displacement in yield line and the moment capacity of the yield line.

Results of the yield line study

In Figs 9 – 11 some results are shown. The curves in these figures clearly show that the total load that the slab carries is constant as long as the average of the three moment capacities of the yield lines remains constant.

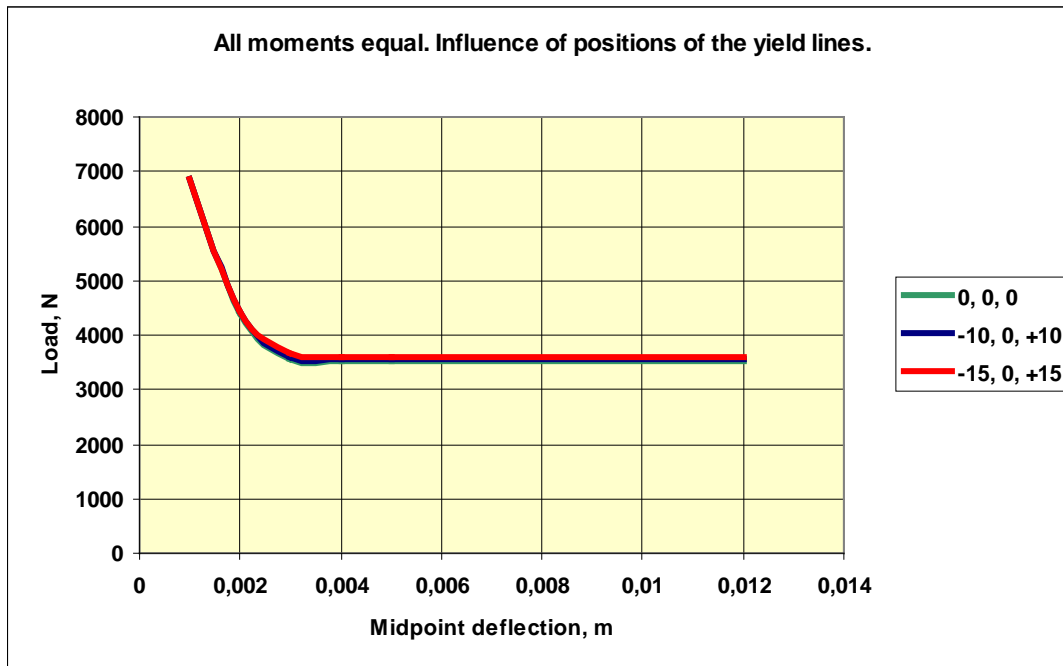


Figure 9 – Load – midpoint deflection curves for different deviations of the yield lines from the theoretical position. All moment capacities are equal.

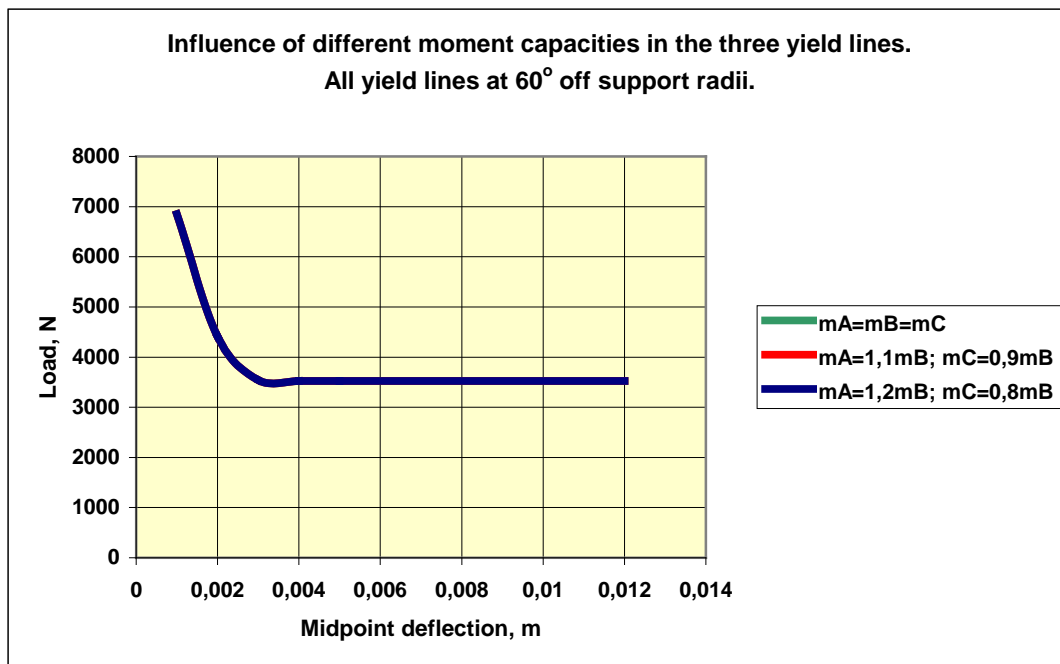


Figure 10 – Load – midpoint deflection curves for yield lines not deviating from the theoretical position. The moment capacities varies but their average is always = m .

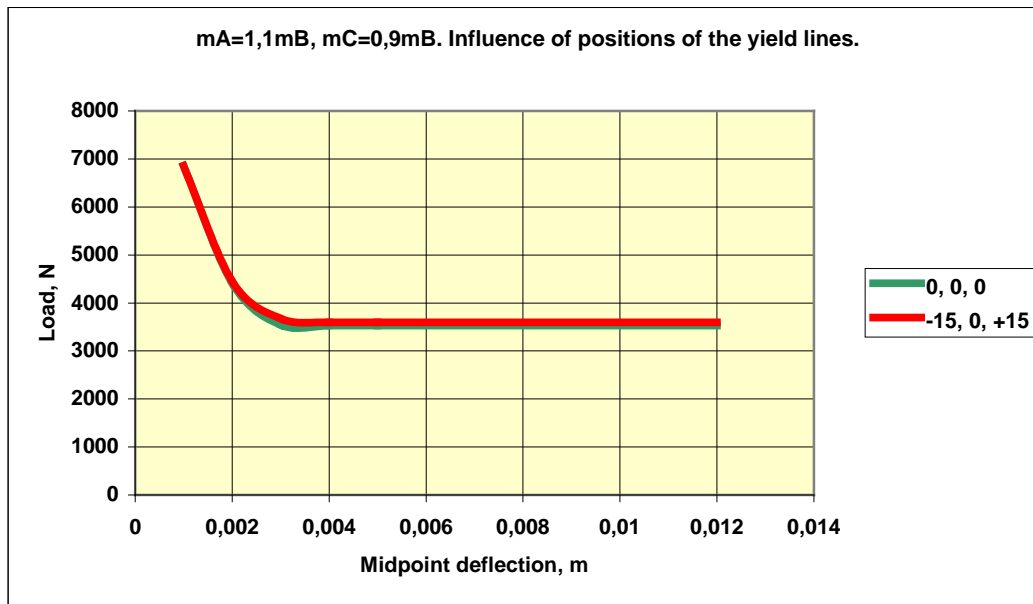


Figure 11 – Load – midpoint deflection curves for different deviations of the yield lines from the theoretical position. The moment capacities varies but their average is always = m

3. TRANSLATIONS FROM SOME BEAM TESTS TO THE ROUND, DETERMINATELY SUPPORTED CONCRETE PANEL TEST

In the Nordic countries the so called EFNARC beam or a modified ASTM C1018 beam are used as a basis for descriptions of the fibre reinforced concrete in contracts. A translation is needed until the round slab has become common in those countries.

The EFNARC test operates with load – deflection relationships for a well-defined beam i.e. for some specific deflection values a minimum nominal bending tensile strength is required. It means that the beam deflection can be translated to an angular displacement of the cracked section. The same angular displacement in the yield lines of the round panel can be translated to a midpoint deflection of the round panel. The required nominal strength of the beam can be translated to a moment capacity of the yield lines of the round panel at least as long as the thicknesses are about the same. Table 1 shows the midpoint deflections of the round panel which corresponds to the normally used deflections of the EFNARC beam.

Table 1 – Midpoint deflections for round panel when compared with EFNARC beam test

Midpoint deflection of EFNARC beam	Angular displacement	Midpoint deflection for round panel
1 mm	0,0044 rad	1,92 mm
2 mm	0,0089 rad	3,85 mm
3 mm	0,0130 rad	5,80 mm

From an equation of equilibrium for one sector, where all moments are assumed equal one obtains

$$m = P \frac{r\sqrt{3}}{9R} \quad (12)$$

With $R = 0,8$ and $r = 0,75$, slab thickness = 0,075 and using Navier's formula for bending stresses one finds

$$f = 192P \quad (13)$$

where f shall be compared with the required nominal flexural strength.

The modified ASTM C1018 test used in Sweden also operates with load – deflection relationships but in a dimensionless form. This is obtained by referring all deflections to the deflection at first crack. Such a method would probably show to be impossible when dealing with the round panel test. Difficult definition problems would occur since there are normally three cracks that forms before the quasi-plastic state is developed. It would also be very difficult to discover the first crack at the soffit of the slab unless the slab is tested upside down. It is not recommended to define the requirements on fibre reinforced concrete in terms of residual strength factors if the intended test specimen is the round panel. For ongoing projects where the requirements are defined according to the modified ASTM C1018 used in Sweden a translation is possible, but then a modulus of elasticity for the concrete and a crack stress have to be assumed.

From $E = 30$ GPa and $f_{cr} = 3$ MPa it follows that $\theta_{cr} = 0,0002556$ rad and the translation table below is obtained.

Table 2 – Translation from modified ASTM C1018 beam test to the round panel test

Toughness index	Angular displacement in crack I	Angular displacement in crack II	Midpoint deflection for round panel
I_5	$3,5\theta_{cr}$	= 0,00089 rad	0,385 mm
I_{10}	$5,5\theta_{cr}$	= 0,0014 rad	0,61 mm
I_{30}	$15,5\theta_{cr}$	= 0,004 rad	1,75 mm
I_{50}	$25,5\theta_{cr}$	= 0,0065 rad	2,82 mm

$f_{5.10} = 192 P_{avg}$, where P_{avg} is the average of P 's at 0,385 and 0,61 mm deflection of the round panel.

$f_{10.30} = 192 P_{avg}$, where P_{avg} is the average of P 's at 0,61 and 1,75 mm deflection of the round panel.

$f_{10.50} = 192 P_{avg}$, where P_{avg} is the average of P 's at 0,61 and 2,82 mm deflection of the round panel.

4 CONCLUSIONS

The following conclusions can be drawn from this limited study.

- i. The round, determinately supported concrete panel test gives the averaged moment capacity of 1,2 m yield lines.
- ii. It is not possible to discover moment capacity variations within the slab.
- iii. The test is insensitive to variations in the position of the cracks.
- iv. The test results can be translated to EFNARC test results.

- v. The test results can be translated to modified ASTM C1018 test results after some approximations.

Load Bearing Capacity of Steel Fibre Reinforced Shotcrete Linings



Ulf Nilsson, M.Sc. Ph.D. Student
Department of Structural Engineering, Concrete structure
Royal Institute Of Technology, Stockholm Sweden
E-mail: ulf.nilsson@struct.kth.se

ABSTRACT

An experimental investigation of the flexural behaviour of Steel Fibre Reinforced Concrete (SFRC) has been carried out in order to improve design methods for SFRC tunnel linings and similar applications. A large number of suspended slabs and beams with fixed ends were tested, with the intention of gaining a clearer understanding of how these structural elements behave during failure. The calculations, which were based on yield line theory, were in poor agreement with the test results in that the estimated capacities were consistently lower than the actual load bearing capacity of the specimens. From the tests it was clear that compressive arch action enhanced the load bearing capacity of the specimens and that this phenomenon led to the error in the calculated values.

Key words: Concrete, fibre reinforced, slabs, structural design, tunnel linings

1. INTRODUCTION

1.1. General

To use SFRC in tunnels in order to secure the rock has become a very common method all over the world in recent years. It proffers a rapid rate of application, saving in labour and a good economy compared to ordinary reinforced concrete, generally in form of steel wire mesh, [1]. However, to make an economical, safe and from an engineers point of view proper design is not possible today. This is due to the non-linear behaviour of fibre reinforced concrete, the lack of design methods, which incorporates this behaviour, and the fact that a tunnel lining is a very complex structure, [2].

1.2 Structural design

If it is assumed that a rock mass cannot support itself even if an adhering shotcrete lining is applied, a rock-anchored reinforced shotcrete lining must be adopted. The gravity load from the

loosened rock has in this work been treated as a uniform load acting on the reinforcement. A tunnel supported by sprayed concrete and rock bolts may then, from a design point of view, be considered as a slab supported by columns where each column represents a rock bolt,[3]. Under loading, this slab works as a number of edge restrained circular slabs with the load at the centre. Furthermore, the interaction between rock bolts and the shotcrete may also be considered as a beam with fixed ends, see Figure 1. Statically indeterminate structures made of ordinary reinforced concrete are often designed using yield line theory because of its simplicity and the efficient use of the material compared to a more conservative design based on elastic theory. It was therefore interesting to determine if yield line theory is applicable for SFRC as well.

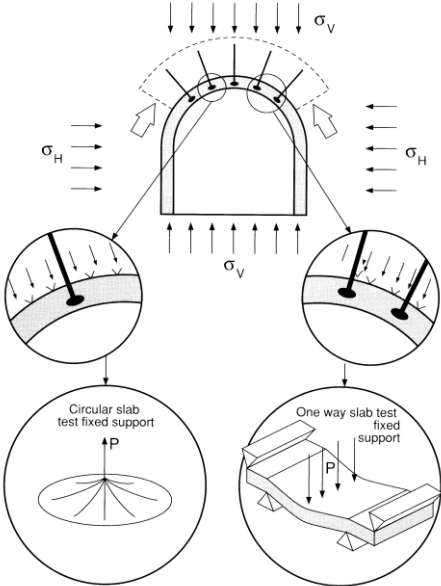


Figure 1 – Analogy between a bolted tunnel lining and test simulation, [4]

A throughout presentation of the study can be seen in, [5].

2. EXPERIMENTAL INVESTIGATION

2.1 General

The concrete used was a standard prescription for shotcrete used in tunnel linings in Sweden. Although the specimens produced in this investigation were intended to simulate a portion of a sprayed tunnel lining, all specimens were produced by casting instead of spraying. This was done because sprayed specimens are difficult to produce with good dimension tolerances in thickness and levelness. Many specimens were made with prefabricated notches in order to initiate rupture in those notches. This was done to make it easier to compare the test results with an expression for the bending moment capacity in the beams and the slabs. The fibre content in the beam tests was 60 kg/m³ and 100 kg/m³, respectively. In the slab tests, the fibre content was 40 kg/m³ and 60 kg/m³ respectively. These two latter amounts were chosen because they are very common in applications such as tunnel linings. The dosage rate of 100 kg/m³ in the beam tests was chosen in an attempt to obtain a strain hardening type of SFRC. The fibres used in this

investigation were Dramix RC-65/35-BN. The variables examined within each set of specimens included: dosage of fibres, specimen dimensions, and location of prefabricated notches. To determine the influence of compressive arch action in the specimens, eight slabs and four beams were manufactured. These were cast with the same type of concrete as the other specimens, except that there were no fibres in the concrete. Before testing, deep notches were sawn in the specimens to eliminate the tension capacity of the concrete during failure. This meant that the resulting load bearing capacity of the specimens could be attributed to the compressive arch action alone.

2.2 Testing of beams

The beams were of uniform rectangular cross section having nominal dimensions of 100 mm height, 250 mm width and a length of 1860 mm. The beams were restrained against rotation and translation at both ends and had a span of 1500 mm, see Figure 2. They were tested under third-point loading. The experimental program included four types of beams, varying in fibre content and position of prefabricated notches. The notches were 50 mm deep in the unreinforced beams and 30 mm deep in the fibre reinforced beams.

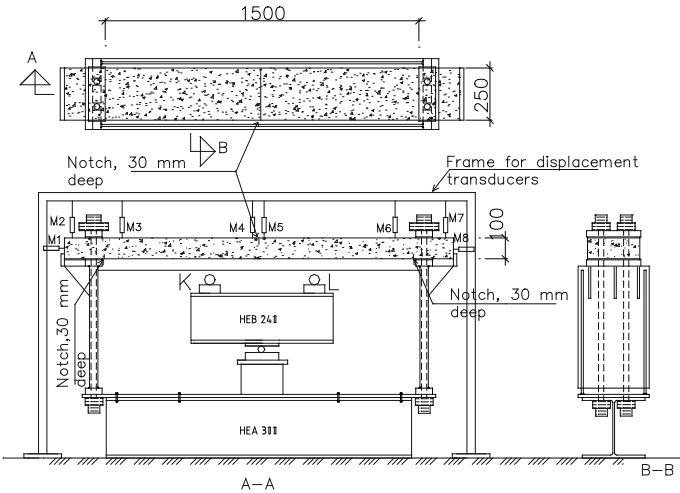


Figure 2 – Test set-up for beam with a notch in the middle

In Figure 3 the support conditions for the beams are detailed.

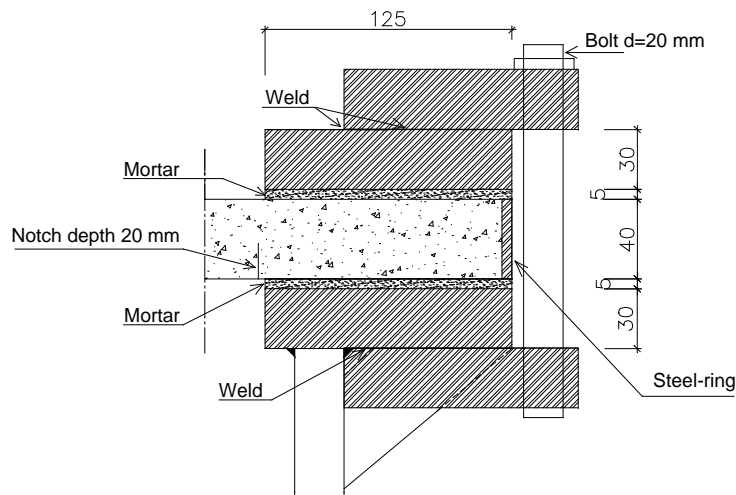


Figure 5 – Support conditions for the slabs

2.4 Results from the beam tests

Almost every beam failed as intended by a bending failure at the prefabricated notches. It was observed that the shape of the loading-displacement curves differed from the normal shape of steel fibre reinforced concrete, since the load-bearing capacity generally increased significantly after the cracking load was reached. The results also indicated that the beams made of plain concrete displayed almost the same peak load capacity as the reinforced beams. However, the capacity to carry load at large deformations was a great deal less for the unreinforced beams. The final condition of one of the beams with a notch in the middle and a fibre content of 60 kg/m³ can be seen in Figure 6.

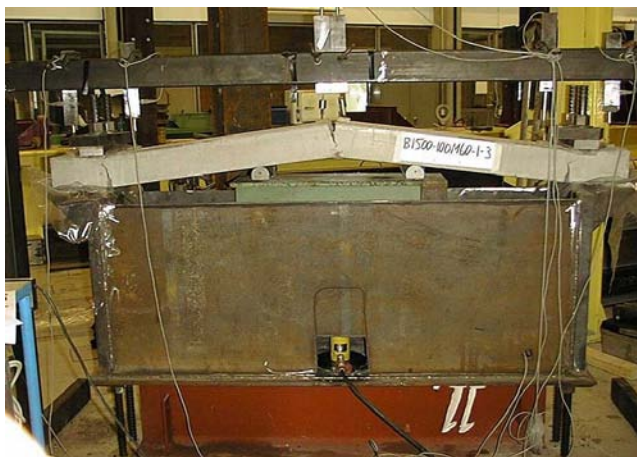


Figure 6 – Final condition of a fibre reinforced beam with a notch in the middle

Examples of load/displacement curves obtained in the tests are shown below. Figure 7 indicate a comparison between a fibre reinforced beam and a beam made of plain concrete.

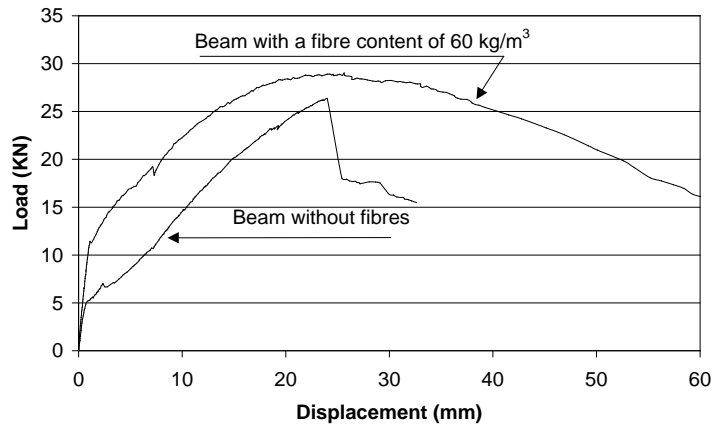


Figure 7 – A comparison between a fibre reinforced beam (60 kg/m^3) and a beam made of plain concrete

2.5 Results from the slab tests

The typical failure mechanism for the slabs was a tough bending failure followed by punching at the centre, which generally occurred after a large deformation. The slabs with the smaller diameter had the greatest peak load capacity, while the bigger slabs generally displayed the toughest type of failure. As can be seen in Figure 8, a large number of radial cracks developed during each test in the slabs without prefabricated radial notches. The slabs with prefabricated notches displayed a failure mode in which radial yield lines mainly developed within the notches.

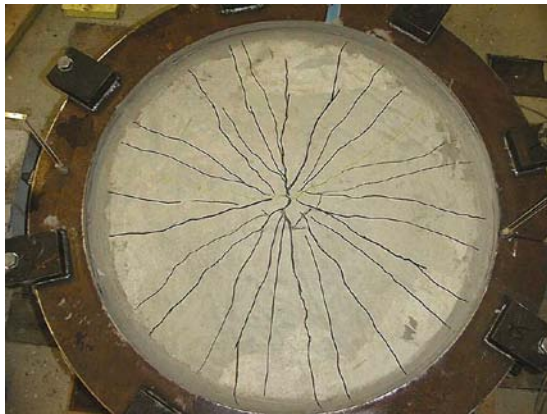


Figure 8 – Final failure of a fibre reinforced slab without notches.

The peak load capacity and the toughness were more or less the same for the slabs whether they were reinforced with fibres or not. Figure 9 displays a comparison of slabs with a span of 936 mm and a thickness of 40 mm.

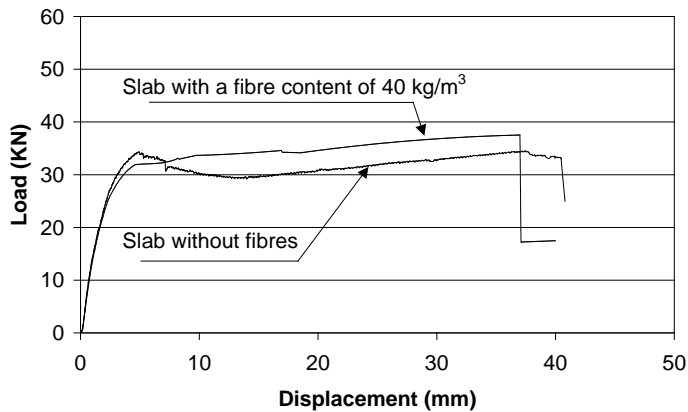


Figure 9 – A comparison between a fibre reinforced slab (40 kg/m^3) and a slab made of plain concrete.

3. ANALYSES

Calculations of structural load capacity in the present specimens have been performed according to yield line theory. Yield lines in the slabs and in the statically indeterminate beams were treated like the cracked section of a statically determinate beam. The beams used for comparisons with the slabs and end restrained beams were cast at the same time and were separated into two categories. One set called reference beams (which had the same depth as the slabs and the statically indeterminate beams) and the other were produced and tested in accordance with the recommendations of the standard-test method, ASTM C1018.

Examples of the comparison between test results and the calculated load capacities can be seen below. The comparison is presented in diagrams where the load-displacement curve from the tests describes the average value obtained from one type of test specimen. The theoretical load capacities are presented as numerical solutions based on the moment crack-rotation relationship in the cracked section of the reference and ASTM beams.

3.1 Beams

The beam is loaded by two point loads according to Figure 10. A moment $m_{2\alpha}$ causes yield on the top of the beam. At the supports of the beam, a moment m_{α} causes yield in the bottom of the beam.

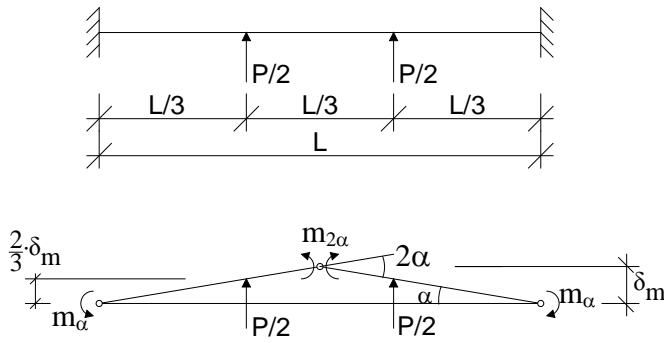


Figure 10 – Yield line pattern of the beams with a notch in the middle.

The failure load can be derived as

$$P_{\alpha} = \frac{6}{L} \cdot (m_{\alpha} + m_{2\alpha}) \quad (1)$$

In Figure 11, an example of comparison between calculated post-crack load capacity and test result for a beam with a fibre content of 60 kg/m^3 can be seen.

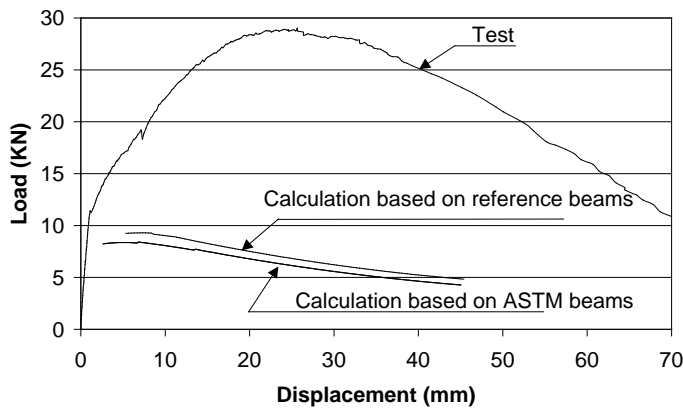


Figure 11 – Comparison between a beam with a fibre content of 60 kg/m^3 and numerical solutions according to yield line theory based on reference and ASTM beam tests

3.2 Slabs

The slab is loaded with a point load in the middle. A moment m_r per unit length causes yield on the upper surface of the slab. A moment m_t per unit length causes yield in the bottom of the slab according to Figure 12.

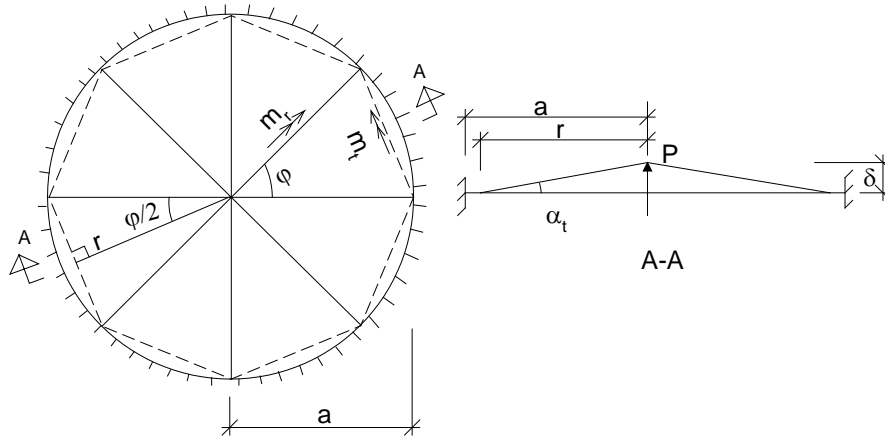


Figure 12 – Yield line pattern of the slabs

The failure load P is obtained as

$$P = 2 \cdot \pi \cdot (m_r + m_t) \quad (2)$$

In Figure 13, an example of comparison between calculated post-crack load capacity and test results for a slab with a span of 682 mm and a fibre content of 60 kg/m³ can be seen.

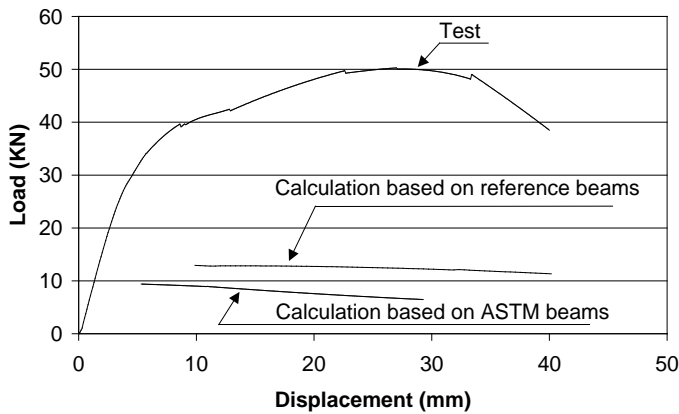


Figure 13 – Comparison between a test on a slab with a span of 682 mm and numerical solutions according to yield line theory based on reference and ASTM beams

4. DISCUSSION AND CONCLUSIONS

It was shown that yield line theory based on the rotation capacity at the yield lines was not able to predict the load bearing capacity of the test specimens. The calculated capacities were consistently lower than the actual capacities of the specimens. This can possibly be explained by the fact that compressive arch action is the main load carrying component of the specimens and that failure will occur when the concrete reaches its compressive strength limit in the compressed zones of the specimens. It was also observed that the calculations that were based on ASTM beam tests consistently resulted in lower load capacities compared with calculations

that were based on reference beams. The explanation of this is probably that a superior fibre effect was obtained in the reference beams, due to the fact that they are thinner than the ASTM beams. It is assumed that the arch effect arises at a deformation level where the concrete stresses are reasonably small when the slab is fibre reinforced. When the slab is bar reinforced it is assumed that the compressive stresses in the concrete because of bending alone are already in the vicinity of the concrete strength when the arch action arises. The remaining capacity of the compression zone is thus rather limited in the later situation. This assumption requires a thorough theoretical investigation, which remains to be performed.

In a structure that consists of several slab elements that cannot rotate and expand freely along its periphery, such as a bolted tunnel lining, compressive arch action will most likely arise in the element that is overloaded if the surrounding structure can resist horizontal forces. The structure will then carry the load by a resistance-moment between compressive forces in the element, instead of equilibrium between the tension zone and the compressive zone of the concrete section as in ordinary bending. This is very beneficial with respect to the peak load capacity of the structure, because the best load-carrying characteristic of concrete is its compressive strength.

REFERENCES

1. Bernard, E.S., The Influence of Edge Restraint on Flexural Behaviour in Square SFRC Slabs, Engineering Report no, CE 5, Dept. Of Civil and Environmental Engineering, Univ. of Western Sydney, Nepean, Kingswood NSW, Australia, July 1997, ISSN 1326-0693.
2. Bernard S., The behaviour of round steel fibre reinforced concrete panels under point loads, Engineering report no.CE8, Dept. of Civil and Environmental Engineering, Univ. of Western Sydney, Nepean, Kingswood NSW, Australia, June 1998, ISSN 1326-0693.
3. Holmgren J., The use of Yield-Line Theory in Design of Steel Fibre Reinforced Concrete Slabs, Proceedings, Advanced Design of Concrete Structures. K. Gylltoft, B. Engström, L.-O. Nilsson, N.- E. Wiberg and P. Åhman (eds) © CIMNE, Barcelona 1997, p. 249
4. Vandervalle M., N. V. Bekaert, Dramix Tunnelling the World, with 7 reference projects, Zwevegem 1991.
5. Nilsson, U., Load bearing capacity of steel fibre reinforced shotcrete linings, Licentiate Thesis, Department of structural engineering, Royal Institute of Technology, Stockholm 2000.

Steel Fibre Corrosion in Cracks – A Design Problem for Shotcrete Applications?



Erik Nordström
MSc., Senior Research Engineer
Vattenfall Utveckling AB, Concrete Technology
814 26 Älvkarleby, Sweden
E-mail: erik.nordstrom@vattenfall.com

ABSTRACT

Steel fibre reinforcement is commonly used for structural purposes in shotcrete applications. The influence on residual load-bearing capacity and mechanisms ruling corrosion of steel fibres in cracked concrete is not fully investigated. By performing field and accelerated exposures on cracked steel fibre reinforced concrete this is investigated. Crack width, fibre length end exposure environment are main parameters. Results from the first preliminary evaluations show that corrosion is a potential problem in environments with presence of chlorides. Measures like addition of extra amount of fibres, usage of other fibre materials or increased concrete thickness might be needed. This to ascertain wanted residual strength in the structure.

Key words: steel fibres, concrete, shotcrete, cracks, corrosion, service-life.

1. INTRODUCTION

1.1 General

From the design process via construction to maintenance of a structure the service-life should be focused on. Today's regulations e.g. TUNNEL 99 (1999) from the Swedish Road Authorities has service life demands for tunnels with an "expected technical service life" of 120 years ("normal" maintenance). A question contractors, designers and purchasers should have is whether steel fibre reinforced shotcrete can fulfil this service life demand. "Normal maintenance" could not possibly be reconstruction e.g. every 15-25 years with all the costs and disturbance to the use of a tunnel that would give (traffic problems, loss of production etc.). All presented experiments and results are from Nordström (2000).

1.2 Steel fibres and the shotcrete technique

Shotcrete is most commonly applied in relatively thin layers (typically 50-100 mm) and the concrete quality is high. This will give a high degree of shrinkage due to drying out and

therefore risk for cracks. High air speeds due to ventilation and usage of accelerators further increase this effect. Loads from movements in the substrate being shot on are another possible source to cracks. A positive property of shotcrete is that it is always applied on another substrate and due to the limited thickness the restraint also limits the crack width.

One could suspect that the relatively thin steel fibres would discontinue to carry load relatively fast due to decrease of fibre diameter caused by corrosion. Especially in cracked concrete. Previous investigations on cracked concrete however show that steel fibres corrode at a lower rate than conventional reinforcement at the same conditions. The parameters giving this positive property are not very well known. It is also possible that the rate of degradation is not linear.

2. FIELD EXPOSURE TESTS

To be able to examine the effect of different parameters on the rate of corrosion, field exposure tests are ongoing. The field exposure tests where started in September 1997.

2.1 Test program & specimen

The test program is showed in Figure 1. The mix type and mix design can be found in Table 1 and 2. The accelerator used was based on sodium silicate. Standard Portland cement (trade name Degerhamn Std P in Sweden) was used. There are three different exposure sites in addition to the control site in the laboratory:

1. National Road 40 (Rv 40) close to Borås, outdoor along a motor highway.
2. River Dal at Älvkarleby, outdoors with specimen partly immersed in river water.
3. Eugenia tunnel, a road tunnel in Stockholm.

To produce the specimens, large slabs where shot (2×1.25 m) after which beams where sawn from the slabs. Cracking of the beams was performed by applying a flexural load.

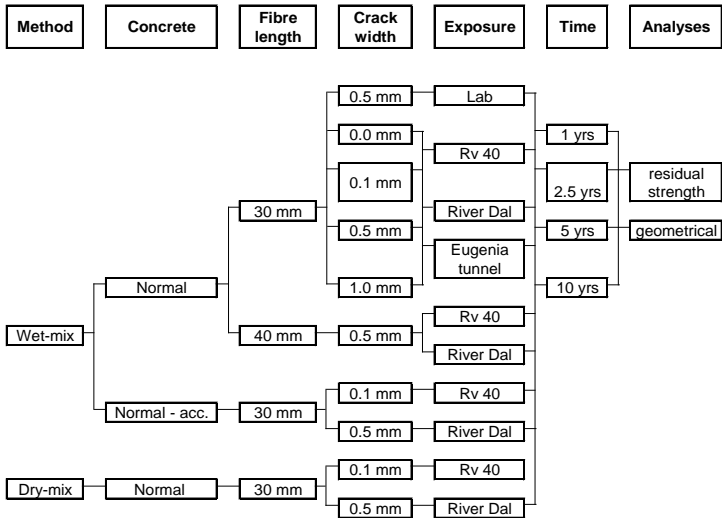


Figure 1 - Field exposure test program

Table 1 - Mix types

Mix	Method	Accelerator	Fibres
WA30	wet-mix	yes	Dramix 30/0.5
WA40	wet-mix	yes	Dramix 40/0.5
W30	wet-mix	-	Dramix 30/0.5
D30	dry-mix	-	Dramix 30/0.5

Table 2 - Mix design used in field exposure tests

		WA30	WA40	W30	D30
w/c		0.42	0.42	0.42	-
cement	(kg/m ³)	510	510	510	500
gravel, 0-8 mm	(kg/m ³)	1202	1202	1202	1101
sand, 0-1 mm	(kg/m ³)	298	298	298	398
plasticiser	(%/kg C)	1.4	1.4	1.4	
accelerator	(%/kg C)	3.5	3.5		
fibre dosage	(kg/m ³)	70	70	70	65

2.2 Evaluation after exposure

Two beams for every combination of mix design and exposure condition were brought back to the lab after exposure. One of the two beams was subjected to continued flexural loading up to 5 mm deflection. The other beam was cut into small plates at different distances from the crack mouth, as shown in Figure 2.

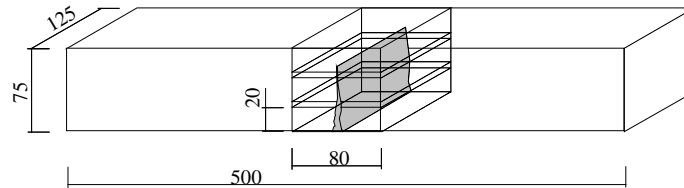


Figure 2 - Dismembering of beams (measurements in mm).

Residual strength

A typical test result is shown in Figure 3 where it can be seen that the residual strength increased ($w = 0.1$ mm) after exposure. In Figure 4 the trend after 1 and 2.5 years of exposure is shown. Beams with a crack width of 0.1 mm show a larger increase in residual strength compared to specimens with larger crack widths.

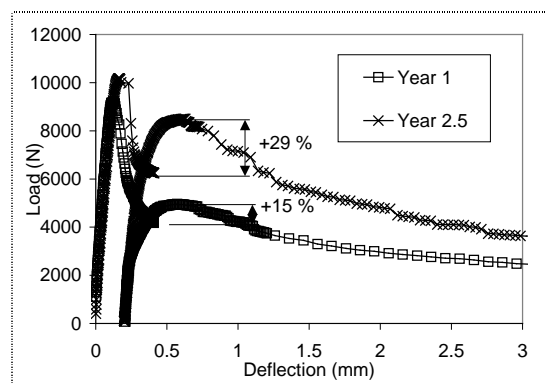


Figure 3 - Residual strength before and after 1 and 2.5 years of exposure (mix WA30, $w = 0.1$ mm, RV40).

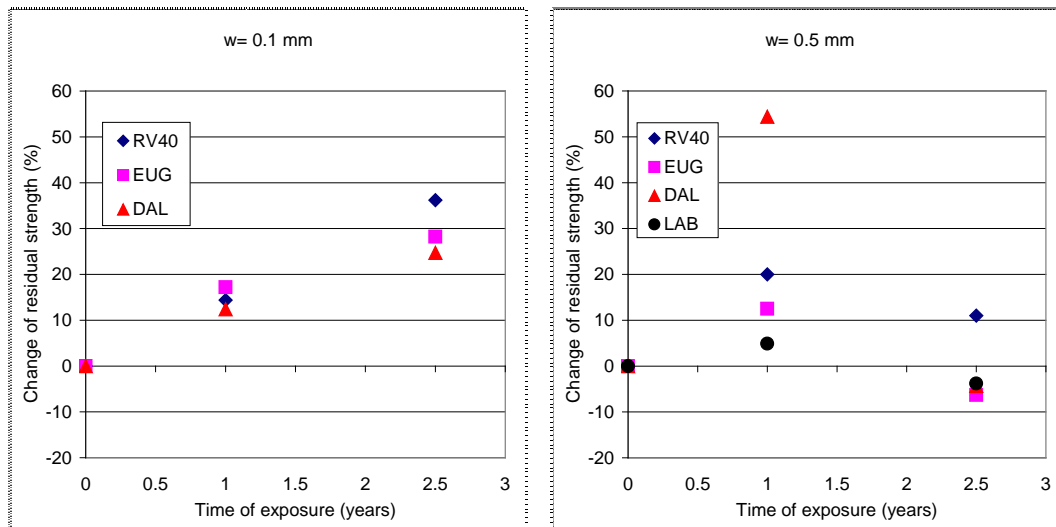


Figure 4 - Development of residual strength with time of exposure. $w = 0.1$ mm (left) and $w = 0.5$ mm (right).

Corrosion of fibres crossing cracks

There was an obvious risk for tensile failure of the fibres if the concrete was broken down by crushing. Break down by freezing was therefore used. Drying (200°C) followed by water saturation with vacuum treatment made it possible to fully degrade the concrete by freezing. After this the fibres crossing the crack could easily be taken out for examination. The depth of corrosion on single fibres was measured by using a micrometer.

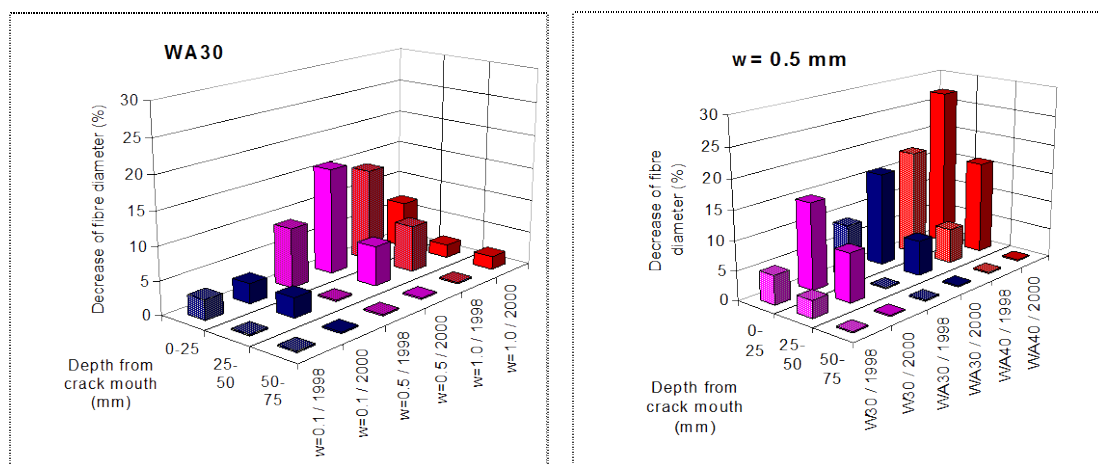


Figure 5 - Decrease of fibre diameter after 1 and 2.5 years of exposure at Rv40. Mix-type WA30 (left). $w = 0.5$ mm (right).

Table 3 - Change of residual strength (in percent) after exposure

Crack width (mm)	Motorway		Road tunnel		River		Lab	
	Rv40		Eugenia		Dal			
	1998	2000	1998	2000	1998	2000	1998	2000
0.1	15	29	17	28	10	25	-	-
0.5	20	11	12	-6	54	-4	5	-4
1.0	10	9	10	9	-2	-6	-	-

2.3 Discussion

Residual strength

The increase in residual strength with exposure was probably caused by continued hydration of the concrete and therefore increased anchorage strength. The increase is still higher for smaller crack widths and the effect of autogenous healing could be one reason. There is a trend that larger crack widths show the same or lowered residual strength at 2.5 years than at year 1 and this is probably due to brittle tensile failure of the corroded fibres.

Extent of corrosion

Corrosion was initiated after only one year of exposure at Rv40. It can be seen (in Figure 8) that the extent of fibre diameter reduction decreased with increased depth into the crack. It also appears that the 40 mm fibres show more severe damage from corrosion. This supports the theory that the galvanic effects related to the ratio of anode to cathode area is important. No significant difference between spraying methods could be seen. The effect of crack width on the extent of corrosion of fibres is no longer clear after 2.5 years. Fibres in the beams with a crack width of 0.5 mm had corroded more than those with a crack width of 1 mm. This supports the theory that crack width mainly affects the time to initiation of corrosion.

Practical consequences

Since corrosion of steel fibres has been initiated after only 2.5 years, the expected performance in a 120 year scenario should be questioned. There are two possible practical consequences of this, but these also depend on the results of further evaluations. Firstly, if it is not possible to achieve a sufficiently long service-life in steel fibre reinforced shotcrete if cracks occur. Then repair of cracks, use of more corrosion resistant fibres, or addition of an extra layer of fibre reinforced shotcrete will be required. Secondly, if the rate of corrosion propagation is so slow for narrow crack widths that cracks up to a certain critical width only decrease the service-life and residual strength to a limited extent. Then no further measures might be needed.

3. LABORATORY EXPOSURE TESTS

The main objective with the laboratory exposure tests was to make a relative comparison between different parameters tested under controlled climatic conditions. The field exposure tests can be used to estimate the degree of acceleration in the laboratory tests.

3.1 Test program & specimen

Three fibre lengths (35, 70 and 105 mm) and three crack widths (0.2 , 0.5 , 1.0 mm) are tested. The mix-composition is generally the same as in the field exposures. To make pouring possible with remained location of fibres the lower part was poured with plastic consistency and the upper part was poured with a more fluid consistency. The cement used is the same type as in the field exposure tests (Swedish standard Portland cement, Degerhamn). The specimen are cylindrical with a diameter of 57 mm and a length of 170 mm with a notch in the middle. The fibres where made from cutting cold-drawn wire into desired lengths. The wire used is the type being used in manufacturing of the Dramix-fibre from Bekaert. Demoulding after one day was followed by three days of water curing. Cracking was performed 5 days after pouring and to create a crack of desired width the samples where subjected to uniaxial stress and displacement

controlled loading (0.02 mm/s) To make the cracking of samples rational a device with friction grips was also constructed. The accelerated exposure test started 30 days after pouring of the samples. The temperature was 20°C for both environments.

CHLORIDE - Submerged in water with 3.5% chlorides (3 days) + Air with RH 50% (4 days).
 TAP WATER - Submerged in water (3 days) + Air with RH 50% (4 days).

3.2 Evaluation after exposure

The dismembering and evaluation was made in the same manner as in the field exposure tests and samples were taken out at 70 and 120 days of exposure.

Fibre corrosion

In general, corrosion have been initiated on all samples after 70 days. Samples stored in the CHLORIDE environment corrode more than samples stored in TAP WATER environment. The influence of both crack width and fibre length is obvious in the CHLORIDE environment.

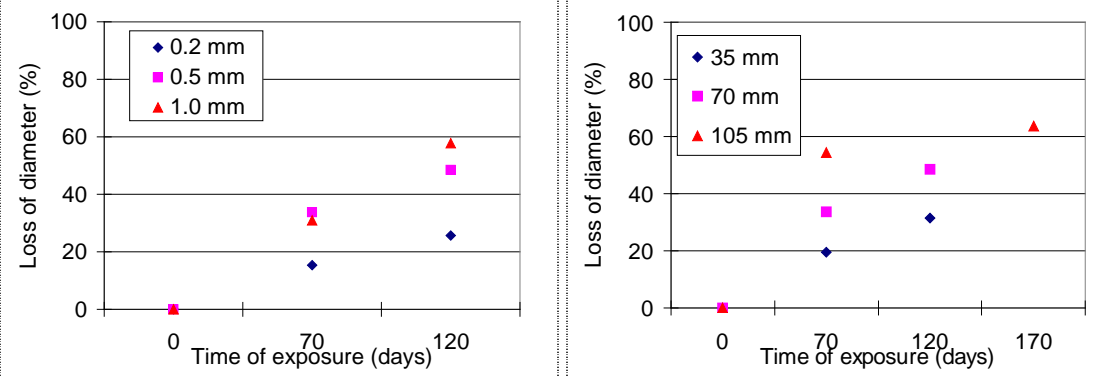


Figure 6 - Average loss of fibre diameter in CHLORIDE environment from one sample (37 fibres). Influence of crack width, L=70 mm (left) and fibre length, w=0.5 mm (right).

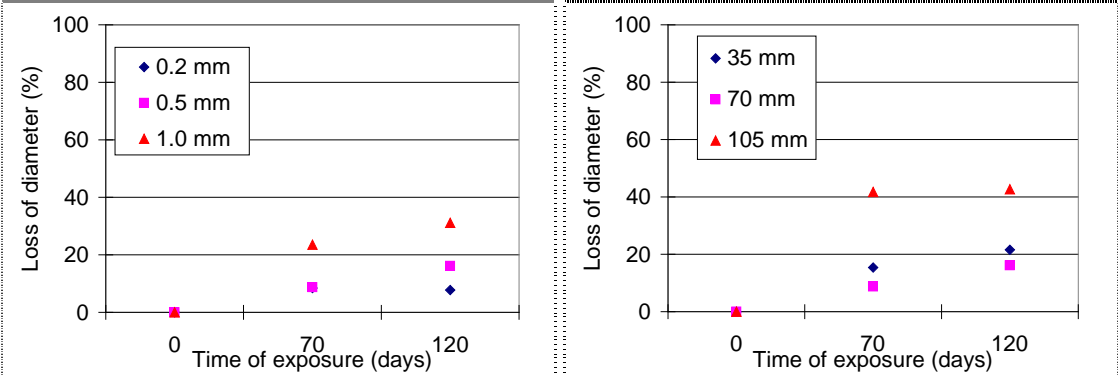


Figure 7 - Average loss of fibre diameter in TAP WATER environment from one sample (37 fibres). Influence of crack width, L=70 mm (left) and fibre length, w=0.5 mm (right).

3.3 Correlation between field and laboratory exposure tests

An attempt to correlate the laboratory exposure tests to the field exposure tests is made below. The shortest fibre length used in the laboratory is 35 mm and 30 mm in field. Studying the right part of figure 6 it can be seen that an increase of fibres length from 35 to 70 mm gives an increase in the loss of fibre diameter from 19 to 33 % after 70 days of exposure. In a rough approximation this can be used to estimate the loss of fibre diameter a 30 mm fibre would have received in the laboratory exposures. Using linear extrapolation from the results a 30 mm fiber would have corroded according to equation (4.1). Studying the field exposure tests for 30 mm fibres and $w = 0.5$ mm exposed at Rv40 give that the plate nearest the crack mouth show a loss of 16% of fibre diameter after 2.5 years of exposure which is fairly similar. Therefore the acceleration factor can be calculated as in equation (4.2).

$$\Delta\phi_{30,cl}(70) = \Delta\phi_{35,cl}(70) - \frac{\Delta\phi_{70,cl}(70) - \Delta\phi_{35,cl}(70)}{l_{70} - l_{35}} * (l_{35} - l_{30}) = 19 - \frac{33 - 19}{70 - 35} * 5 = 17\% \quad (4.1)$$

$$A_{RV40} = \frac{t_{field}}{t_{lab}} = \frac{365 * 2.5}{70} = 13 \quad (4.2)$$

If a rough estimations is used to extrapolate the future behavior, the samples with 30 mm fibres and 0.5 mm crack width will have lost about 20% of the fibre diameter (according to the results after 120 days) after 4 years in the Rv40 environment.

4. SERVICE-LIFE MODEL

4.1 Analytical model

A reduced cross section due to corrosion gives a more brittle tensile failure of the fibres instead of a ductile pull-out failure. Kosa (1988) has suggested a simplified model for calculation of the effect. Input needed in the model is the number of fibers in the tensile zone, bond strength, fiber tensile strength, embedded length of fibers etc. In the model it is assumed that $\frac{1}{4}$ of the fibre length is contributing to the bond-strength. The strength ratio (S) represents the residual moment capacity in percent of the original, uncorroded state. To be taken into consideration when using the above mentioned model is that only straight fibres is simulated with this model.

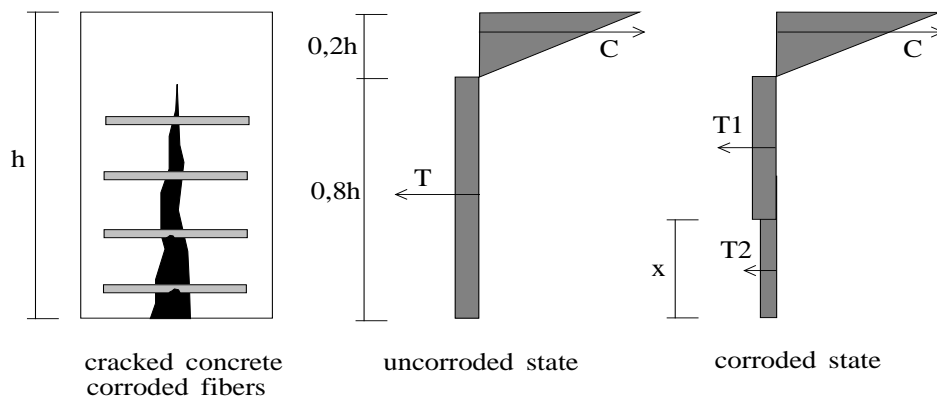


Figure 8 - Analytical model for flexural load test on a cracked specimen, Kosa (1988)

Table 4 – Parameters used in analytical and service-life model

Parameter	Description
x	depth of the corroded area
N	number of fibres in tensile zone
M_1, M_2	moment capacity for non corroded / corroded fibres
ϕ, ϕ_C	original / minimum fibre diameter
T_1, T_2	tension force in non-corroded / corroded area
l	fibre length
h	height of concrete
f_b	average bond strength
r	rate of corrosion
f_s	tensile strength of the fibre
t_c	service life (years)
S_c	critical strength ratio

4.2 Definition of limit state

For conventionally reinforced concrete the limit state when the service life ends is defined by Sarja & Vesikari (1996) as:

- 1 The steel is depassivated
- 2 Corrosion of rebars leads to cracking and spalling.

For steel fibres these two criteria are very unfavorable. The first criterion is not suitable since the propagation of corrosion is much slower than for conventional reinforcement, even with chlorides present. Therefore the propagation rate should be taken into consideration. Fibres are also distributed all over the crack plane. Therefore the effect of reduced fibre diameter in a part of the crack is not as dramatic as corrosion on rebars all in one level. Criteria no. 2 is not valid at all since the amount of corrosion products is too small to exceed the tensile strength of the concrete. Taking the propagation period into consideration a suitable limit state is to define an acceptable reduction in load bearing capacity (i.e. an acceptable/critical strength ratio S_c).

4.3 Service life

As mentioned earlier the initiation of corrosion is more or less instantaneous for cracked steel fibre reinforced concrete. The service life (time to reach limit state) should therefore be a function of the corrosion rate and a critical strength ratio. With an assumed rate of corrosion and a critical strength ratio the service life can be calculated as in equation (4.3). A full derivation of the equations and figures used can be found in Nordström (2000).

The calculated service life with different corrosion rates and critical strength ratios can be found in figure 9. With an accepted strength ratio reduction to 70 % this would give a service life of only 4.23 years with a corrosion rate of 0.06 mm/year. The corrosion rate is taken from the field exposures where the WA30-mix with a crack width of 1 mm showed an average corrosion of 15 % in the upper 25 mm of the crack. at Rv40. Other assumptions in the calculation can be

found in table 4. When designing a conventionally reinforced structure durability is taken into consideration by defining a minimum concrete cover over the reinforcement. In a steel fibre reinforced concrete structure the designer has to estimate the resulting crack widths from the design load. With knowledge of crack width, expected environmental exposure and designed service life the designer can compensate the loss in load-bearing capacity due to corrosion by increasing the amount of fibers, prescribe stainless steel fibres or increase the concrete thickness.

$$t_c = \frac{\phi - \phi_c}{r} = \frac{\phi}{r} - \sqrt{\frac{4}{r^2 \cdot \pi} \left[\frac{\pi \cdot \phi \cdot l \cdot f_b}{2 \cdot f_s} \cdot \left(1 + \sqrt{1 - \frac{1,6 \cdot h \cdot (M_1 \cdot S_c - T_1 \left(\frac{0,8 \cdot h - x}{2} \right))}{x \cdot N \cdot \pi \cdot \phi \cdot l \cdot f_b}} \right) \right]} \right]} \quad (4.3)$$

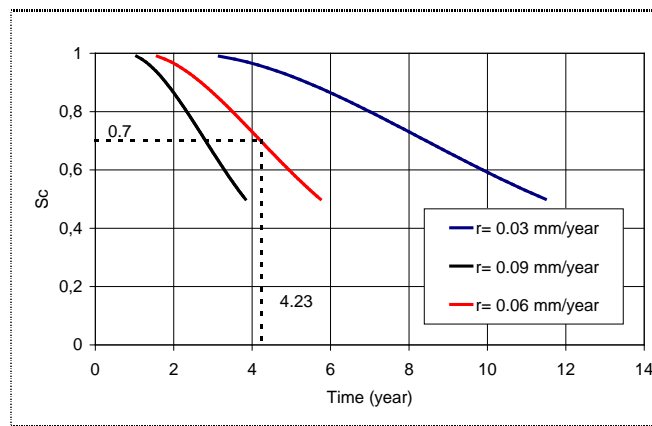


Figure 9 - Propagation scenario for corrosion of steel fibres in cracked concrete.

4.4 Discussion

The use of a model as the one presented is not an attempt to make accurate estimations of the service-life. It has been presented just to illuminate the need for taking corrosion in cracks into consideration already in the design stage. In the presented model only a linear elastic approach is used. Bond-slip behavior and/or friction is not considered at all in the model. Since hooked end fibres are most commonly used in Scandinavian sprayed concrete applications, an analytical model requires that friction between fibre and concrete during pull-out has to be taken into consideration. The loss of fibre diameter is also depending on the actual depth down in the crack and this effect must be included in a refined model. The model does not either take into consideration the continued hydration and therefore increased strength or the effect of self-healing.

5. CONCLUSIONS

Generally the results indicate that corrosion of steel fibres in cracked concrete must be regarded as a potential service-life problem. Measures taken in the design stage could be addition of extra amount of fibres, usage of fibres with stainless steel or increased concrete thickness.

5.1 Field exposures

- The amount of corrosion is limited after 2.5 years and is most severe for specimens subjected to a high degree of exposure to deicing-salts at the motorway during the winter-time.
- The residual flexural strength continues to increase after exposure for small crack widths. Probably due to increased anchorage strength for the steel fibres due to continued hydration of the concrete. For larger crack widths the trend is that corrosion leads to similar or reduced residual strength.
- The 40 mm long fibres corroded more than the 30 mm long fibres at the same crack width.
- The amount of corrosion decreased with an increasing depth from the crack opening.
- No significant difference can be seen between different mix-types.

5.2 Laboratory exposure tests

- In the chloride environment longer fibres corrode faster than shorter ones. An approximation is that a change of fibre length with 10 mm should give a change in loss of diameter in a crack of roughly 5%. In the tap water environment the results are more contradictory.
- An increased crack width gives a larger loss of fibre diameter.
- The acceleration factor is roughly estimated as 10 times the environment at Rv40. Future evaluations will give information about the validity of the calculated acceleration factor.

5.3 Service-life model

- A limit state criterion for obtained service-life of steel fibre reinforced concrete should be an acceptable level of load-bearing capacity.

6. REFERENCES

Kosa, K. (1988). Corrosion of fibre reinforced concrete. PhD thesis, University of Michigan, Ann Arbor.

Nordström, E. (2000) Steel fibre corrosion in cracks – Durability of sprayed concrete. Licentiate thesis, 2000:49, Luleå University of Technology, Sweden.

Flexural Behaviour of Steel-Fibre-Reinforced High-Performance Concrete



Manouchehr Hassanzadeh
Ph.D., Lecturer
Division of Building Materials
Lund Institute of Technology
P.O. Box 118
221 00 LUND, SWEDEN
E-mail: m.hassanzadeh@byggtek.lth.se

ABSTRACT

The combined effects of two different aspects of concrete (3 levels of each) were examined: the fibre volume and the matrix water/binder ratio. The volume fractions of the fibres were 0.5%, 1% and 2%, respectively. The three levels of the water/binder ratio of the concrete matrix were 0.38, 0.33 and 0.27. The concrete was subjected to bending, uniaxial tension and compression tests. An analytical model was used to predict the flexural behaviour of fibre-reinforced concrete beams on the basis of the tensile test results.

Key words: Steel-fibre, flexural strength, fracture mechanics, high-strength concrete, tensile strength.

1. INTRODUCTION

The development of super plasticizers has made it possible to produce concrete with a low W/B (water/binder) ratio. Concrete with a W/B ratio of less than 0.40 is now easy to manufacture and to utilize in practical applications. Such concrete is usually referred to as high-performance concrete or HPC. The advantages of HPC compared with conventional concretes, i.e. concretes with W/B ratios greater than 0.40, include its having greater strength and durability. HPC has also been shown, however, to be more brittle than conventional concretes. One way of reducing the brittleness of HPC is by the admixture of fibres. The aim of the present investigation was to study the fracture behaviour of HPC that has been reinforced with steel fibres.

Three types of concrete matrixes were compared. These had W/B ratios of 0.38, 0.33 and 0.27, corresponding to compressive strengths of 106, 111 and 133 MPa. The volume fractions of the fibres were 0.5%, 1% and 2%, respectively. The fibres had an indented surface and were made of high-strength steel. Their length and diameter were 35 mm and 0.6 mm, respectively.

The load-deflection and tensile stress-displacement curves of the different fibre-reinforced HPCs were determined. The geometry of the specimens and the bending-test setup are shown in figure 1. Two transducers (LVDTs) with a ± 2.5 mm measuring range were used to measure the deflection of the beam. The transducers recorded the displacement of the middle point of the

beam relative to the supports on both the rear and front side of the beam. In the following, deflection of the beam refers to the mean value of the relative displacements as just described. Displacement was the controlling parameter during the tests. The beams were 100 mm thick.

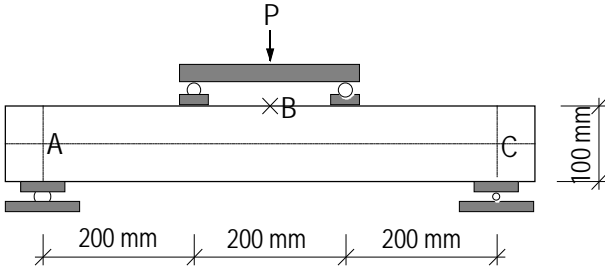


Figure 1 – Bending-test setup..

Figure 2 shows the type of specimens used in the tension tests. The specimens were sawn from the beams with a diamond saw. The necklines were produced using a core drill 100 mm in diameter. The position and direction of the specimens in the beams are likewise shown in the figure. As one can note, the direction of the tensile stresses in the beams and in the tensile test specimens is the same. The specimens were 50 mm thick.

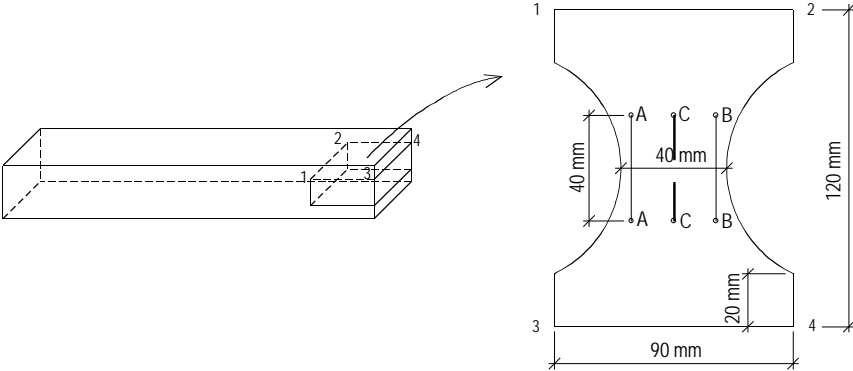


Figure 2 –A specimen for the uniaxial tension tests.

A theoretical model was employed to predict the load-deflection curves of the beams by means of tensile-stress-displacement curves. The results of the tests and of applying the model are described in [1] and [2]. In the present paper, further applications of the model are presented.

2. RELATION BETWEEN UNIAXIAL TENSILE AND FLEXURAL BEHAVIOUR

2.1 Introduction

Figure 3a presents a tensile stress-displacement curve schematically. The curve consists of three major parts, parts 1 and 3 corresponding to a monotonically increasing tensile displacement and part 2 to the unloading of the specimen. The curve in figure 3a can be decomposed into curves b and c. Curve b describes the material behaviour of those parts of the specimen in which the tensile displacement does not exceed the displacement that corresponds to the tensile strength of

the material. Curve *c* describes the material behaviour for those parts of the specimen in which the tensile displacement corresponding to the tensile strength of the material is exceeded. Curve *c* is obtained from curve *a* by subtracting the displacements obtained in part 2 from those obtained in part 3.

The tensile behaviour just described is in accordance with the “Fictitious Crack Model, FCM” [3]. Curve *b* in figure 3 describes the behaviour of the material outside the fracture process zone and curve *c* the behaviour of the material inside the fracture process zone. The former will be referred to as the stress-strain curve and the latter as the stress-displacement curve.

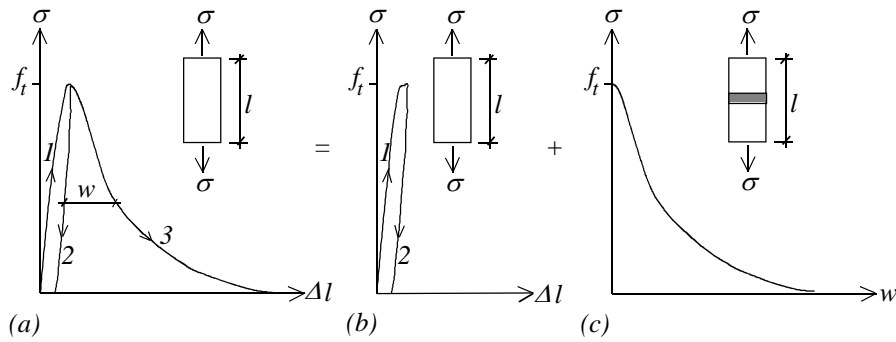


Figure 3 – Tensile stress-displacement curve.

2.2 The moment-curvature relationship and the load-deflection curve

Using the notations employed in figure 4 and assuming linear elastic unloading, the total tensile strain (ε_t , m/m) can be obtained as

$$\varepsilon_t = \frac{\Delta l_e}{l_g} + \frac{\Delta l_p}{l_g} + \frac{w}{l_g} = \varepsilon_e + \varepsilon_p + \frac{w}{l_g} \quad (1)$$

where Δl_e and Δl_p are elastic and plastic displacement, respectively, outside the fracture process zone, ε_e and ε_p are the corresponding strains, and l_g is the gauge length. Since w is not proportional to l_g , ε_t is a function of l_g . Due to derivation of the moment-curvature relationship being based on the strains involved, a gauge length needs to be introduced. In the analytical model for fictitious crack propagation in plain concrete beams as derived by Ulfkjær et al. [4], l_g is set to $0.5d$ (d = beam depth). According to [4], the results of the analytical model agree well with the results of a more detailed finite-element model. In forthcoming applications, however, l_g will be set to 40 mm, i.e. to $0.4d$. The reason for setting it to $0.4d$ instead of to $0.5d$ is that in the tension tests l_g is 40 mm. There was found to be no significant difference between the results obtained by use of the one set of assumptions or the other.

The model presented below is based on a model described in [5]. The model is derived from an analysis of simply reinforced concrete beams that fail, due either to failure of the reinforcement bar or failure of the concrete during compression. The basic ideas of the model presented in [5] are utilized here for the analysis of fibre-reinforced concrete beams. It should also be noted that

the basic conception of the model to be presented next is the same as that of the model described in [4].

Three assumptions are made: (1) plane sections before bending remain plane after bending, (2) when the concrete is under compression, the stress-strain curve is linear, (3) each beam fibre deforms independently.

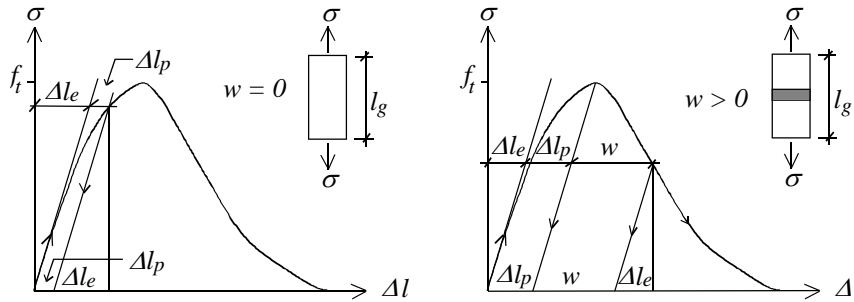


Figure 4 – Loading and unloading components of a complete stress-displacement curve.

Figure 5 shows the distribution of the strains and stresses over the cross-section. ε_t and ε_c are the tensile and compressive strains, respectively, at distance y from the neutral axis. σ_t and σ_c are the corresponding tensile and compressive stresses at distance y from the neutral axis. ε_{tm} and ε_{cm} are the tensile and compressive strains, respectively, on the outside fibres of the beam. σ_{tm} and σ_{cm} are the corresponding stresses. P_t and P_c are the resultant of the tensile and of the compressive forces, respectively. κd is the distance from the outside tensile fibres to the neutral axis. $\gamma \kappa d$ is the distance from the point upon which P_t impinges to the outside tensile fibre of the beam. b is the width of the beam.

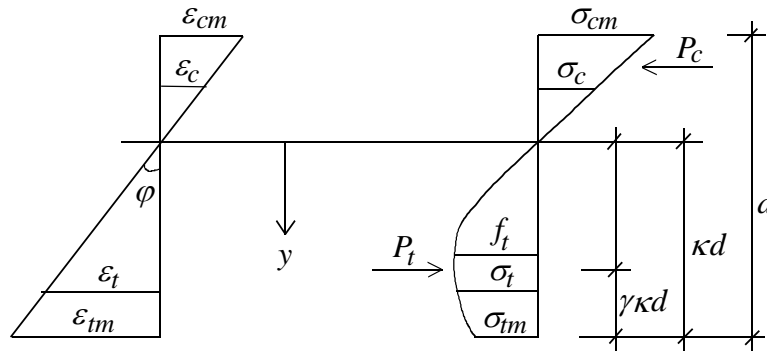


Figure 5 – Distribution of strains and stresses over the cross-section.

It can be shown that

$$\kappa = \frac{1}{1 + \sqrt{A}}, \quad A = \frac{2}{E \varepsilon_{tm}^2} \int_0^{\varepsilon_{tm}} \sigma_t d\varepsilon_t \quad (2)$$

$$\varphi = \frac{\varepsilon_{tm}}{\kappa d} \quad (3)$$

$$\gamma = 1 - \frac{\int_0^{\varepsilon_m} \sigma_t \varepsilon_t d\varepsilon_t}{\varepsilon_m \int_0^{\varepsilon_m} \sigma_t d\varepsilon_t} \quad (4)$$

$$P_t = \frac{b\kappa d}{\varepsilon_m} \int_0^{\varepsilon_m} \sigma_t d\varepsilon_t \quad (5)$$

$$\frac{\varepsilon_m}{\varepsilon_{cm}} = \frac{\kappa}{1 - \kappa} \quad (6)$$

$$P_c = 0,5b(d - \kappa d)E\varepsilon_{cm} \quad (7)$$

$$M = \kappa d(1 - \gamma)P_t + \frac{2}{3}d(1 - \kappa)P_c \quad (8)$$

For each prescribed value of ε_m , φ and M can be determined using equations 2-8. Observe that σ_t and $\sigma_t \varepsilon_t$ need to be integrated with regard to ε_t . The integration can be performed analytically if the relation between σ_t and ε_t can be expressed by a function, see e.g. [4]. Otherwise, the tensile stress-strain curves obtained using the tension tests can be employed instead. In the latter case the integration can only be performed numerically. By use of equations 1-8, the tensile stress-strain curves can be converted into moment-curvature curves. The results presented here were obtained using the stress-strain curves and numerical integration.

For any load, the distribution of the curvature over the beam length can be determined by means of the moment-curvature relationship and the moment distribution over the beam length. The moment distribution corresponding to a four-point bend test is shown in figure 6. The deflection of the midpoint of the beam can be determined as

$$\delta = \int_0^{l/2} \varphi(l/2 - x) dx \quad (9)$$

The notations are the same as in figure 7.

Note that in the ascending part of the load-deflection curve the curvature at any point along the beam increases with increasing moment. When the load approaches the failure load of the beam, a fracture zone develops, in this case at the midpoint of the beam. After the maximum load in a displacement-controlled test has been reached, all additional rotations take place inside the fracture zone, whereas in the other parts of the beam the curvature decreases. Since linear elastic unloading is assumed, the curvature decreases linearly by the same slope as the initial part of the moment-curvature curve. Consequently, the part of the beam in which the fracture zone is contained follows the moment-curvature curve entirely, whereas the other parts become unloaded before reaching their moment capacity.

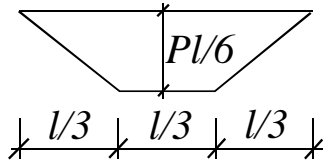


Figure 6 – Distribution of moments.

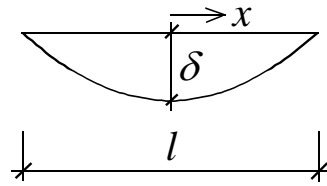


Figure 7 – Notations for equation 9.

2.3 Simulation of the model

The load-deflection curves predicted by the model were shown in [1] to agree well with the average experimentally determined load-deflection curves, provided the inputs of the model are derived from the weakest tensile stress-strain and stress-displacement curves. It was also shown that using the average stress-strain and stress-displacement curves as input parameters leads to an overestimation of both the failure load and the ductility of the beams. Note that “stress-displacement curve” refers to the stress-displacement curve of the fracture process zone described in section 2.1.

The load-deflection curve calculated using the model is very sensitive to the slope of the first part of the stress-displacement curve, figure 3c. The higher the slope, the lower the load capacity and the ductility of the beam are. For design purposes, one needs to determine the most unfavourable tension curves that can be used to predict the lower bound of the load-deflection response of the beam. Since only a small number of tensile tests were performed, determining the most unfavourable tension curves here is statistically uncertain. However, results of the numerical simulation presented in the next section indicate the influence which the scatter of the stress-strain and stress-displacement curves has on the load-deflection curves.

3. THE INFLUENCE OF THE SCATTER IN THE TENSION TESTS ON THE LOAD-DEFLECTION CURVES

Figures 8-9 show the stress-strain (a), stress-displacement (b) and load-deflection curves (c). The solid curves labelled as “Experiments” indicate the results of the experiments that were performed. Mean curves for the stress-strain and stress-displacement relationships are included. The mean curves are determined by calculating the mean stress that a given strain or displacement involves.

The mean curves shown have been used to determine the lower stress-limit of the 90% confidence interval, σ .

$$\sigma = \bar{\sigma} - k \quad (10)$$

$$k = \frac{s \cdot c_t}{\sqrt{n}} \quad (11)$$

where $\bar{\sigma}$ = mean value of the stress caused by a given strain or displacement, s = standard deviation of the stress, n = number of samples, which in most of the series is 3. $c_t = 2.92$ is obtained from the table of a t-distribution with $n-1 = 2$ degrees of freedom. Equation 10 can be rewritten as

$$\sigma = \bar{\sigma} - 1.69 \cdot s \quad (12)$$

The standard deviation of the stresses are calculated for each strain and displacement separately.

The stress-strain and stress-displacement curves determined by use of equation 12 are shown in figures 8-9, labelled as “90% conf. Int.”. These curves have been used to determine the load-deflection curves, again designated as “90% conf. Int.”, in figures 8c – 9c.

Load-deflection curves have also been calculated using the material model presented in figure 10. The model consists of a linear stress-strain curve, figure 10a, and a bilinear stress-displacement curve, figure 10b. The stress-strain curve is defined in terms of the ultimate stress, σ_0 , and the modulus of elasticity, E . The stress-displacement curve is defined in terms of three points: σ_i , w_i , and $i = 0, 1, 2$.

where w_0 , w_1 and w_2 are set to 0 mm, 0.05 mm and 0.4 mm, respectively, and the stresses, σ_i , are determined by use of the following equations:

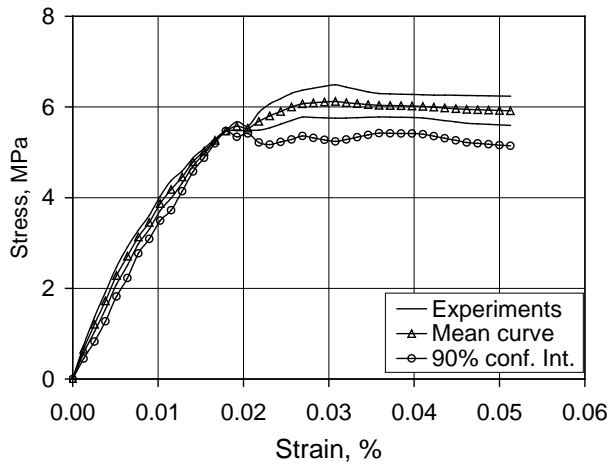
$$\sigma_i = \bar{\sigma}_i (1 - \nu \cdot c_n) \quad (13)$$

$$\nu = \frac{1}{m} \sum_{j=1}^m \frac{s_j}{\bar{\sigma}_j} \quad (14)$$

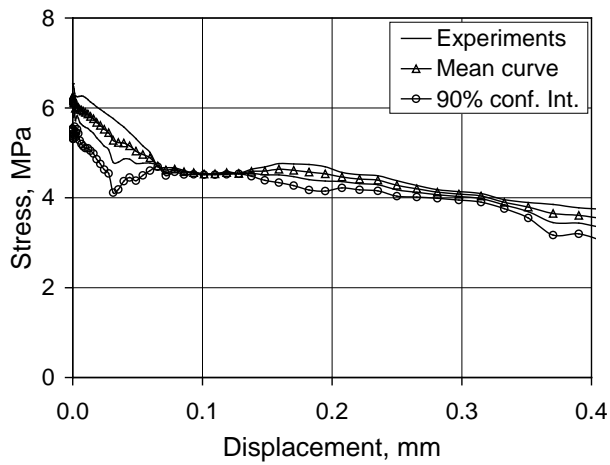
where $\bar{\sigma}_i$ is the mean value of the stress at displacement w_i , $\bar{\sigma}_i$ is calculated from the experimental stress-displacement curves, ν is the coefficient of variation, set to 0.23 in the calculations, ν is calculated on the basis of the results of all the test series, $\bar{\sigma}_j$ is the mean value of the stress at a given displacement, s_j is the standard deviation corresponding to $\bar{\sigma}_j$, and c_n is obtained from the table of the normal distribution, where for the 95% confidence interval c_n is 1.96. Inserting values for ν and c_n into equation 13 leads to the following equation for σ_i :

$$\sigma_i = 0.55 \cdot \bar{\sigma}_i \quad (15)$$

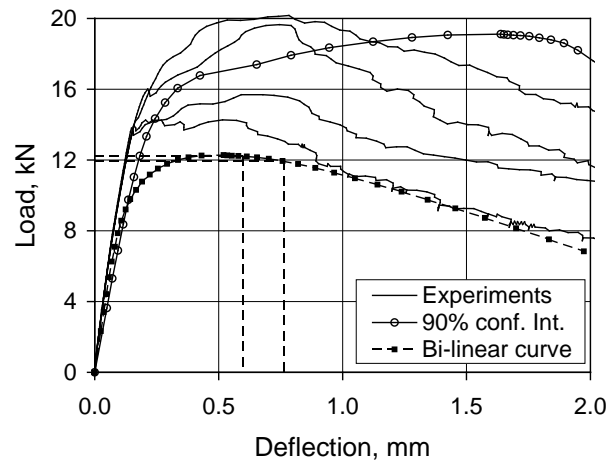
Table 1 shows the modulus of elasticity and the stress levels used as input in the model. The results of the calculations are shown in figures 8c – 9c, where they are designated as “Bilinear curve”. Loads and deflections corresponding to tensile crack-opening-displacements of 0.1 mm and 0.2 mm are shown by the horizontal and vertical dashed lines, respectively. These crack-opening-displacements correspond to those crack widths that do not endanger durability of the steel fibres in a corrosive environment, see e.g. [6].



(a)

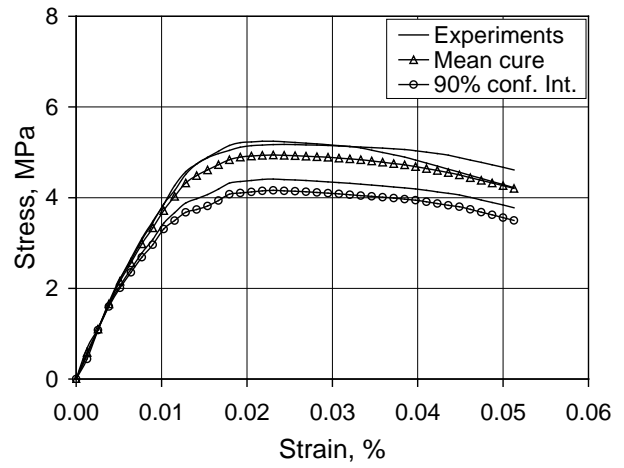


(b)

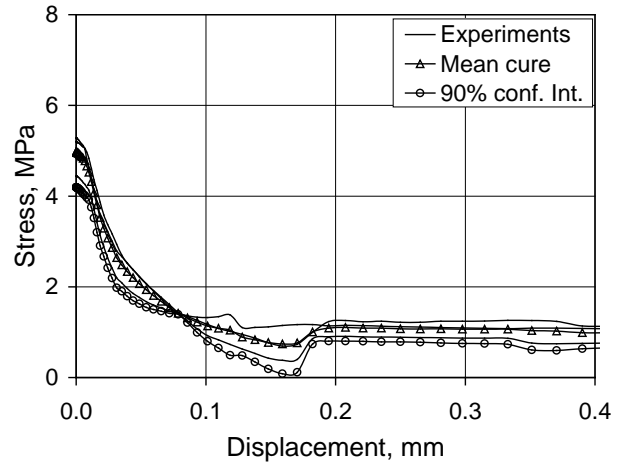


(c)

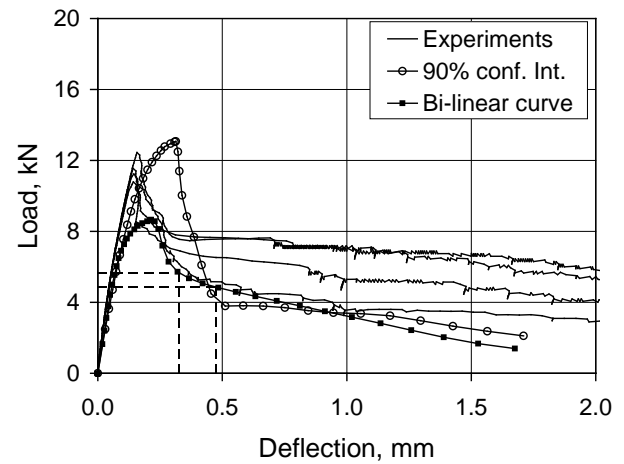
Figure 8 – Stress-strain, stress-displacement and load-deflection curves of fibre-reinforced concrete. W/B ratio = 0.33, Fibre content = 2.0%.



(a)

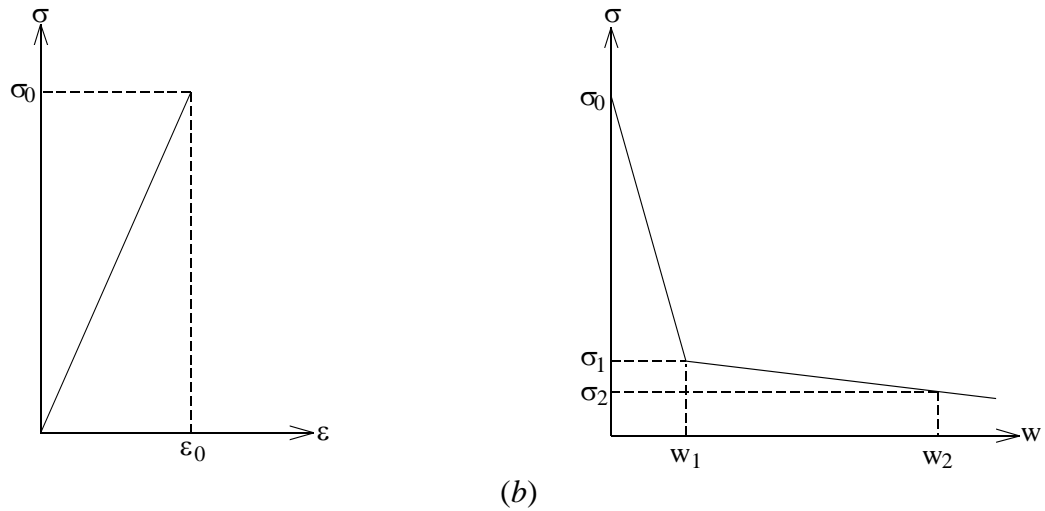


(b)



(c)

Figure 9 – Stress-strain, stress-displacement and load-deflection curves of fibre-reinforced concrete. W/B ratio = 0.38, Fibre content = 0.5%.



(a) (b)
 Figure 10 – Linear stress-strain curve (a), and bilinear stress-displacement curve (b) of fibre-reinforced concrete.

Table 1 – The modulus of elasticity and stress levels used as inputs in the model.

W/B	V_f (%)	E (GN/m ²)	σ_0 (MN/m ²)	σ_1 (MN/m ²)	σ_2 (MN/m ²)
0.27	0.5	40	3.2	1.2	0.7
	1.0	45	3.1	1.9	1.2
	2.0	45	3.8	2.8	2.0
0.33	0.5	41	3.1	0.9	0.6
	1.0	39	3.3	2.5	1.8
	2.0	43	3.4	2.8	2.0
0.38	0.5	42	5.0	2.0	1.0
	1.0	42	2.7	1.4	0.7
	2.0	39	3.3	2.6	1.9

4. DISCUSSION

The fracturing of a beam is a complex process governed by the strength and brittleness of the cross-sections of the beam. In tests similar to that shown in figure 1, cracks seldom propagate along the same cross-section. The direction of a cracks changes several times during propagation. The first crack occurs in the weakest cross-section. What happens after initiation of the first crack depends on the distribution of strength and ductility within the beam. A crack seeks sections of lower strength and ductility. The distribution of the fibres has a strong influence on the direction of cracks that occur.

The model presented in the paper accounts neither for changes in the direction of a crack nor the influence of the distribution of the strength and ductility of the beam on its load-deflection response. The model assumes that a crack initiates and propagates on the same cross-section. This is the cross-section with the lowest tensile strength, moment capacity and ductility. The changes in crack direction observed in the tests suggest, however, that in practice such cross-sections do not exist.

The statistical approaches described above should be considered as attempts to find the properties of the cross-section that has the lowest tensile strength, moment capacity and ductility. Although agreement between the calculated load-deflection curves and the curves obtained from tests is not good, the results show that it is possible - if the tensile stress-strain and stress-displacement curves correspond to the cross-section that is lowest in tensile strength, moment capacity and ductility - to predict the lower bound of the load-deflection response of the beams through use of the tensile stress-strain and stress-displacement curves. It is also possible to determine the lower bound of the load that corresponds to a given crack opening displacement.

5. CONCLUSIONS

The load-deflection response of the beam here is sensitive to the slope of the first part of the stress-displacement curve. The higher the slope is, the lower the failure load of the beam and the more brittle the fracture behaviour of the beam are.

The model presented in the paper is able to predict the lower bound of the load-deflection response of the steel-fibre-reinforced concrete beams, provided the tensile stress-strain and stress-displacement curves used in the model correspond to the cross-section having the lowest tensile strength, moment capacity and ductility.

REFERENCES

1. Hassanzadeh, M. "The Strength and Ductility of Steel Fibre-Reinforced High-Strength Concrete", in Proceedings of 5th international Symposium on Utilization of High Strength/High Performance Concrete, Sandefjord, Norway, 1999.
2. Hassanzadeh, M. "Steel-Fibre-Reinforced High-Strength Concrete", in Proceedings of the Nordic Concrete Research Meeting, Reykjavik, Island, 1999.
3. Petersson, P.E. "Crack Growth and Development of Fracture Zones in Plain Concrete and Similar Materials". Report TVBM-1006, Division of Building Materials, Lund Institute of Technology, Lund, Sweden, 1981.
4. Ulfkjær, J.P., Krenk, S. and Brincker, R. "Analytical Model for Fictitious Crack Propagation in Concrete Beams". Journal of Engineering Mechanics, Vol. 121, No. 1, 1995, 7-15.
5. Park, R. and Paulay, T. "Reinforced Concrete Structures". John Wiley & Sons, Inc, 1987, ISBN 0-471-04655-8.
6. De Place Hansen, E.J. "Holdbarhet af Fiberarmeret Beton og Revnet Beton – State-of-the-art". Series R No 48, Department of Structural Engineering and Materials, Technical University of Denmark, 1998.

Influence of Steel Fibre Reinforcement on Punching Shear Capacity of Column Supported Flat Slabs



Ghassem Hassanzadeh, Ph.D. Candidate
E-mail: ghassem.hassanzadeh@struct.kth.se

Håkan Sundquist, Prof. Structural Design and Bridges
E-mail: hakan.sundquist@struct.kth.se

Royal Institute of Technology, KTH
Department of Structural Engineering
SE – 100 44 Stockholm – Sweden



ABSTRACT

Punching shear, caused by a concentrated load, induces a complex crack pattern and different failure modes in concrete flat slabs. A series of experiments was conducted to study the influence of steel fibres on punching shear strength of concrete flat slabs. Five slabs on columns were tested in this investigation. The main aim of this investigation was to elucidate if any improvement in the failure behaviour of the slabs could be observed by using steel fibres. Steel fibre reinforced concrete has been used both with and without ordinary flexural reinforcement. The studied variables were concrete compressive strength, the local usage of steel fibre reinforced concrete and the usage of post-tensioned unbonded tendons placed in the slabs without ordinary flexural reinforcement. The beneficial effects of adding steel fibres to the high strength concrete are demonstrated. The use of prestressed tendons and steel fibres increases remarkably the ultimate load capacity and stiffness of the slab. Replacing the normal strength concrete in the area over the column with steel fibre reinforced high strength concrete provides an efficient means of increasing the punching shear capacity of the slab.

Keywords: concrete; high strength concrete; flat plates; punching shear; reinforced concrete slabs; fibre reinforced slabs; tests; prestressing; unbonded tendons

1 INTRODUCTION

Due to the flexibility of planning and the low structural depth, which results in economic structures, the use of concrete flat slabs supported by columns has consistently increased. In general, concentrated high stresses at the slab-column connection may lead to punching shear failure. Punching shear failures occur suddenly and the results are catastrophic.

Ordinary concrete is brittle and has very low tensile strength, and cracks at very low applied loads. Steel bars are used in concrete structures in order to eliminate the insufficiency of tensile strength and toughness of concrete. Reinforcing work constitutes about 50 % of design, 30 % of

total labour and 20 % of total production cost of the slab structure. Design engineers must assign, draw and specify every rebar in the construction. The steel fixing work consumes a lot of time and causes many injuries and a high level of absenteeism, Ay (1999).

The large quantity of the often different types of reinforcement, i.e. flexural reinforcement, shear reinforcement and even prestressed tendons, makes it difficult to cast the concrete directly over the columns. Reduction of the amount of reinforcing rebars is economically advantageous, which must be taken into consideration in order to achieve cost-effective structures.

High strength concrete (HSC) with compressive strengths in excess of 60 MPa are now available and have not only higher strength, both in compression and tension, but shows also higher durability compared to ordinary concrete. The comparison of test results shows that the utilisation of HSC can result in a significant increase in punching shear strength of slabs, Hallgren (1996).

The utilisation of steel fibres in concrete has increased considerably, due to its advantages in stress redistribution and control of cracking, especially in the serviceability limit state. During hardening, steel fibres prevent expansion of the cracks, caused by the hydration process in the filler material. That is due to the closer location of the fibres to the concrete surface and well dispersion of the fibres in the concrete. Steel fibres can also eliminate cracks caused by differences in temperature or differential hardening. This results in a better control of leakage and penetration of liquids.

The improvement in the mechanical properties of concrete due to steel fibres is well known. It commences after cracking and causes a significant enhancement of the loading resistance. This is due to the redistribution of stresses even after the onset of the cracking. The energy absorption in the fibre bridging zone of a fibre reinforced concrete (FRC) is a result of several types of interactions between fibre and matrix, e.g. interface debonding, frictional sliding and inclined angle effects associated with random fibre orientations. The large amount of fibres, bridging over an extended length can contribute enormously to the toughening effect of the composite, Li and Maalej (1996). By contrast, what is not very well known is the steel fibre effectiveness in arresting crack propagation in a brittle fracture process like punching shear in concrete slabs without any longitudinal reinforcement, Prisco and Felicetti (1997).

The first objective of this paper is to study the influences of steel fibre on the punching shear strength of concrete slabs. The other investigated parameters are the influence of the steel fibre reinforced high strength concrete (SFHSC) and the punching shear strength in the absence of ordinary flexural reinforcement. The present paper even attempts to identify the effectiveness of locally placed SFHSC above the column with normal strength concrete cast wet-to-wet around the SFHSC portion.

2 PREVIOUS RESEARCH

In recent decades, the problem of shear strength in slabs subjected to concentrated loading has been studied extensively, since it can result in the collapse of flat slab floor systems and column footings. Punching shear is a brittle failure with little or no warning prior to collapse. This phenomenon is often coupled with bending and cracking, which changes the post-peak behaviour of the slab drastically.

Swamy et al. (1979) and, Swamy and Ali (1982) reported the effects of fibre-reinforced concrete on the punching shear behaviour of slab-column connections. The observed improvements due to the addition of the 1 % of steel fibres included a 30 % reduction of service

load deflection and a 40 % increase in the punching shear capacity. The fibres also gave a 40 % to 50 % reduction of the tensile strains in the flexural reinforcement at the service load level. Swamy and Ali also reported that placing of fibre reinforced concrete within a distance of $3h$ from the column faces was as effective as constructing the entire slab of fibre reinforced concrete.

Alexander and Simmonds (1992) tested six specimens in order to investigate the effects of the fibre reinforced concrete on the punching shear behaviour of slabs. A 0,4 % dosage of 50 mm long corrugated steel fibre increased the ultimate shear capacity of the slab by 20 %. With a fibre content of 0,8 %, the shear capacity of the slab increased about 7 %. They also concluded that adding fibres to the concrete increased the slab ductility and the punching capacity of slab-column connection.

Shaaban and Gesund (1994) investigated the effects of using steel fibres in the concrete by testing 13 slab-column specimens. They concluded that using steel fibre reinforced concrete significantly increases the punching shear capacity of the slab.

Adebar et al. (1997) summarised many of the shear strength tests with steel fibre reinforced concrete beams without stirrups. The increase in shear strength provided by the fibres ranged from the highest 170 % to the lowest of about 10 %. Due to different used approaches to conduct shear tests, it was difficult to identify consistent trends in the experimental results. The measured results in their investigation showed that at low fibre volumes, the increase in shear strength was proportional to the amount of fibres, but the rate of increase was reduced at higher fibre volumes.

McHarg et al. (2000) studied the strategic use of steel fibre reinforced concrete in two-way slabs by testing six slab-column specimens. Using concrete with 0,5 % steel fibre in the slab around the column for a distance of at least $3,5h$ from the column face resulted in a significant improvement in performance. This included an increase in the punching shear resistance, a significant increase in the ductility, a greater postcracking stiffness and smaller cracks widths at service load levels. Furthermore, providing fibre reinforced concrete cover resulted in an increase in punching shear resistance and better crack control.

3 TESTS

3.1 Test specimens

The experimental program comprises two test series with totally five slabs, series C with two slabs and series E with three slabs, on punching shear capacity of concrete slabs on circular column stubs. The slabs had the same dimensions as previously tested slabs in order to make the comparison easier. The diameter c , at which the slabs were loaded, was 2380 mm which approximately corresponds to zero-moment distribution around a column in a real flat slab structure. The slabs had a length of 2600 mm and a thickness of 220 mm on a 250 mm circular column at the centre.

The series C consisted of two slabs, which were cast with normal strength concrete, Swedish Grade K40, reinforced with steel fibre (SFNSC) without any ordinary flexural reinforcement. The notation K40 stands for concrete with compressive cube strength of 40 MPa at the age of 28 days measured on at least three cubes. The main reason for this series was to study the influence of steel fibres on the punching shear strength and on the deformation capacity of the slabs compared with similar concrete slabs reinforced with ordinary flexural reinforcement. The total

steel fibre amount in slabs C1 and C2 was 120 kg/m^3 ($\sim 1,5 \text{ vol-\%}$) consisting of *Dramix RC-65/35-BN* (fibre length, $L = 35 \text{ mm}$, fibre diameter, $d = 0,55 \text{ mm}$, $L/d = 65$) and *RC-80/60-BN* (fibre length, $L = 60 \text{ mm}$, fibre diameter, $d = 0,75 \text{ mm}$, $L/d = 80$), 60 kg/m^3 each. The abbreviations stand for $R =$ hooked fibres, $C =$ glued fibres into small bundles, $B =$ Bright and $N =$ steel with normal tensile strength.

The first specimen C1 was solely cast with steel fibre reinforced concrete, without any flexural reinforcement bars or any prestressed tendons. The second slab, C2, was arranged with parabolically aligned prestressed tendons, which were placed according to the current design codes as shown in Figure 1. No flexural reinforcement bars were used in the slab C2, however steel fibres were used with the content and type described previously.

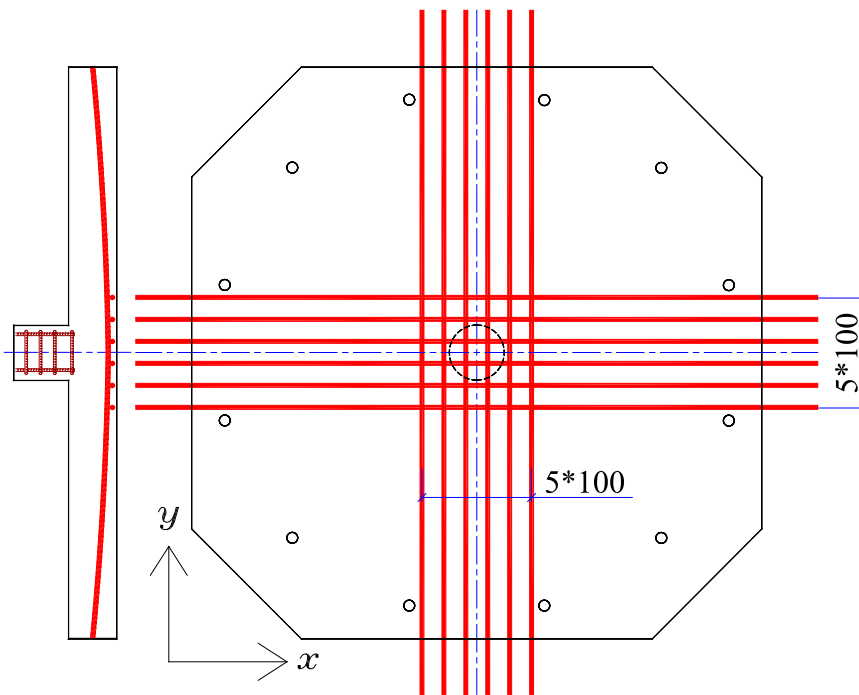


Figure 1 - The distribution of the tendons in slabs C2 and E3.

The series E consisted of three slabs, which were cast with high strength concrete, Swedish Grade K80, reinforced with steel fibres. The steel fibre amount in these slabs was 120 kg/m^3 ($\sim 1,5 \text{ vol-\%}$) consisting of *Dramix RC-65/35-BN* (fibre length = 35 mm , fibre diameter = $0,55 \text{ mm}$, $L/d = 65$).

The specimens E1 and E2 were reinforced with ordinary flexural reinforcement bars and the reinforcement ratio was $7,8 \%$. The reinforcement was arranged as shown in Figure 2. The specimen E1 was cast entirely with steel fibre reinforced high strength concrete (SFHSC), Swedish Grade K80, while the specimen E2 had SFHSC only within the immediate column region. The remaining part of the slab was cast with normal strength concrete (NSC), Swedish Grade K40. These two different concrete types were cast wet to wet and vibrated afterwards. The slab E3 had no ordinary flexural reinforcement but prestressed tendons in both directions placed along the column band, see Figure 1. The concrete used in the slab E3 was SFHSC, Swedish Grade K80.

The bottom reinforcement consisted of a net with $17\phi 6$ bars in each direction and was placed in all slabs in order to avoid cracks at the lower side of the slabs during handling and transportation

of the slabs. The influence of the bottom reinforcement on punching shear capacity of the slabs is not investigated in this project.

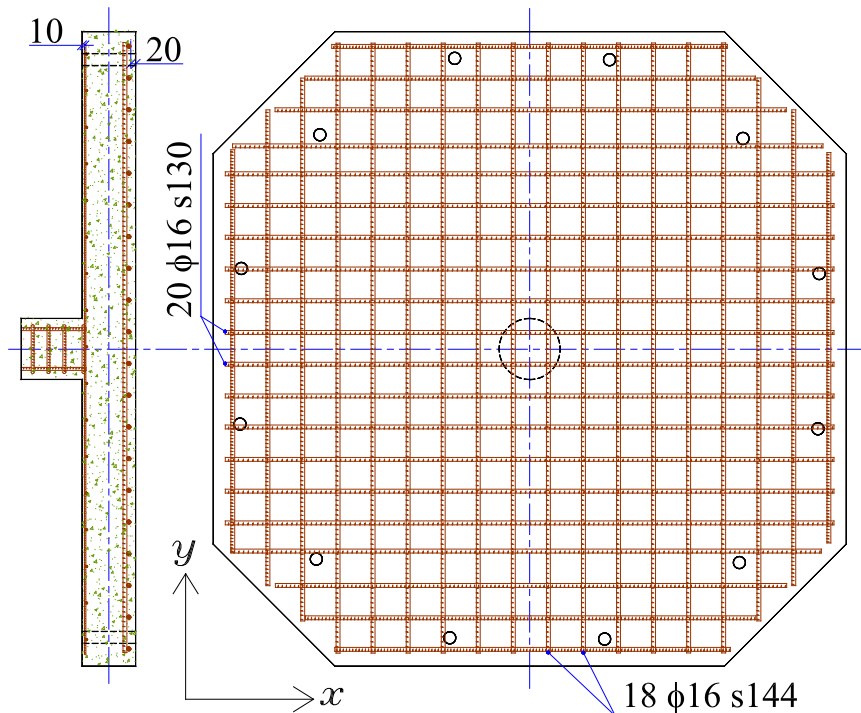


Figure 2 - Flexural reinforcement distribution in the slabs E1 and E2.

Each specimen of those with unbonded tendons, slabs C2 and E3, had six tendons in each direction. The tendons were of type BRIDON WIRE 15,7 mm PC STRAND SS 21 36 20 with 0,2-percent proof stress $f_{0,2} = 1729$ MPa and with $f_{st} = 1852$ MPa. The relative distance between the tendons was 100 mm as shown in Figure 1.

The measured results of these slabs are compared to the results of some earlier tested slabs by Hallgren (1996) and Hassanzadeh (1998). The slab B1 was cast with ordinary flexural reinforcement and normal strength concrete to estimate the punching shear capacity of the slab. The specimen B1 had a thickness of 220 mm and a length of the 2600 mm but with chamfered edges. The ratio of ordinary flexural reinforcement for this slab was 2,86 ‰, consisting of a net with 18φ10 bars in each direction Swedish Grade K500 and with a yield stress about 582 MPa.

The other two slabs used for comparison were HSC2 and N/HSC8, which were tested by Hallgren (1996). The slab HSC2 was cast with high strength concrete, the Swedish Grade K100. The slab had a thickness of 240 mm and a ratio of reinforcement of 0,82 ‰. The slab N/HSC8 had high strength concrete only in the area above the column with a radius of at least $B+3,5d$ on the top surface of the slab and $B+7,5d$ on the bottom surface of the slab, where B is the diameter of the column and d is the effective depth of the slab. The remaining part of the slab was cast with normal strength concrete. The slab had a thickness of 242 mm and a ratio of reinforcement of 0,8 ‰.

3.2 Test set-up, instrumentation

The test set-up is shown in Figure 3. A hydraulic jack was used to apply load to the slabs through the column stub. 12 tie rods, Dywidag φ 26,5, and 12 spreader beams distributed the

load uniformly along a circle with diameter $c = 2380$ mm. A heavy, reinforced concrete counter slab was used to hold back the tie rods.

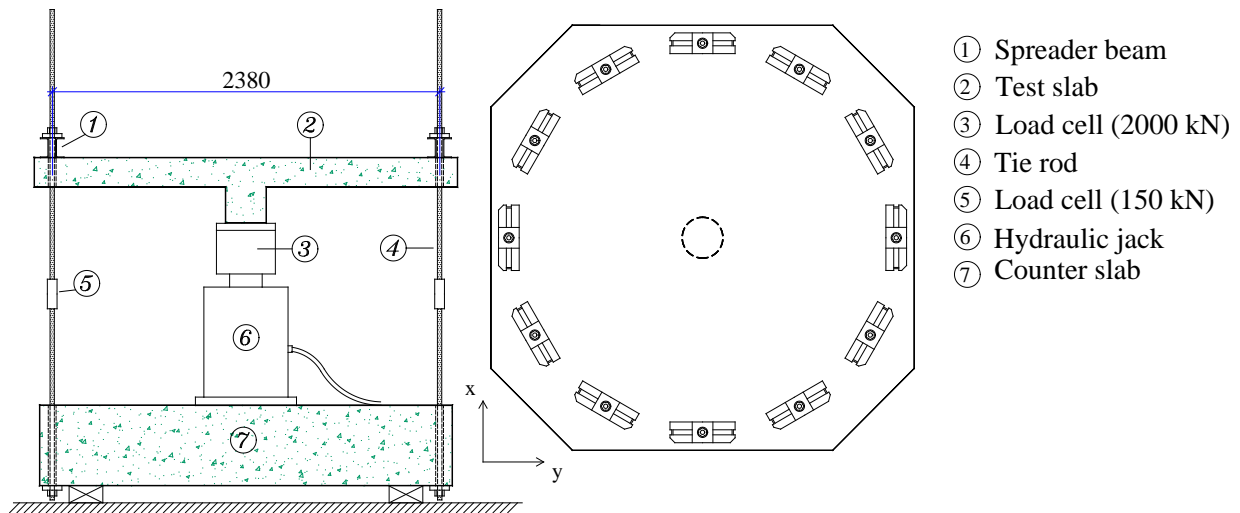


Figure 3 - Test set-up.

The column load was applied in steps of 80 kN during a time period of two minutes. The load was then kept constant for the next 13 minutes. During this time, the crack pattern was carefully inspected and marked. In addition, the maximum crack widths were measured in four points on the topside after each load step.

In order to measure the strains in the concrete in both tangential and radial directions, electrical gauges were glued to the bottom surface of the slabs at several points in both x - and y -direction. The slab deflection was continuously measured at seven points along a centre line in the y -direction on the upper surface of the slabs.

3.3 Materials properties

The mixture properties of concrete used in each specimen are summarised in Table 1. In addition, the information concerning the mixture properties of both the normal strength concrete and the high strength concrete used in the slab E2 and the slab N/HSC8 are given.

Table 1 - Concrete mixture proportions kg/m³.

Slab	B1	C1-C2	E1	E2		E3	HSC2	N/HSC8	
				NSC	HSC			NSC	HSC
Cement, <i>c</i>	432	444	485	342	486	486	450	302	483
Fine aggregates, 0-8 mm	866	950	920	1035	967	960	828	1021	850
Coarse aggregates, 8-18	869*	895*	886	870	880	880	980	779	937
Silica fume, <i>s</i>	-	-	19	-	24,7	29,3	50	-	49
Superplasticizer	-	7	7**	1.9	5***	4.2	20	-	12
Water reducer (Lignin)	-	-	2.6	1.1	3	-	-	-	-
Water, <i>w</i>	158	203	159	184	174	164	132	206	130
Air entrainer agent	2.4	7	1	-	-	-	-	-	-
<i>w / (c+s)</i>	0.67	0.46	0.32	0.54	0.34	0.32	0.26	0.68	0.24
Retarder	-	-	-	-	-	-	5.5	-	3.0
Steel fibre, <i>V_f</i> %	-	1.5	1.5	-	1.5	1.5	-	-	-

* 8-16 mm ** Sika (Melamin based) *** Sika (Glenium based)

The different properties of the concrete were measured on both cubes and cylinders. The specimens were cured according to the Swedish Standard SS 13 11 12. Compression and split strengths of the concrete used in each slab were measured on both cubes and cylinders. The cubes had a side length of 150 mm, and the cylinders had a diameter of 150 mm and a height of 300 mm. A part of the test results are given in Table 2. The results are based on three cubes for each slab, measured at the time of testing of the slab. The results of the slabs HSC2 and N/HSC8 are also given as they were reported by Hallgren (1996).

Table 2- Measured concrete properties

Slab	B1	C1	C2	E1	E2		E3	HSC2	N/HSC8	
					NSC	HSC			NSC	HSC
Age /days	39	28	29	34	28	28	28	28	42	42
<i>f_{csp,cube}</i> /MPa	4.0	-*	3.7	8.8	3.7	5.5	5.1	5.7	3.2	6.9
	(0.1)		(0.1)	(0.2)	(0.1)	(0.3)	(0.1)	(0.1)	(0.2)	(0.2)
<i>f_{cc,cube}</i> /MPa	51.2	52.4	52.2	86.9	48.9	74.8	75.0	98.8	34.5	100.1
	(0.3)	(0.3)	(0.7)	(0.4)	(0.6)	(0.9)	(1.3)	(1.9)	(0.6)	(6.5)

Notation: *f_{csp,cube}* = splitting tensile strength, measured on 3 cubes; *f_{cc,cube}* = compressive cube strength, measured on 3 cubes; * no cube available for splitting tensile strength test

4 RESULTS

In the tests, the applied load, deflection and the concrete strain at the compressive side of the slab were continuously recorded. The crack widths were measured at four points on the upper

side located near the slab centre. Some of these data are presented in Table 3 and discussed in the following paragraphs.

Table 3 - Summary of the test results

Slab	h /mm	d /mm	ρ_{flex} /‰	ρ_{id} /‰	ρ_{tot} /‰	Failure mode	δ_{max} /mm	V_f /%	P_u /MPa	f_{vp} /MPa
B1	220	190	2.86	-	2.86	P	33	-	437	1.7
C1	220	220	0	0	0	F	5.8	1.5	342	1.1
C2	220	180	0	4.1	4.1	F	21.8	1.5	931	3.8
E1	220	184	7.6	-	7.6	P	24	1.5	1210	4.8
E2	220	184	7.6	-	7.6	P	23	1.5	1057	4.2
E3	220	190	-	4.1	4.1	F	18	1.5	949	3.6
HSC2 *	240	194	8.2	-	8.2	P	11	-	889	3.3
N/HSC8 *	242	198	8.0	-	8.0	P	14	-	944	3.4

Notation: ρ_{flex} = ratio of flexure reinforcement; ρ_{id} = reinforcement ratio used when the prestressed slab is treated as though ordinarily reinforced; $\rho_{tot} = \rho_{flex} + \rho_{id}$ = total ratio of reinforcement; V_f = fibre content by volume; P = brittle punching; F = flexural failure; δ_{max} = maximum deflection of the slab; P_u = observed ultimate load; f_{vp} = punching shear strength according to eq.(1); * Slab tested by Hallgren(1996).

Also given in the table is the punching shear strength f_{vp} , which is the nominal shear stress in a cylindrical control section at the distance $d/2$ from the column. This is calculated using the following formula, without consideration of its validity to the slab in question, where P_u is the observed ultimate load, d is the effective depth and B is the column diameter.

$$f_{vp} = \frac{P_u}{\pi(d + B)d} \quad (1)$$

The first observed crack in all slabs was in the radial direction at the top of slab centre running towards the slab edge. The slabs C1, C2 and E3 had two wide cracks extending over the total slab width. For slab C2 and E3, these cracks were parallel to the tendons in both x - and y -direction. The failure mode for slabs C1, C2 and E3 was flexural failure. For the rest of the slabs, a punching failure was observed. The deflections of the slabs were measured throughout the tests at seven points along a diameter. The deflections of the slabs at the circumference are shown in Figure 4 as a function of the measured load. The total load reported is the sum of applied loads and the self-weight of the slab. Since the load was applied upwards through the column, the deflections shown are the average of the difference between the upward movement measured at the centre of the slab and the deflections measured at the perimeter.

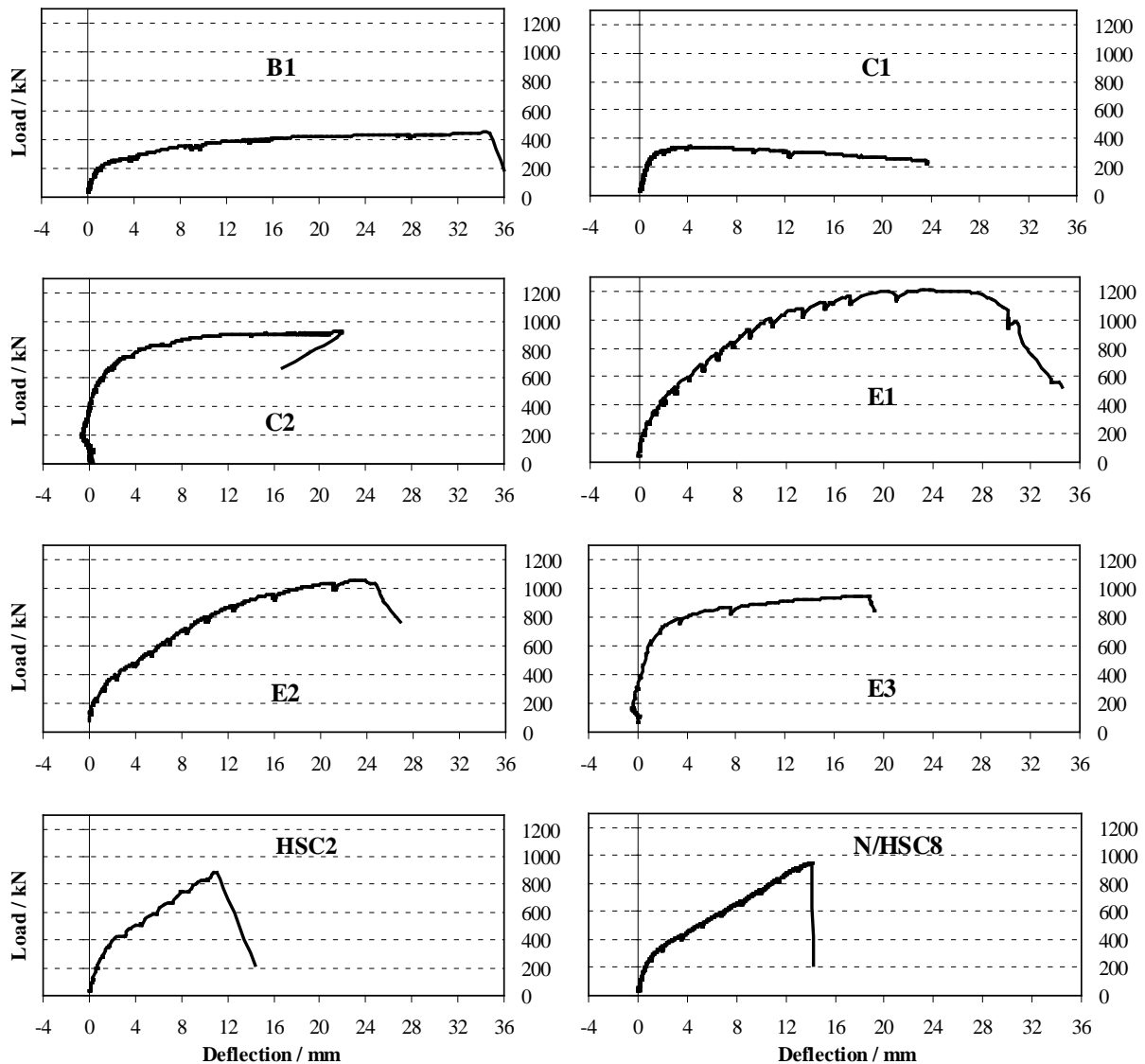


Figure 4 - The load-deflection curves of the slabs.

Figure 5 compares the total measured load versus deflection of the tested slabs in order to study the influence of the different variables on the punching shear capacity of the slabs. The comparison between the failure load of the slabs B1 and C1 shows that steel fibre reinforced concrete, SFRC, can not be used alone due to its deficient post-cracking tensile strength. The utilisation of prestressed tendons and SFRC in slab C2 increased the load capacity of the slab by about 113 % but decreased the deflection at ultimate load approximately by 35 %. The failure mode was changed from brittle punching failure for slab B1 to flexural failure for slab C2.

For all slabs in series E, a remarkable increase of the ultimate load capacity was observed. For slab E1, using SFHSC increased the punching shear capacity of the slab by about 176 % compared with slab B1. Also, comparison of the result for slab E1 with the result for the slabs HSC2 showed an increase of approximately 36 % of the punching shear capacity of the slab E1, though the concrete used in slab E1 had 13 % lower compressive cube strength but 53 % higher splitting tensile strength.

Using SFHSC locally in the slab E2 reduced the punching shear capacity of the slab by about 13 % compared with slab E1 but increased the punching shear capacity of the slab by approximately 140 % compared with slab B1 and 12 % compared with slab N/HSC8. For both slabs E1 and E2, the deflection at ultimate load increased by about 100 % compared with HSC2 and N/HSC8, respectively.

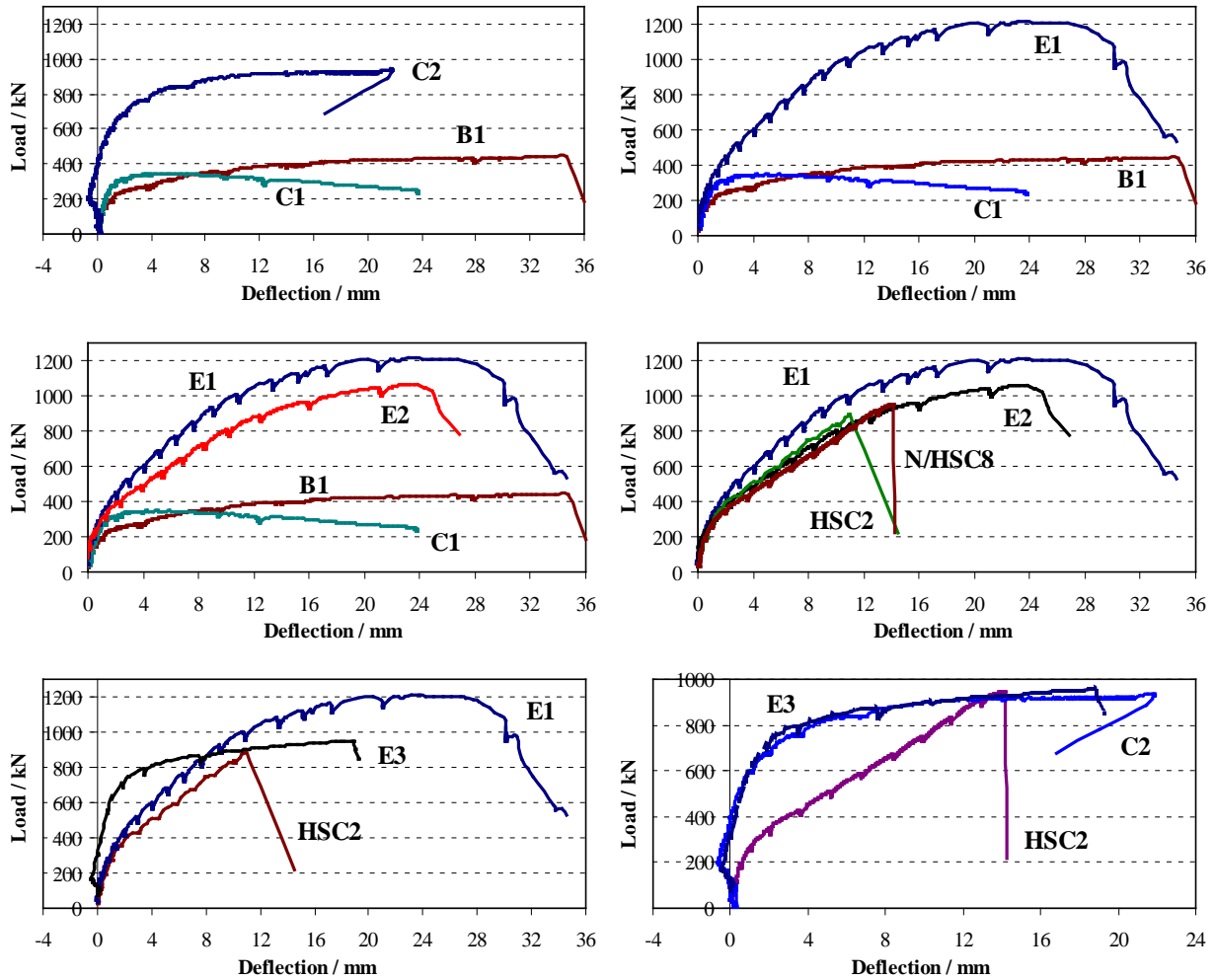


Figure 5 - Comparison of the measured load-deflection

A comparison between the measured ultimate load for slabs C2 and E3, which had prestressed tendons in both directions, showed that the utilisation of the SFHSC had no influence on the ultimate load but a significant improvement of the slab stiffness.

The deflection curves at different distances from the column centre at various load levels are shown in Figure 6.

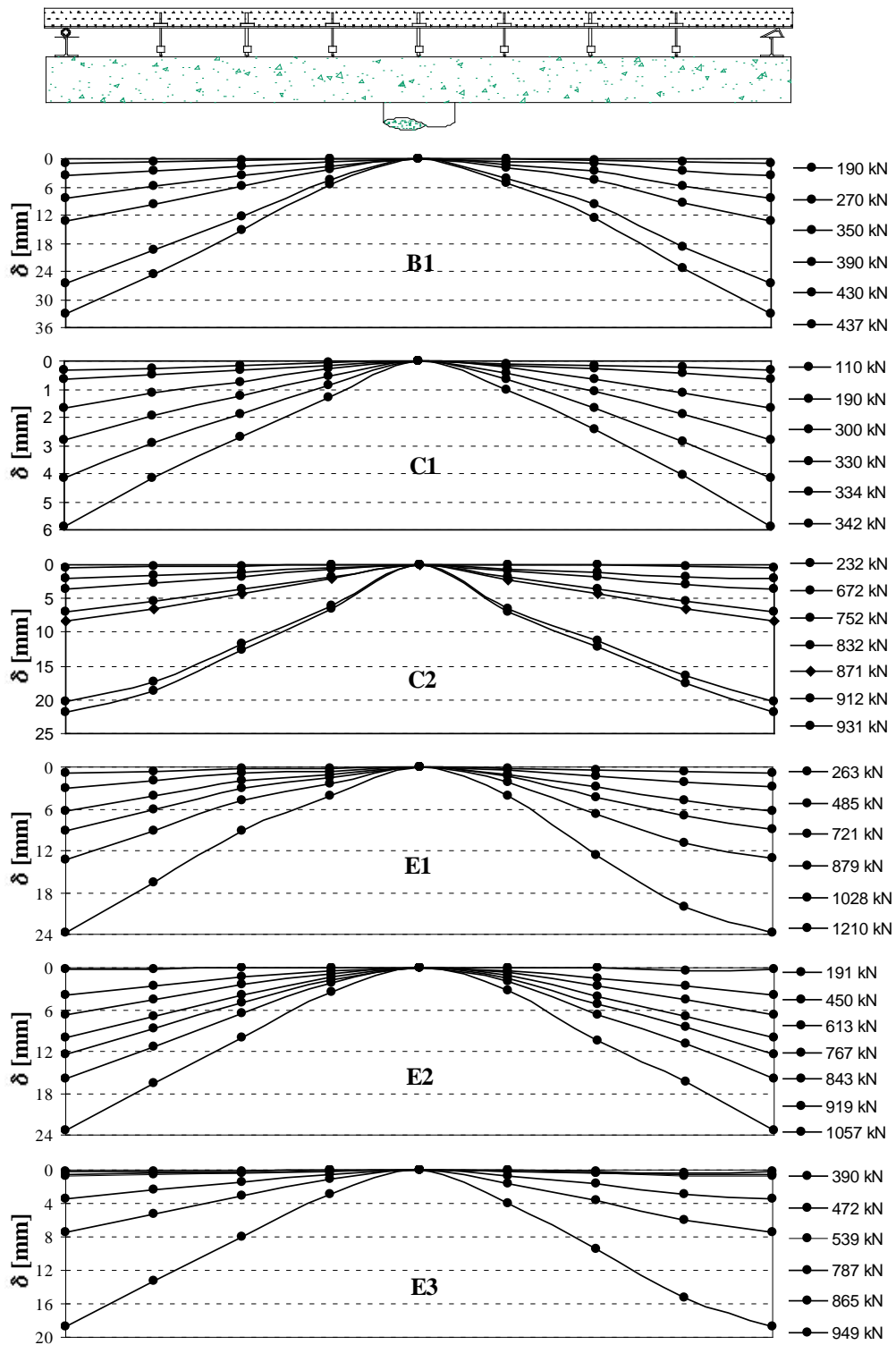


Figure 6 - Deflection curves at different distances from the column centre at various load levels measured in mm.

5 CONCLUSIONS

The following conclusions can be drawn from the results of the experimental program on the two-way slab specimens, though the reinforcement ratio were not exactly the same for the compared slabs.

The observed first crack load for the tested slabs with steel fibres were higher compared to the slabs without steel fibres. Also, the reduction in the crack width for the slabs with steel fibre reinforced concrete was significant in comparison to those with ordinary reinforcement.

Comparison between the observed ultimate loads indicates that the utilisation of steel fibres in concrete has a significant influence on increasing the ultimate load capacity of the slabs. The increase of the punching shear capacity of slabs due to adding steel fibre to the high strength concrete was about 36 %. Also, the deflections at the same load level was reduced for the slabs with steel fibres and a larger deflection for these slabs was measured at ultimate load.

Using SFHSC locally in the slab had no significant influence on the slab stiffness but increased both the punching shear capacity of the slab and its maximum deflection. Hence, It appears that a significant increase of the punching shear capacity can be gained by replacing the normal strength concrete in a certain small area over the column with SFHSC.

The comparison between the observed punching loads for two slabs, B1 and C1, shows that the flexural reinforcement can not totally be replaced by steel fibres. The results of the other investigations indicate the possibility of replacing the shear reinforcement with steel fibres in beams and slabs. However, for slabs with both steel fibres and prestressed tendons, i.e. slabs C2 and E3, a remarkable increase in ultimate load capacity and stiffness of the slab was observed. More investigations are required in order to produce a mechanical model to study the consequence of omitting the flexural reinforcement at punching failure.

ACKNOWLEDGEMENTS

The project is financially supported by the *Development Fund of the Swedish Construction Industry (SBUF)*, *J. Gust Richert Foundation* and *KTH*. Concrete and reinforcement, used in series E were delivered free of charge by *Swerock AB* and *Fundia Bygg AB*, respectively. The C series were conducted at *Skanska Prefab* in *Strängnäs*. Steel fibres *Dramix*[®], used in series C, were delivered free of charge by *Leon Bekaert Svenska AB*. *Internordisk Spännarmering AB* has supported the project by equipment and personal to prestress the slabs. The authors gratefully acknowledge all these supports.

REFERENCES

1. Ay L. (1999); "Using Prestressed Steel Fiber Reinforced High Performance Concrete in the Industrialization of Bridge Structures"; Licentiate Thesis, Bulletin 49, Dept. of Structural Engineering, Royal Institute of Technology, Stockholm; 129 pp.
2. Hallgren M. (1996); "Punching Shear Capacity of Reinforced High Strength Concrete Slabs", Doctoral Thesis, Bulletin 23, Dept. of Structural Engineering, Royal Institute of Technology, Stockholm; 206 pp.
3. Prisco M. di and Felicetti R. (1997); "Some results on punching shear in plain and fibre-reinforced micro-concrete slabs"; Magazine of Concrete Research 49, No. 180, Sept.; pp. 201-219.

4. Li V. and Maalej M. (1996); "Toughening in Cement Based Composites. Part II: Fiber Reinforced Cementitious Composites"; *Cement & Concrete Composites* 18, pp. 239-249
5. Swamy R. N., Al-Ta'an S. and Ali S. A. R (1979); "Steel fibers for Controlling Cracks and Deflection"; *Concrete International*, V. 1, No. 8, Aug.; pp.41-49.
6. Swamy R. N. and Ali S. A. R. (1982); "Punching Shear Behaviour of Reinforced Slab-Column Connections with Steel Fiber Concrete", *ACI Journal*, Proceeding V. 79, No. 5, Sept.-Oct.; pp.392-406.
7. Alexander S. D. B. and Simmonds S. H. (1992); " Punching Shear Tests of Concrete Slab-Column Joints Containing Fiber Reinforcement"; *ACI Structural Journal*, V. 89, No. 4, July-Aug.; pp.425-432.
8. Shaaban A. M. and Gesund H. (1994); " Punching Shear Strength of Steel Fiber-Reinforced Concrete Flat Slabs"; *ACI Structural Journal*, V. 91, No. 4, July-Aug.; pp. 406-414.
9. Adebar P., Mindes S., St-Pierre D. and Olund B. (1997); "Shear Tests of Fiber Concrete Beams Without Stirrups"; *ACI Structural Journal*, V. 94, No. 1, Jan.-Feb.; pp. 68-76.
10. McHarg P., Cook W. D., Mitchell D. and Yoon Y.-S. (2000); "Benefits of Concentrated slab Reinforcement and Steel Fibers on Performance of Slab-Column Connections"; *ACI Structural Journal*, March-April, Title No. 97-S24, pp. 225-234.
11. Hassanzadeh G. (1998), "Betongplattor på pelare – Dimensioneringsmetoder för plattor med icke vidhäftande spännarmering", Licentiate Thesis, *Bulletin* 43, Dept. of Structural Engineering, Royal Institute of Technology, Stockholm, 160 pp., (in Swedish with a summary in English).

Behaviour of Fibre Reinforced Concrete for Different Structures



Keivan Noghabai
 Ph.D., Associated Professor
 Luleå University of Technology
 Div. of Structural Engineering
 S-971 87 Luleå, Sweden
 E-mail: keivan.noghabai@ce.luth.se

ABSTRACT

The paper discusses FRC in the context of three different structures based on results of experiments and models. Various fibres were tested for (1) notched prisms under uniaxial tension, (2) reinforced elements in tension, and (3) reinforced beams under transverse loading. A FRC labelled “tough” in one case does not necessarily give a tough response in all other cases. Instead, the quality of a FRC must be viewed in its structural context, where the variables *Geometry*, *Material* and *Environment* (including loading and restraints) interact. This interaction can be quantified by numerical methods.

Key words: Metallic fibres, Nonmetallic fibres, High-strength concrete, Uniaxial tension, Reinforcing bar, Shear.

1. DEFINITION OF PROBLEM

In moderate amounts (i.e., up to 1 volume-%), fibres are meant to arrest further opening of arisen tensile cracks. Cracks arise and develop in a reinforced concrete structure (RCS) during its entire life span. They are caused by mechanical loads (e.g., imposed loading and dead weights) in combination with the surrounding environment, and external as well as internal restraints. There is, however, no commonly accepted theoretical basis for *how* cracks arise and develop in different concrete structures, and consequently, the contribution of fibres to the overall performance of RCS under load is not fully understood. The important question is, then, how to use fibres efficiently, especially considering the current high cost of fibres. Unavoidably, for a rational composition of fibre reinforced concrete (FRC) there must exist guidelines based on models that are able to describe and quantify the contribution of fibres to the overall mechanism of function of the RCS. In fact, the lack of guidelines is the main reason why fibres are not used more extensively in RCS, also to enhance its torsional or shear capacity, or the bar-to-concrete bonding.

2. METHOD

In the above discussion, the main function of fibres was defined as to arrest tensile cracking in concrete. The theory describing the function of a RCS, thus, ought to be based on tensile behaviour of concrete. Figure 1 schematises a theoretical concept that more explicitly takes into account the tensile behaviour of concrete. In mechanical terms, the behaviour of each substructure in Fig. 1 is

used as a local (constitutive) law for describing the behaviour of structures at higher levels. Different theories may coexist for the same problem, because the behaviour of the substructure is also complex. In civil engineering it is problematic to obtain true material properties that are not influenced by the size and shape of the test piece, and the testing procedure. In fact, it seems quite realistic to suppose that there is a coupling of the *Material-Geometry-Environment* at all levels in Fig. 1, [1, 2]. Here, *Environment* involves all types of influences exerted by the surrounding on the boundaries of the structure, be they variations in temperature and moisture, chemical or biological attack, or types of mechanical loading and restraints. Because the contribution of each variable to the whole structure is not deterministic, the description of the problem ultimately becomes a matter of interpretation; hence the lack of consensus on theories mentioned previously. Experiments alone are not enough to bring clarity to the complexity (or indeterminism) of parameters. There must also exist numerical tools in which the theory is implemented and by which the contribution of essential parameters is quantified, through an iterative procedure.

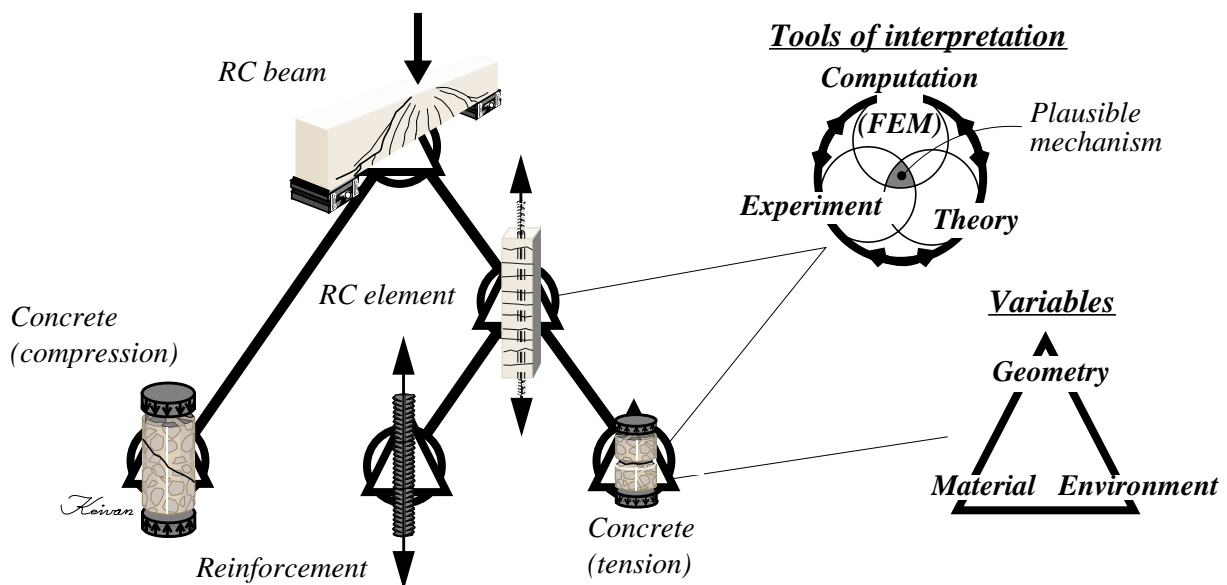


Figure 1 - Theoretical concept for reinforced concrete beams.

3. EXPERIMENTS

The effect of fibres on the behaviour of three different types of structures will be discussed here:

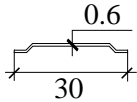
- (1) Notched concrete cylinder subjected to uniaxial tension test
- (2) Pull-tension test on reinforcement bars embedded in concrete prisms
- (3) Simply supported slender beams loaded in flexural-shear

The studied cases may be viewed on their own, but a major objective of this paper is to show how the effects of fibres can be retraced in the performance of the different structures, based on Fig. 1.

3.1 Combination of concrete and fibres

The fibres used in this study are presented in Table 1. They were added to mixtures of high-strength concrete (HSC) containing around 490 kg/m^3 cement, 48 kg/m^3 silica fume, and $4.6\text{-}5.2 \text{ kg/m}^3$ superplasticizer, [1]. The mixtures had a water-to-cement ratio between 0.32-0.38.

Table 1 - Types and combination of fibres used in the investigation

Notation	Fibre content kg/m ³	Material	Configuration	Density kg/m ³	Strength MPa	Elastic modulus GPa	
S30/0.6	80 (1.0%)	Steel		7800	1100	200	
S60/0.7/0.75	60 (0.75%)	Steel		7800	2200	200	
S60/0.7/0.5	40 (0.50%)	Steel		7800	2200	200	
S6/0.15	80 (1.0%)	Steel	—	7800	2600	200	
Smix	S30/0.6	40 (0.5%)	Steel		7800	1100	200
	S6/0.15	40 (0.5%)	Steel	—	7800	2600	200
P50/0.63	9.1 (1.0%)	Polyolefin		910	275	2.6	
P25/0.38	9.1 (1.0%)	Polyolefin		910	275	2.6	
Carbon	16 (1.0%)	Carbon	—	1600	4350	230	

3.2 Uniaxial tension test

The opening resistance of a typical crack can be quantified by uniaxial tension test. The tests here are according to [1] and carried out on notched concrete cylinders, see Fig. 2. The tension softening (i.e., increasing crack opening displacement, COD, for decreasing load) is monitored over the notch and structural effects are eliminated using a deformation control procedure. Some typical results are given in Fig. 2. The results can be used directly as a “material” law in numerical models where the FRC is assumed “homogeneous”. In reality, the given curves indirectly reflect various micro-mechanical effects related to aggregate interlocking, local bonding between matrix and fibres, amount and direction of fibres bridging a crack, and fibre strength. On a general level, possible spurious structural effects of the testing procedure may question whether the results can be viewed as a true material attribute; hence returning to the discussion in Section 2.

The amount of fibres used here (up to 1 volume-%) enhanced the crack opening resistance (that is, tension softening) and had virtually no influence on the tensile strength (f_{ct}). The only exception was fibre S6/0.15, which enhanced both the elastic modulus and the f_{ct} of the concrete. Apparently, due to their small dimensions, these fibres also increased resistance of cracks that occur prior to the f_{ct} . Furthermore, the small fibres are much better dispersed, making the scatter in test results smaller. According to Fig. 2, steel fibres become active as soon as the major fracture localizes, whereas concrete specimens containing polyolefin fibres behave, at first, very much like a plain concrete. These fibres offer resistance when the CODs are in the range of 0.2 to 0.3 mm. The chosen carbon fibres have not changed the tensile behaviour of the concrete. In fact, they seem to have reduced the compressive strength of the plain concrete by approximately 25% [1].

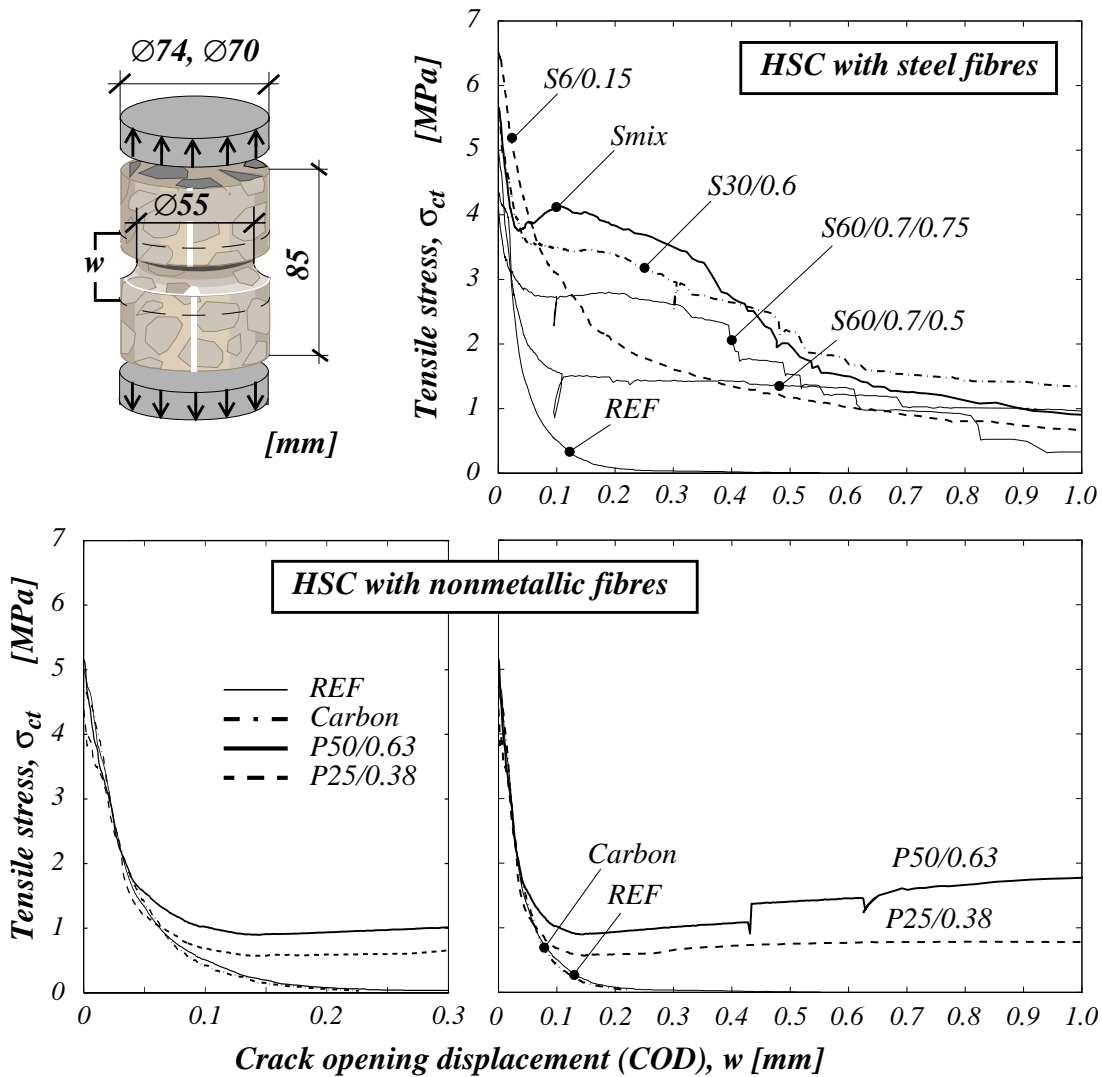


Figure 2 - Response of specimens according to inlaid figure made of different high-strength concrete (HSC) mixtures to uniaxial tension with restrained rotation at load application.

3.3 Reinforced concrete elements in tension

The testing procedure and general behaviour of the elements are described in more details in [1, 2] and more results are presented in [1, 3]. The test shows the combined effect of fibres and ordinary reinforcing bar. A deformed reinforcing $\text{Ø}16$ bar (Swedish Grade Ks500), embedded in a $80 \times 80 \times 960 \text{ mm}^3$ concrete prism, is subjected to axial tension. The results are presented in Fig. 3(a)-(b). At the beginning, the elements behaved almost elastically until transverse cracks appeared (at around 20-30 kN). The arisen cracks did not open uniformly along the elements, mainly because of nonsymmetric surface configuration of the bar. The created crack fronts are sensitive to various time-dependent effects, e.g., the rate of loading. Concrete softens along the discrete cracks according to Fig. 2. In the reference prism of plain concrete (REF), for high load levels, the cracks penetrated the entire cross-section ceasing to transfer any tensile stresses (i.e., the cracks became stress-free with widths wider than 0.3 mm, cf. Fig. 2). The loads were then carried by the confined steel bar. In prisms of FRC, on the other hand, the post-peak softening behaviour contributed to the behaviour of the elements also beyond yielding of the steel, cf. Fig. 2 and Fig. 3.

Based on what is described above, if the load carried by the confined steel reinforcement bar is deducted from the test results, what remains would represent the accumulative load transferred in cracks (i.e., tension softening). This is illustrated by Fig. 3(c), and indeed, there is a similitude between the “softening curves” in Fig. 3(c) and the tension softening curves of single cracks presented in Fig. 2. The stiffness of the confined reinforcement bar is assumed higher than the bare steel of the same length (Fig. 3(a)-(b)), because the strains in the steel bar localize to the location of cracks. The bar stiffness, however, is limited to its “material” stiffness E_s . This is clearly due to a structural effect which also depends on the cover thickness, see [1, 2, 3]. The stiffness of the confined bar increases with the crack spacing which, in turn, increases with the concrete cover. Other tests have indicated that when the element dimensions are doubled, the behaviour of the element changes proportionately. These observations imply that the carrying mechanism for the RC element is more predictable; hence the problem lends itself to analytical modelling. In [1, 3], the RC elements were modelled by parallel-coupled springs. The model will later be instrumental for modelling the RC beam, based on the method given in Fig. 1.

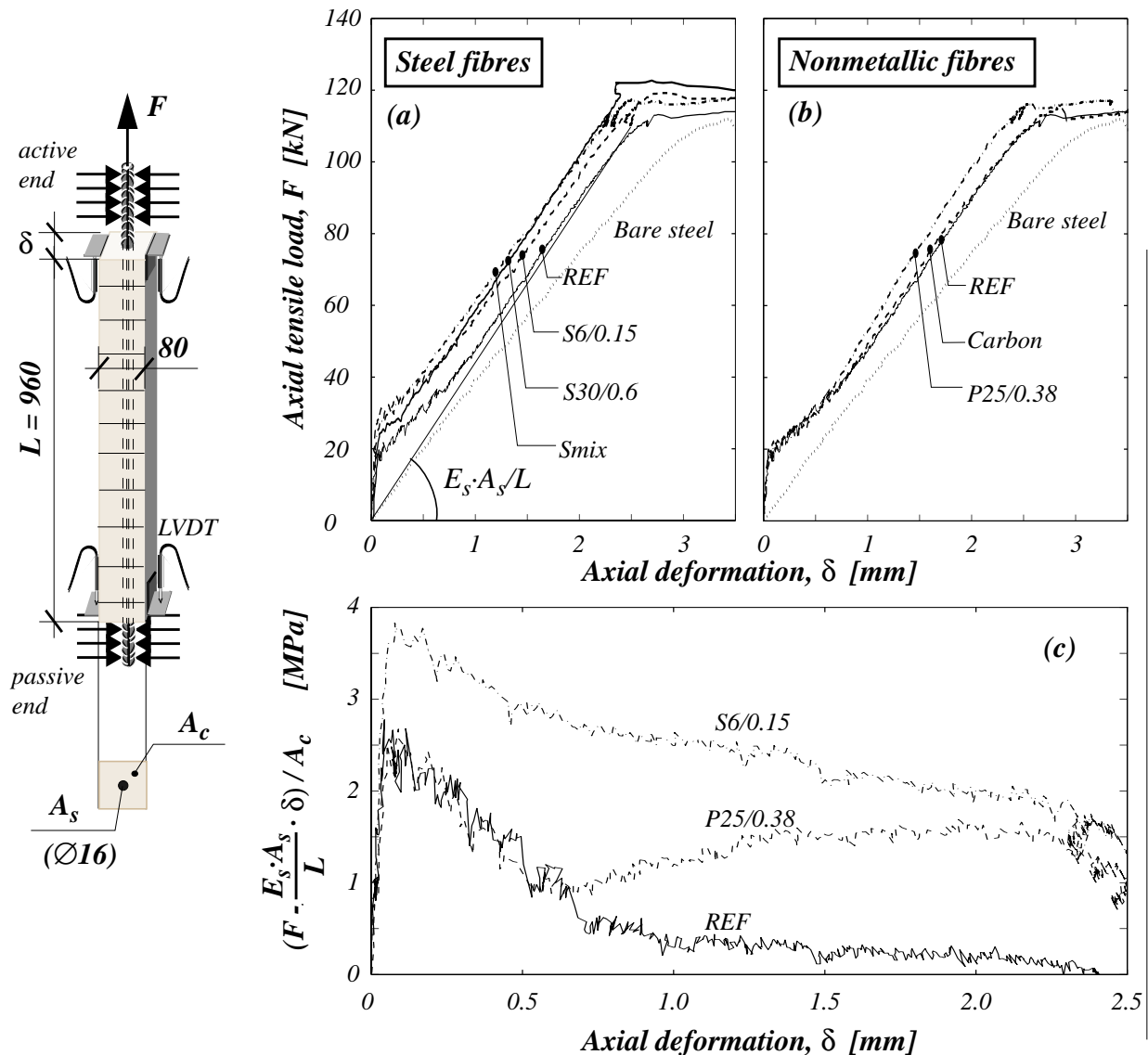


Figure 3 - Reinforced concrete elements under axial tension. Experimental results are shown in (a) and (b). In (c) contribution of confined steel ($E_s \cdot A_s \cdot \delta / L$) is deducted from test results, thus showing accumulated softening in localized cracks in elements.

3.4 Reinforced concrete beams in shear and bending

A major incentive using fibres for load-carrying is to reduce or where possible eliminate conventional reinforcement in RCS, such as the stirrups in beams under transverse loading. One of the most important aspects here, apart from the composition of FRC, is variations in structural dimensions, see Fig. 4. The beams were reinforced with enough bending reinforcement to avoid a yielding of the steel and a flexural failure. The reinforcement ratio ($\rho = A_s / (b \cdot d)$) and the aspect ratio (between shear-span and effective depth, a/d) were fairly similar for the beams. The testing procedure is described in details in [1, 4].

The behaviour of beams of type B is shown in Fig. 4(a). Results of other beams are presented in [1, 4]. The appearance of diagonal cracks corresponds to the two jumps on the curve for the reference beam REF and Carbon-beam. Note that despite lower compressive strength of Carbon-concrete, the beam behaviour is almost identical to the REF-beam, as is the softening behaviour of the two concretes. In fact, there is a connection between the behaviour of all the B-beams and results of the uniaxial tension tests in Fig. 2. The steel fibres start to act as soon as cracks arise in the beam and help redistributing the stresses among other existing cracks. Consequently, the fibres not only make the beam stiffer, the diagonal “shear” cracks become much finer compared with those observed in the beam with stirrups. Polyolefin fibres become active for larger crack widths and the beam behaviour initially resembles the REF-beam’s. Clearly, fibres may all together alter the mechanism of failure in the beam depending on when they start to become active. The beam capacity is limited by the mechanism to which fibres no longer contribute. Thus, the total structural failure coincides with local failure either at zones where compressive stresses prevail (cf. beam of Smix or with stirrups) but also at the anchoring zone of the reinforcing bars (as a bond failure).

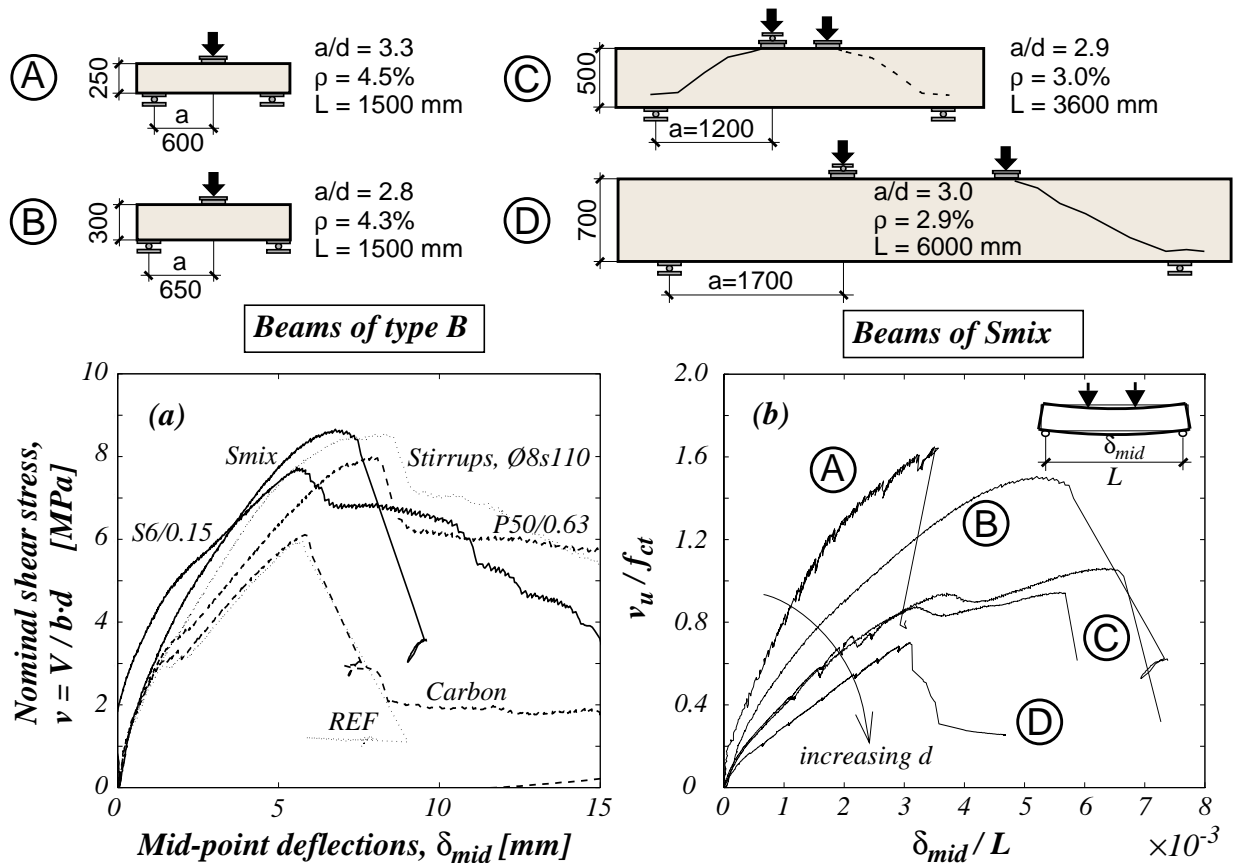


Figure 4 - Experimental results on beam under bending and shear.

Previously, in Fig. 4(a), *Material* was the main variable whereas *Geometry* and *Environment* were kept constant. In Fig. 4(b) the FRC mixture is kept (fairly) constant whilst the beam dimensions (and, to some degree, also the loading conditions) are changed. When normalizing the curves with respect to the tensile strength, the relative capacity of the beams decreases with increasing beam depth. Although the C-beams showed a very tough behaviour, beams of both types A and D failed very abruptly, but apparently for different reasons. In general, failure occurred in the A-beams when the compressive capacity of the beams was reached, whereas for the D-beams failure corresponded to formation of a single asymmetric diagonal crack.

4. MODELLING

Apparently, the behaviour of beams is very complex and cannot be predicted with resort to simple analytical models. Instead, in accordance to the methodology described in Fig. 1, the beams of type B are modelled by axially loaded elements; hence using a nonlinear truss model, see Fig. 5. Results from the uniaxial tension tests are used for representing cracks in both the RC elements and in the RC beam. The RC element, in turn, represents the tensile zone in the RC beam. Based on what was described in Section 3.3, the RC elements are modelled by coupled spring and cohesive elements, representing the elastic and softening concrete, and the steel. By onset of concrete softening (i.e., cracking) the forces in concrete and steel (that balance the applied load $F = F_c + F_s$) are calculated under condition that the system deforms equally (i.e., $\delta = \delta_s = \delta_c$), see [1, 3]. Some comparison between experimental and analytical results are presented in Fig. 5(b).

According to Fig. 5(c), the nonlinear truss model gives good predictions of the ultimate beam loads, albeit the deformations are too stiff. Also important was that the model indicated an alternate mode of failure for the Smix-beam, which, according to Fig. 4(a), seemed to have reached the ultimate capacity for the beam type. Note that, the obtained variation in predicted load capacity would not have been possible using strength-based empirical models, because the FRC used had almost the same f_{ct} . Furthermore, such models consider only specific types of fibre, and cannot handle a mixture of fibres. On the other hand, according to [5], an empirical model that accounts for the tension softening of FRC gives better predictions and is independent of the type, amount, and combination of fibres. The nonlinear truss model better describes bending and arching actions in beams under transverse loading and the predictions become poorer for the largest beams [1, 4].

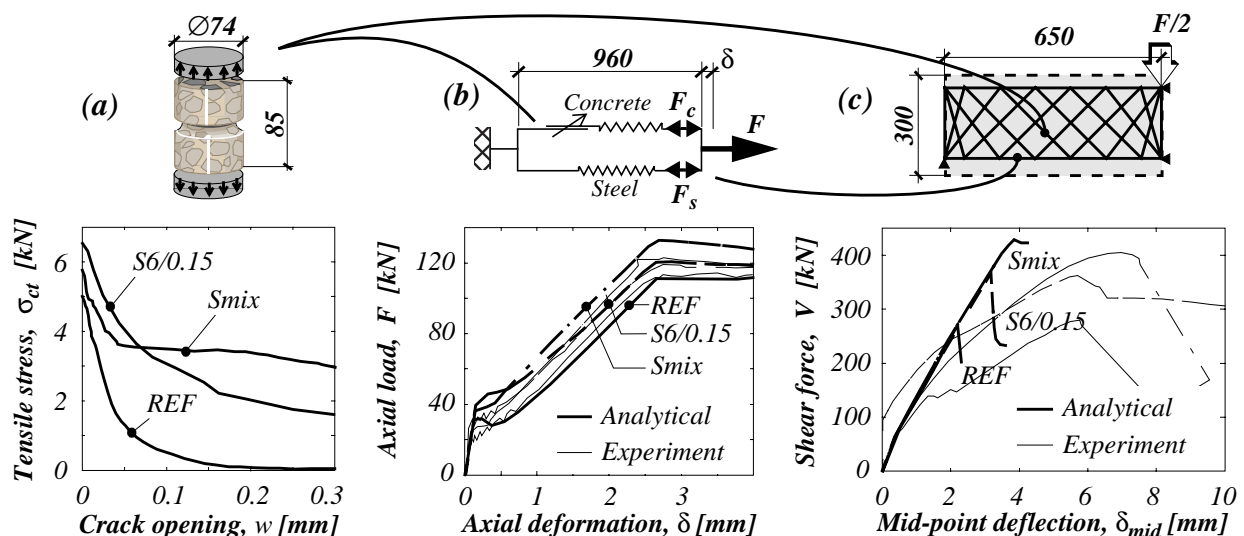


Figure 5 - Application of method in Fig. 1 for modelling some beams of type B.

5. CONCLUSIONS

A FRC labelled “tough” (or high-performance) according to, e.g., the uniaxial tension test (or a standardized test method) can for RC beams under transverse loading give *both* a very tough *and* a very brittle behaviour. The amount and efficiency of fibres in beams must be related to the prevailing load carrying mechanism in the structure. Based on experimental evidence and numerical modelling it was shown that the mechanisms vary for different beam dimensions. Conclusively, under the same loading conditions (*Environment*), in smaller beams structural effects (*Material* and *Geometry* interaction) dominate, whereas for larger beams the tension softening along and stability in propagation of the skew crack (*Material*) become decisive. The ultimate capacity of beams obtained by experiments cannot explain the complexity in structural behaviour, and a numerical tool becomes necessary. Accordingly, for smaller beams where bending and arching action seem to prevail, the nonlinear truss model used here is sufficient as a tool of prediction, whereas for increasing beam depth, a finite element method based on a discrete crack model (of the skew crack) is more suitable, see further [1, 4].

From a practical point of view, the study here implied that 1% of the chosen types of fibre was in excess for the A-beams ($d = 180$ mm) and some of the B-beams ($d = 230$ mm), which failed very abruptly (probably in compression). Other experiments on beams of small depths have also shown a practically nonexistent contribution of steel fibres [6, 7]. On the other hand, 1% fibres seemed ideal for the C-beams ($d = 410$ mm) which showed a very ductile post-peak behaviour. For the D-beams ($d = 565$ mm) 1% fibres was not enough to keep the skew diagonal crack together in order to facilitate a shift of load-carrying mechanism to a more favourable one.

REFERENCES

1. Noghabai, K., “Effect of Tension Softening on the Performance of Concrete Structures - Experimental, Analytical and Computational Studies”, PhD thesis 1998:21, Luleå University of Technology, Luleå, Sweden, 1998, 147 pp.
2. Noghabai, K., “Reinforced Concrete Elements under Combined Loading and Environmental Exposure - Survey on Degradation Processes and Experimental Study”, Research report 2001:07, Luleå University of Technology, Luleå, Sweden, 2001, 120 pp.
3. Noghabai, K., “Behavior of Tie Elements of Plain and Fibrous Concrete and Varying Cross Sections”, *ACI Structural Journal*, ACI, Vol. 97, No. 2, 2000, pp. 277-284.
4. Noghabai, K., “Beams of Fibrous Concrete in Shear and Bending - Experiment and Model”, *Journal of Structural Engineering*, American Society of Civil Engineers, Vol. 126, No. 2, 2000, pp. 243-251.
5. Noghabai, K., Olofsson, T., and Gustafsson, J. “Fiber reinforced high-strength concrete beams in shear”, *Proceedings*, First Int. Conf. on High Strength Concrete (eds. A. Azizinamini, D. Darwin and C. French), Kona, Hawaii, July 13-18, 1997, American Society of Civil Engineers, 1999, pp. 480-493.
6. Balazs, G.L., and Kovacs, I., and Erdelyi, L. “Flexural Behavior of RC and PC Beams with Steel Fibers”, *Proceedings*, High Performance Fiber Reinforced Cement Composites (HPFRCC 3, eds. H. W. Reinhardt, and A. E. Naaman), RILEM, 1999, pp. 499-508.
7. Campione, G., and Mindess, S. “Fibers as Shear Reinforcement for High Strength Reinforced Concrete Beams Containing Stirrups”, *Proceedings*, High Performance Fiber Reinforced Cement Composites (HPFRCC 3, eds. H. W. Reinhardt, and A. E. Naaman), RILEM, 1999, pp. 519-529.